

Università degli Studi di Padova  
DIPARTIMENTO DI MATEMATICA "TULLIO LEVI-CIVITA"  
CORSO DI LAUREA IN INFORMATICA



**Fast Message Propagation  
Over IoV Scenarios**

*Tesi di Laurea Magistrale*

*Relatore*

Prof. Claudio E. Palazzi

*Co-relatore*

Dott. Armir Bujari

*Laureando*

Jordan Gottardo

---

ANNO ACCADEMICO 2018-2019



# Contents

<b>1</b>	<b>Introduction</b>	<b>1</b>
1.1	Emergency Message Dissemination and broadcasting protocols . . . . .	1
1.1.1	Single-hop Broadcasting Protocols . . . . .	2
1.1.2	Multi-hop Broadcasting Protocols . . . . .	3
1.2	Radio Propagation Models . . . . .	5
<b>2</b>	<b>Models</b>	<b>7</b>
2.1	Obstacle Shadowing propagation loss model . . . . .	7
2.2	Junction modeling . . . . .	8
<b>3</b>	<b>Fast-Broadcast</b>	<b>11</b>
3.1	Estimation Phase . . . . .	11
3.2	Broadcast Phase . . . . .	12
3.3	Multiple dimensions extension . . . . .	13
3.3.1	Hello Message Header Structure . . . . .	16
3.3.2	Alert Message Header Structure . . . . .	16
3.4	Smart Junction Fast-Broadcast (SJ-Fast-Broadcast) . . . . .	16
3.4.1	Alert Message Header Structure . . . . .	19
<b>4</b>	<b>ROFF</b>	<b>21</b>
4.1	Forwarder Selection Problem . . . . .	21
4.1.1	Collision Analysis . . . . .	21
4.1.2	Latency Analysis . . . . .	22
4.2	ROFF Algorithm . . . . .	24
4.2.1	ESD Bitmap Construction . . . . .	24
4.2.2	Forwarding Priority Acquisition . . . . .	26
4.2.3	Waiting Time Assignment . . . . .	27
4.3	Multiple dimensions extension . . . . .	28
4.3.1	Hello Message Header Structure . . . . .	29
4.3.2	Alert Message Header Structure . . . . .	29
4.4	Smart Junction ROFF (SJ-ROFF) . . . . .	30
4.4.1	Alert Message Header Structure . . . . .	31
<b>5</b>	<b>Tools and applications</b>	<b>33</b>
5.1	Network Simulator 3 . . . . .	33
5.1.1	Modules and module structure . . . . .	33
5.1.2	Key elements . . . . .	34
5.1.3	Structure of a simulation . . . . .	35
5.1.4	NetAnim . . . . .	35

5.2	Simulation of Urban MObility . . . . .	36
<b>6</b>	<b>Simulations</b>	<b>39</b>
6.1	Metrics . . . . .	39
6.1.1	Total Delivery Ratio (TDR) . . . . .	39
6.1.2	Total Delivery Ratio On Circumference (TDROC) . . . . .	39
6.1.3	Number Of Hops (NOH) . . . . .	40
6.1.4	Number Of Slots (NOS) . . . . .	41
6.1.5	Forwarding Node Number (FNN) . . . . .	41
6.2	Platoon scenario . . . . .	42
6.3	Grid scenario . . . . .	45
6.4	Los Angeles urban scenario . . . . .	54
6.5	Padua urban scenario . . . . .	64
6.6	Los Angeles smart city scenario . . . . .	71
6.7	Hello Message forging scenario . . . . .	80
6.7.1	Low severity attack . . . . .	81
6.7.2	High severity attack . . . . .	81
6.8	Different vehicle density scenario . . . . .	82
6.9	Smaller contention window . . . . .	90
	<b>Acronyms</b>	<b>95</b>
	<b>Bibliography</b>	<b>97</b>

# List of Figures

2.1	Example of obstacle shadowing in vehicle-to-vehicle communication. Walls encountered by the signal are surrounded in red circles . . . . .	8
2.2	Example of data about a junction retrieved from OpenStreetMap and elaborated through SUMO . . . . .	9
2.3	Junction modeling process . . . . .	9
2.4	Example of 6 junctions in an urban scenario . . . . .	10
3.1	Example of Fast-Broadcast in 2D scenario . . . . .	14
3.2	Fast-Broadcast Hello Message header structure . . . . .	16
3.3	Fast-Broadcast Alert Message header structure . . . . .	16
3.4	Usual Fast-Broadcast Alert Message propagation . . . . .	17
3.5	SJ-Fast-Broadcast Alert Message propagation . . . . .	18
3.6	SJ-Fast-Broadcast Alert Message header structure . . . . .	19
4.1	Definition of <i>minDiff</i> between $f_N$ and $f_{N-1}$ ([21]) . . . . .	22
4.2	Definition of empty space ([21]) . . . . .	23
4.3	Components of ROFF algorithm . . . . .	24
4.4	Example of Neighbor Table of node with ID 0 . . . . .	25
4.5	ESD Bitmap construction with $k = 1$ . . . . .	25
4.6	Resulting ESD Bitmap with $k = 2$ . . . . .	26
4.7	ID-based contention: node A defers its transmission . . . . .	27
4.8	Waiting time assignment based on vehicle distribution depicted in Figure 4.5 . . . . .	27
4.9	ROFF Hello Message header structure . . . . .	29
4.10	ROFF Alert Message header structure . . . . .	30
4.11	SJ-ROFF Alert Message header structure . . . . .	31
5.1	ns-3 module structure . . . . .	34
5.2	Packet transmission in NetAnim . . . . .	35
5.3	Steps to generate necessary files using SUMO ([19]) . . . . .	36
5.4	Padua scenario with vehicle distance equals to 15 meters (top) and 45 meters (bottom) . . . . .	37
6.1	Example of <i>NOH</i> calculation with Alert Message starting from node S	40
6.2	Example of <i>NOS</i> calculation with Alert Message starting from node S	41
6.3	<i>TDR</i> , <i>TDROC</i> , <i>NOH</i> and <i>NOS</i> metrics for Platoon scenario . . . . .	43
6.4	<i>FNN</i> metric for Platoon scenario . . . . .	44
6.5	<i>TDR</i> without buildings (top) and with buildings (bottom) for Grid scenario . . . . .	46

6.6	<i>TDROC</i> without buildings (top) and with buildings (bottom) for Grid scenario . . . . .	46
6.7	<i>NOH</i> without buildings (top) and with buildings (bottom) for Grid scenario . . . . .	47
6.8	<i>NOS</i> without buildings (top) and with buildings (bottom) for Grid scenario . . . . .	47
6.9	<i>FNN</i> without buildings (top) and with buildings (bottom) for Grid scenario . . . . .	48
6.10	Fast-Broadcast after 1 hop (top) and 2 hops (bottom) in Grid scenario with 500 meters transmission range and without the Obstacle model . . . . .	49
6.11	Fast-Broadcast after 1 hop (top) and 2 hops (bottom) in Grid scenario with 500 meters transmission range and with the Obstacle model . . . . .	50
6.12	<i>ROFF</i> after 1 hop (top) and 2 hops (bottom) in Grid scenario with 500 meters transmission range and without the Obstacle model . . . . .	51
6.13	<i>ROFF</i> after 1 hop (top) and 2 hops (bottom) in Grid scenario with 500 meters transmission range and with the Obstacle model . . . . .	52
6.14	Collision area in 2D <i>ROFF</i> . . . . .	54
6.15	Los Angeles urban scenario depiction . . . . .	55
6.16	Los Angeles urban scenario test overview . . . . .	55
6.17	<i>TDR</i> for Los Angeles urban scenario . . . . .	57
6.18	<i>TDROC</i> for Los Angeles urban scenario . . . . .	58
6.19	<i>NOH</i> for Los Angeles urban scenario . . . . .	59
6.20	<i>NOS</i> for Los Angeles urban scenario . . . . .	60
6.21	<i>FNN</i> for Los Angeles urban scenario . . . . .	61
6.22	Alert Message delivery for Los Angeles scenario with buildings and without junctions (Fast-Broadcast with 100 meters transmission range) . . . . .	62
6.23	Padua urban scenario depiction . . . . .	64
6.24	<i>TDR</i> for Padua urban scenario . . . . .	66
6.25	<i>TDROC</i> for Padua urban scenario . . . . .	67
6.26	<i>NOH</i> for Padua urban scenario . . . . .	68
6.27	<i>NOS</i> for Padua urban scenario . . . . .	69
6.28	<i>FNN</i> for Padua urban scenario . . . . .	70
6.29	Los Angeles smart city scenario with real height buildings (top) and very high buildings (bottom) . . . . .	72
6.30	Test overview of Los Angeles smart city scenario . . . . .	73
6.31	<i>TDR</i> for Los angeles smart city scenario . . . . .	75
6.32	<i>TDROC</i> for Los angeles smart city scenario . . . . .	76
6.33	<i>NOH</i> for Los angeles smart city scenario . . . . .	77
6.34	<i>NOS</i> for Los angeles smart city scenario . . . . .	78
6.35	<i>FNN</i> for Los angeles smart city scenario . . . . .	79
6.36	<i>TDR</i> for Fast-Broadcast (top) and <i>ROFF</i> (bottom) with different distance between vehicles and transmission ranges . . . . .	84
6.37	<i>TDROC</i> for Fast-Broadcast (top) and <i>ROFF</i> (bottom) with different distance between vehicles and transmission ranges . . . . .	85
6.38	<i>NOH</i> for Fast-Broadcast (top) and <i>ROFF</i> (bottom) with different distance between vehicles and transmission ranges . . . . .	86
6.39	<i>NOS</i> for Fast-Broadcast (top) and <i>ROFF</i> (bottom) with different distance between vehicles and transmission ranges . . . . .	87
6.40	<i>FNN</i> for Fast-Broadcast (top) with different distance between vehicles and transmission ranges . . . . .	88

6.41	<i>FNN</i> for Fast-Broadcast (top) and ROFF (bottom) with different distance between vehicles and transmission ranges (alternative angle) . . . . .	89
6.42	<i>TDR</i> for [16, 128] contention window (top) and [32, 1024] ] contention window (bottom) . . . . .	91
6.43	<i>TDROC</i> for [16, 128] contention window (top) and [32, 1024] contention window (bottom) . . . . .	91
6.44	<i>NOH</i> for [16, 128] contention window (top) and [32, 1024] ] contention window (bottom) . . . . .	92
6.45	<i>NOS</i> for [16, 128] contention window (top) and [32, 1024] ] contention window (bottom) . . . . .	92
6.46	<i>FNN</i> for [16, 128] contention window (top) and [32, 1024] ] contention window (bottom) . . . . .	93

# List of Tables

6.2	Platoon scenario configuration . . . . .	42
6.4	Grid scenario configuration . . . . .	45
6.6	Los Angeles urban scenario configuration . . . . .	56
6.8	Los Angeles urban scenario configuration . . . . .	65
6.10	Los Angeles urban scenario configuration . . . . .	74
6.12	Low severity forging attack scenario configuration based on Los Angeles urban scenario . . . . .	81
6.14	High severity forging attack scenario configuration based on Los Angeles urban scenario . . . . .	82
6.16	Different vehicle densities scenario configuration based on Padua urban scenario . . . . .	83
6.18	Contention window scenario configuraton based on Los Angeles urban scenario . . . . .	90



# Chapter 1

## Introduction

### 1.1 Emergency Message Dissemination and broadcasting protocols

Emergency Message Dissemination (EMD) is a fundamental application in [VANET](#) to prevent traffic accidents, thereby reducing death and injury rates. Such task can be executed by the VANET itself by turning it into an infrastructure-less self-organizing network, where the dissemination is carried out by specific protocols.

Since traffic information, especially emergency data, has a broadcast-oriented nature (i.e. it is of public interest), it is more appropriate to disseminate it using broadcasting routing scheme rather than unicast or multicast ones. [1]

This choice leads to some advantages, such as:

- \* the fact that vehicles do not need to know the destination address and how to calculate a route towards it;
- \* a greater coverage of vehicles interested in the information, useful also in lossy scenarios, especially when paired with controlled redundancy schemes;
- \* a greater efficiency in bandwidth usage.

The idea behind existing algorithms consists in designating the next forwarder in the multi-hop chain from the source of the alert to the target region where the sensitive data has to be delivered. Ideally, the farthest vehicle from a previous forwarder in the dissemination direction should be given priority when designating the next forwarder. However, due to unreliable wireless channel, the designation of farthest vehicle can fail and interrupt the message dissemination. Due to this, next forwarder designation keeps into consideration also other vehicles (called potential forwarder candidates, PFCs) which have received an Alert Message. The PFCs participate in contention to elect the farthest forwarder candidate (FFC) who will continue disseminating the message.

In order to carry out the forwarder designation process, the main idea consists in differentiating waiting times (WT) of PFCs. Each PFC should select a waiting time ranging from 0 to a predefined upper bound (PUB). To guarantee the correct designation of the farthest vehicle as forwarder, PFCs choose their waiting time inversely proportional to the distance between the PFC and the previous forwarder. This way other candidates can detect the transmission from the FFC and suppress their transmission.

Advancements in research on Emergency Message Dissemination has lead to the development of a number of broadcasting protocols. However, as identified by Panichpapiboon et al.[1], most of them belong to one of two main categories:

- \* Single-hop Broadcasting Protocols, in which no flooding is employed. Instead, vehicles periodically select and broadcast only a subset of the packets it has received;
- \* Multi-hop Broadcasting Protocols, in which packets are transmitted through the network via flooding by some of the neighbors of the source. It is of utmost importance to reduce the number of redundant transmission in order not to waste bandwidth and saturate the channel.

### 1.1.1 Single-hop Broadcasting Protocols

Vehicles employing Single-Hop Broadcasting protocols will not flood received packets immediately through the network. Instead, vehicles use information from packets to update their database and periodically rebroadcast only a fraction of that information. The two variables these kind of protocols can work on to aim for network efficiency are:

- \* *Broadcast Interval*, i.e. the amount of time between retransmissions, which should keep into consideration both freshness of information and potential redundancy in transmissions;
- \* *Relevancy of information* to broadcast: as stated before, only relevant information (i.e. a subset of all the information) should be broadcast.

Single-Hop protocols can be further subdivided into two categories:

1. Fixed Broadcast Interval, which keep the Broadcast Interval fixed. Some examples are:
  - *TrafficInfo*[2], a protocol in which vehicles record, among other information, travel times on road segments (identified by an ID) and keep them on their on-board database. Vehicles periodically exchange information about the learned travel times based on the relevance of such information. The relevance is calculated using a ranking algorithm which uses the current position of the vehicle and the current time (i.e. relevance decreases with distance and time), broadcasting only the  $k$  most important information.
  - *TrafficView*[3], in which vehicles exchange information about speed and position and record it in their database. Data about different vehicles is then aggregated into a single record using one of two aggregation algorithms:
    - the *ratio-based* algorithm, which assigns an aggregation ratio to each portion of a road: the more important the road is, the higher the aggregation ratio will be, increasing the accuracy of the information of that area;
    - the *cost-based* algorithm, an algorithm which keeps into consideration the cost of aggregating different records. The aggregation cost is defined as the loss of accuracy the aggregation will bring about.
2. Adaptive Broadcast Interval, which adapt the Broadcast Interval based on dynamic information. Some examples are:

### 1.1. EMERGENCY MESSAGE DISSEMINATION AND BROADCASTING PROTOCOLS

- *Collision Ratio Control Protocol (CRCP)*[4], a scheme according to which vehicles exchange information about location, speed and road ID. The Broadcast Interval is dynamically controlled based on the amount of detected collisions and bandwidth efficiency: the protocol tries to maintain the number of collisions under a certain threshold by doubling the Broadcast Interval every time the threshold is exceeded. Otherwise, the Broadcast Interval is decreased by one second when the bandwidth efficiency decreases too much. Moreover, the authors propose three different methods for selecting the data to be transmitted:
  - *Random Selection*: a vehicle selects a random information in its database and broadcasts it;
  - *Vicinity Priority Selection*: vehicles give priority to information of nearby areas;
  - *Vicinity Priority Selection with Queries*: similar to Vicinity Priority Selection, with the possibility of querying information for a certain area.
- *Abiding Geocast*: [5], which aims to deliver an Alert Message to a specific area where the warning is still relevant. Only vehicles that are travelling towards the effective area can participate in contention to broadcast the message. Moreover, broadcast is dynamically adjusted based on transmission range, speed, and distance between the potential forwarder and the destination area, increasing when such distance increases or the potential forwarder's speed decreases.
- *Segment-oriented Data Abstraction and Dissemination (SODAD)*[6], a protocol according to which roads are divided into segments and each vehicle can both discover information itself and collect it from neighbor's transmissions. Whenever a vehicle receives a transmission from another vehicle, the information received will be classified as either one of two events:
  - a *provocation* event that will decrease the Broadcast Interval;
  - a *mollification* event that will increase the Broadcast Interval.

The classification is done via comparison of the newly received data with the information stored in the vehicle's on-board database. The vehicle assigns a higher weight if the difference between information coming from these two sources is high. The weight will be then compared against a threshold to establish whether a provocation or mollification event has taken place.

#### 1.1.2 Multi-hop Broadcasting Protocols

Multi-hop Broadcasting Protocols can be further subdivided into two categories:

- (a) Delay based protocols, which assign a different waiting time before re-broadcasting the message to each vehicle. This delay is usually inversely proportional to the distance between the source and the potential sender. Some examples are:
  - *Urban Multi-hop Broadcast (UMB)* [7], designed to solve the broadcast redundancy, hidden node and reliability problems in multi-hop broadcasting using *Request-to-Broadcast (RTB)* and *Clear-To-Broadcast (CTB)* packets;

- *Smart Broadcast (SB)* [8] and *Efficient Directional Broadcast (EDB)* [9], which try to reduce the delay introduced by *UMB* and remove the *RTB* and *CTB* packets, respectively;
  - *Vehicle-density-based Emergency Broadcasting (VDEB)* [10], a slotted broadcasting protocol which keeps vehicle density into consideration when computing waiting time slots;
  - *Reliable Method for Disseminating Safety Information (RMDSI)* [11], which aims to offer better performances when the network becomes fragmented by making a forwarder keep a copy of the packet it has broadcasted until it hears a retransmission (or until the packet lifetime expires). If no retransmission is heard within a certain time limit, the forwarder tries to find the next node which can relay the message using a small control packet;
  - *Multi-hop Vehicular Broadcast (MHVB)* [12], a protocol that keeps traffic congestion into consideration by checking whether the number of neighbors of a vehicle is greater than a certain threshold and its speed is smaller than another threshold. When a node detects congestion, it increases its broadcast interval in order to try to reduce the network load;
  - *Reliable Broadcasting of Life Safety Messages (RBLSM)* [13], whose main objective is reliability, and a higher priority is given to the vehicle nearest to the sender instead to the one farthest from it, due to the assumption that the closer the vehicle is, the more reliable it is considered since its received signal strength is higher.
- (b) Probabilistic-based Multi-hop Broadcasting Protocols. The idea behind these kind of protocols is similar to the one behind Delay based protocols, but instead of assigning a different rebroadcast delay to each vehicle, a different rebroadcast probability is assigned. Each protocol differs in the function that assigns probabilities. Some examples of probabilistic-based protocols are:
- *Weighted p-Persistence* [14], in which every PFC computes its own rebroadcast probability based on distance between itself and the transmitter. The formula used is the following:
- $$p_{ij} = \frac{D_{ij}}{R} \quad (1.1)$$
- where  $D_{ij}$  is the distance between transmitter  $i$  and PFC  $j$  and  $R$  is the transmission range. Based on this function, the probability to rebroadcast is proportional to the distance between the PFC and the transmitter. The abovementioned formula does not keep into account vehicle density and also assumes that the transmission range is fixed and known to all vehicles.
- *Optimized Adaptive Probabilistic Broadcast (OAPB)* [15] and *AutoCast (AC)* [16], which both keep the vehicle density into consideration when computing the forwarding probability by making vehicle periodically exchange Hello Messages. Thanks to those messages, each vehicle can compute the number of neighbors and then use this information accordingly.

- *Irresponsible Forwarding (IF)* [17][18], a protocol that considers vehicle density like *OAPB* and *AC*, but the formula used is not a simple linear function. In fact, the rebroadcast probability assignment function is the following:

$$p = e^{-\frac{\rho_s(z-d)}{c}} \quad (1.2)$$

where  $\rho_s$  is the vehicle density,  $z$  is the transmission range,  $d$  is the distance between the PFC and the transmitter and  $c \geq 1$  is a shaping parameter which influences the rebroadcast probability. *Irresponsible Forwarding* aims to offer a solution that can scale with network density.

The previous work[19] focused on the implementation and testing of Fast-Broadcast, a Multi-hop delay based protocol firstly presented in [20]. The main focus of the algorithm is to try to overcome the assumption of a fixed and known transmission range, which other protocols often tacitly assume. The protocol will be further analyzed in Chapter 3.

The authors of ROFF [21], another Multi-Hop delay based protocol, state that existing protocols are affected by two problems:

- \* the perfect suppression of redundant transmissions, by which potential forwarders which have lost the contention detect the transmission from the farthest vehicle and suppress their transmission. However this suppression can not always be guaranteed due to short difference between waiting times. In fact, if the timer of a potential forwarder expires before it has heard the transmission from the FFC, a redundant transmission will occur;
- \* the disuniformity and the constant change in spatial vehicle distribution in VANETs. Existing protocols which keep into consideration the distance between PFC and previous forwarder do not keep into consideration large empty spaces in the waiting time computation, leading to unnecessary wait.

ROFF's solutions to these problems and the implementation of the protocol will be analyzed in Chapter 4.

## 1.2 Radio Propagation Models

Since field testing in VANETs, especially in large scenarios, is usually expensive and difficult to execute in real settings, researchers usually carry out their tests in a simulated environment, such as ns-3 (Section 5.1). In order to model the transmission of signal throughout various media, several radio propagation models have been developed. A **Radio Propagation Model (RPM)** is an empirical mathematical formulation used to model the propagation of radio waves as a function of frequency, distance, transmission power and other variables. Over the years various RPMs have been developed, some aiming at modelling a general situation, and others more useful in specific scenarios. For example, implementations range from the more general free space model, where only distance and power are considered, to more complex models which account for shadowing, reflection, scattering, and other multipath losses. Moreover, it is important to keep into consideration the computational complexity and scalability of the model: some have poor accuracy but are scalable, while others have very

good accuracy but can only work for small sets of nodes. As always, it is very important to find the right trade-off between complexity and accuracy.

The authors of [22] classify the propagation models offered by the network simulator ns-3 in three different categories:

- \* **Abstract** propagation loss models, for example the Maximal Range model (also known as Unit Disk), which establishes that all transmissions within a certain range are received without any loss;
- \* **Deterministic** path loss models, such as the Friis propagation model, which models quadratic path loss as it occurs in free space, and Two Ray Ground, which assume propagation via two rays: a direct (**LOS**) one, and the one reflected by the ground;
- \* **Stochastic** fading models such as the Nakagami model, which uses stochastic distributions to model path loss.

These traditional models, especially the stochastic ones, work quite well to describe the wireless channel characteristics from a macroscopic point of view. However, given the probabilistic nature of the model, single transmissions are not affected by the mesoscopic and microscopic effects of the surrounding environment. To keep these effects into consideration, researchers have utilized Ray-Tracing, a geometrical optics technique used to determine all possible signal paths between the transmitter and the receiver, considering reflection, diffraction and scattering of radio waves, suitable both for 2D and 3D scenarios [23] [24].

However, a Ray-Tracing based approach, while producing a fairly accurate model, is not very scalable due to its high computational complexity, especially in a real-time scenario. To overcome this problem, the authors of [25] have resorted to a fairly computationally expensive pre-processing, but this leads to the need of pre-processing every scenario (and also every change in the scenario).

The RPM utilized in this work will be presented in Section 2.1.

# Chapter 2

## Models

In this Chapter the models implemented and utilized in this work will be presented, namely the Obstacle Shadowing propagation loss model and the Junction model.

### 2.1 Obstacle Shadowing propagation loss model

The original thesis [19], after having analyzed various works concerning shadowing in urban scenarios [26] [27] used a deterministic RPM called Obstacle Shadowing propagation loss model presented in [28] and implemented by the authors of [29]. This propagation model calculates the loss in signal strength due to the shadowing effect of obstacles such as buildings.

The authors of [28] designed the model as an extension of well-established fading models, which can be expressed by Equation 2.1, where:

- \*  $P$  are the transmit or receive powers of the radios;
- \*  $G$  are the antenna gains;
- \*  $L$  indicate the terms capturing loss effects during transmission.

$$P_r[dBm] = P_t[dBm] + G_t[dB] + G_r[dB] - \sum L_x[dB] \quad (2.1)$$

Common RPMs can be written as components  $L$  of 2.1 and chained to obtain the compound attenuation. For example, Equation 2.2 and 2.3 represent respectively the Two-Ray Ground and Log-Normal models.

$$L_{TwoRayGround} = 10 \lg \left( \frac{d^4 L}{h_t^2 h_r^2} \right) \quad [dB] \quad (2.2)$$

$$L_{LogNorm} = 10 \lg (X_\sigma) \quad [dB] \quad (2.3)$$

The authors extended the general model shown in 2.1 adding a  $L_{obs}$  term for each obstacle in the line of sight between sender and receiver. The term is described by Equation 2.4, where:

- \*  $n$  is the number of times that the line of sight intersects the borders of the obstacle;

- \*  $d_m$  is the length of the obstacle's intersections;
- \*  $\beta$  represents the attenuation due to the exterior wall of a building, in dB per wall;
- \*  $\gamma$  represents an approximation of the internal structure of a building, in dB per meter.

Parameters  $\beta$  and  $\gamma$  can be fitted to represent different types of buildings.  $\beta \approx 9.6$  dB per wall and  $\gamma \approx 0.4$  dB/m are the values proposed by the authors for buildings in suburban areas.

$$L_{obs} = \beta n + \gamma d_m \quad (2.4)$$

[Figure 2.1](#) shows an example of transmission where the signal encounters  $n = 4$  walls.

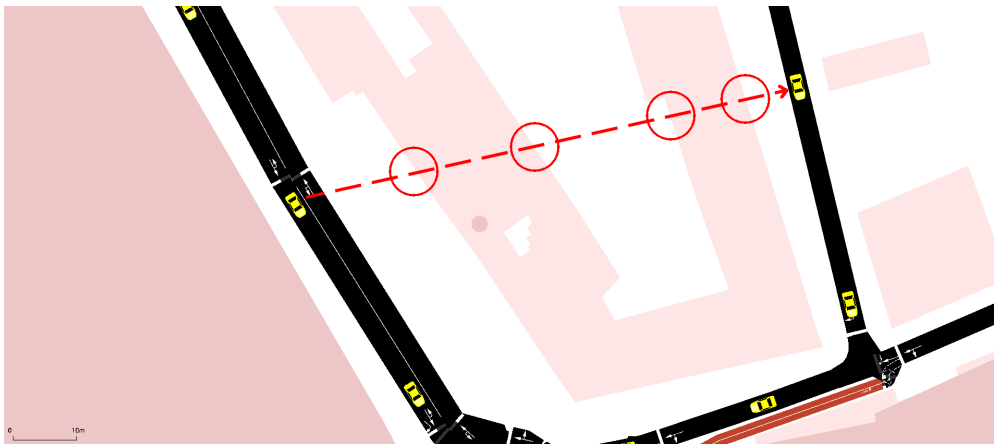


**Figure 2.1:** Example of obstacle shadowing in vehicle-to-vehicle communication. Walls encountered by the signal are surrounded in red circles

## 2.2 Junction modeling

Part of this work consisted in implementing extensions for the algorithms which will be presented in Chapter 3 and 4 to utilize junctions in a smart way. These extensions aim to reach a higher number of vehicles during the Alert Message propagation. In order for those extension to work, a model to identify and represent junctions was necessary. Using data retrieved from OpenStreetMap elaborated through SUMO (see Section 5.2 for the full process), it has been possible to retrieve information about junctions present inside a urban scenario. Figure 2.2 shows the JSON representation of a junction.

```
<junction id="122666592" type="priority" x="1204.30" y="2735.10" intLanes="13446476#0_0
-13433275#0_0 -13446476#1_0" intLanes="122666592_0_0 :122666592_9_0 :122666592_10_0
:122666592_3_0 :122666592_4_0 :122666592_5_0 :122666592_6_0 :122666592_7_0 :122666592_11_0"
shape="1205.98,2741.13 1210.40,2736.50 1208.80,2733.84 1208.24,2731.90 1207.84,2729.55 1207.61,
2726.79 1207.54,2723.62 1201.14,2723.60 1200.81,2725.51 1200.41,2725.91 1199.85,2725.92 1199.13,
2725.56 1198.25,2724.82 1193.81,2729.43">
```

**Figure 2.2:** Example of data about a junction retrieved from OpenStreetMap and elaborated through SUMO

Among other data, the most useful information about a junction are:

- \* the *x* and *y* coordinates, which identify its center;
- \* the *shape* attribute, containing coordinates which represent its shape.

Using from this data it was possible to establish the junction modeling process, represented in Figure 2.3. Since the *shape* attribute resulted in a polygon too small for the purpose of this work, a bounding box which extends the polygon by 20 meters in each direction has been implemented.

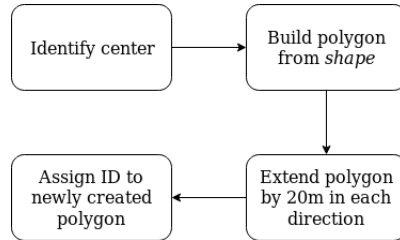


**Figure 2.3:** Junction modeling process

Figure 2.4 shows the results of the above-mentioned process executed on six different junctions. The red polygon is the polygon defined by the *shape* attribute in the JSON definition of a junction, while the yellow rectangle is the bounding box. Each vehicle knows whether it is inside a junction based on its coordinates. A vehicle is inside a junction only if its coordinates are inside of one of the bounding boxes.

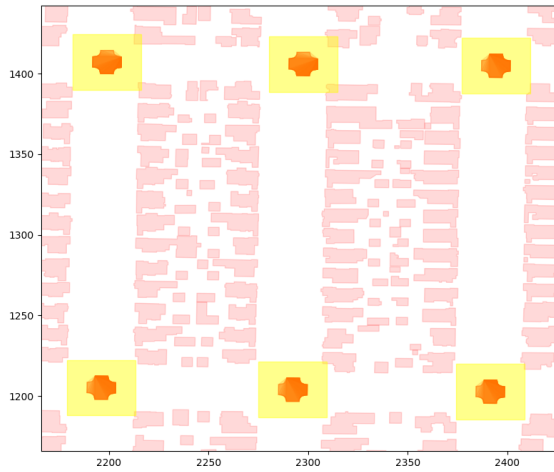


**Figure 2.4:** Example of 6 junctions in an urban scenario

# Chapter 3

## Fast-Broadcast

Fast-Broadcast [20] is a multi-hop routing protocol for vehicular communication. Its main feature consists in breaking the assumption that all vehicles should know, *a priori*, their fixed and constant transmission range. This assumption is often unreasonable, especially in VANETs and urban environments, where electromagnetic interferences and obstacles such as buildings heavily influence the transmission range.

Fast-Broadcast employs two different phases:

1. the **Estimation Phase**, during which vehicles estimate their frontward and backward transmission range;
2. the **Broadcasts Phase**, during which a vehicle sends an Alert Message and the other cars need to forward it in order to propagate the information.

### 3.1 Estimation Phase

During this phase, vehicles try to estimate their frontward and backward transmission range by the means of Hello Messages. These beacons are sent periodically via broadcast to all the neighbors of a vehicle.

Time is divided into turns and, in order to keep estimations fresh, data collected during a certain turn is kept for the duration of the next turn, then discarded. The parameter *turnSize* specifies the duration of a turn: the authors suggest a duration of one second. A bigger *turnSize* could guarantee less collisions to the detriment of freshness of information. On the other hand, the effects of a smaller *turnSize* are specular to those just presented.

Using this approach, vehicles can estimate two different values:

- \* *Current-turn Maximum Front Range (CMFR)*, which estimates the maximum frontward distance from which another car can be heard by the considered one;
- \* *Current-turn Maximum Back Range (CMBR)*, which estimates the maximum backward distance at which the considered car can be heard.

When the turn expires, the value of these variables is stored in the *LMFR* and *LMBR* variables (*Latest-turn Maximum Front Range* and *Latest-turn Maximum Back Range*, respectively). The algorithm uses both last turn and current turn data because the former guarantees values calculated with a larger pool of Hello Messages, while the latter considers fresher information.

When sending a Hello Message (Algorithm 1), the vehicle initially waits for a random time between 0 and *turnSize*. After this, if it has not heard another Hello Message or a collision, it proceeds to transmit a Hello Message containing the estimation of its frontward transmission range.

When receiving a Hello Message (Algorithm 2), the vehicle retrieves its position and the sender's position, calculates the distance between these two positions and then updates the CMFR field if the message comes from ahead, otherwise CMBR is updated. The new value is obtained as the maximum between the old CMFR or CMBR value, the distance between the vehicle and the sender, and the sender's transmission range estimation included in the Hello Message.

---

**Algorithm 1** Hello message sending procedure for 1D

---

```

1: for each turn do
2:   sendingTime  $\leftarrow$  random(turnSize)
3:   wait(sendingTime)
4:   if  $\neg$  (heardHelloMsg()  $\vee$  heardCollision()) then
5:     helloMsg.declaredMaxRange  $\leftarrow$  max(LMFR, CMFR)
6:     helloMsg.senderPosition  $\leftarrow$  retrievePosition()
7:     transmit(helloMsg)
8:   end if
9: end for
```

---



---

**Algorithm 2** Hello message receiving procedure for 1D

---

```

1: myPosition  $\leftarrow$  retrievePosition()
2: senderPosition  $\leftarrow$  helloMsg.senderPosition
3: declaredMaxRange  $\leftarrow$  helloMsg.declaredMaxRange
4: d  $\leftarrow$  distance(myPosition, senderPosition)
5: if receivedFromFront(helloMsg) then
6:   CMFR  $\leftarrow$  max(CMFR, d, declaredMaxRange)
7: else
8:   CMBR  $\leftarrow$  max(CMBR, d, declaredMaxRange)
9: end if
```

---

### 3.2 Broadcast Phase

This phase is activated once a vehicle sends an Alert Message. The other cars can exploit the estimation of transmission ranges to reduce redundancy in message broadcast. Each vehicle can exploit this information to assign itself a forwarding priority inversely proportional to the relative distance: the higher the relative distance, the higher the priority.

When the Broadcast Phase is activated, a vehicle sends an Alert Message with application specific data. Broadcast specific data is also piggybacked on the Alert Message, such as:

- \* *MaxRange*: the maximum range a transmission is expected to travel backward before the signal becomes too weak to be received. This value is utilized by following vehicles to rank their forwarding priority;
- \* *SenderPosition*: the coordinates of the sender.

Upon reception, each vehicle waits for a random time called *Contention Window* (*CW*). This window ranges from a minimum value (*CWMin*) and a maximum one (*CWMax*) depending on sending/forwarding car distance (*Distance*) and on the estimated transmission range (*MaxRange*), according to formula 3.1. It is quite easy to see that the higher the sender/forwarder distance is, the lower the contention window is.

$$\left\lfloor \left( \frac{\text{MaxRange} - \text{Distance}}{\text{MaxRange}} \times (\text{CWMax} - \text{CWMin}) \right) + \text{CWmin} \right\rfloor \quad (3.1)$$

If another forwarding of the same message coming from behind is heard during waiting time, the vehicle suppresses its transmission because the message has already been forwarded by another vehicle farther back in the column. On the contrary, if the same message is heard coming from the front, the procedure is restarted using the new parameters. The vehicle can forward the message only if the waiting time expires without having received the same message.

Algorithm 3 and 4 describe the logic behind the Broadcast Phase.

---

**Algorithm 3** Alert Message generation procedure for 1D

---

```

1: alertMsg.maxRange ← max(LMBR, CMBR)
2: alertMsg.position ← retrievePosition()
3: transmit(alertMsg)

```

---



---

**Algorithm 4** Alert Message forwarding procedure for 1D

---

```

1: cwnd ← computeCwnd()
2: waitTime ← random(cwnd)
3: wait(waitTime)
4: if sameBroadcastHeardFromBack() then
5:   exit()
6: else if sameBroadcastHeardFromFront() then
7:   restartBroadcastProcedure()
8: else
9:   alertMsg.maxRange ← max(LMBR, CMBR)
10:  alertMsg.senderPosition ← retrievePosition()
11:  transmit(alertMsg)
12: end if

```

---

### 3.3 Multiple dimensions extension

The original work [20] considered only a strip-shaped road, where it was easy to define directions and establish when a message came from the front or the back. In [30] an extension considering two dimensions was proposed. This work proposes a modification to that version, since it caused some delivery problems in particular scenarios. This section will firstly present the original extension of [30] and then discuss the proposed modification.

The modifications to the Fast-Broadcast algorithm are the following:

- Utilizing only one parameter between CMBR and CMFR (thus considering only CMR):

2. Including the position of the vehicle which originally generated the Alert Message in addition to the position of the sender of the message.

When a vehicle receives an Alert Message, the origin-vehicle distance is confronted with the origin-sender distance: the vehicle can forward the message only if the former is greater than or equal to the latter, otherwise it simply discards the message.



**Figure 3.1:** Example of Fast-Broadcast in 2D scenario

For example, suppose that vehicle A is the origin of the Alert Message and B receives it, but C doesn't due to an obstacle in the line of sight. B computes origin-vehicle distance,  $d(A, B)$ , and origin-sender distance,  $d(A, A)$ , which in this case are respectively 120 and 0m. Since origin-vehicle is greater than origin-sender, B can forward the Alert Message.

Now suppose that C receives the message from B. C computes origin-vehicle distance,  $d(A, C)$ , and origin-sender distance,  $d(A, B)$ , which amount to 70 and 120m respectively. Since the former is not greater than or equal to the latter, C is not a candidate for forwarding and suppresses the transmission.

D receives the message from B as well. D is a good candidate for transmission since the origin-vehicle distance, which amounts to 180m, is greater than origin-sender distance, equal to 120m.

However, the condition by which vehicles suppressed their transmission when the origin-sender distance was smaller than the origin-sender distance causes delivery

problems in particular scenarios, reported in Appendix TODO

. Hence, that condition has been dropped in the algorithm implemented in this work. Referring to the example in Figure 3.1, this change makes vehicle C a forwarder candidate as well.

Algorithm 5, 6, 7 and 8 show the implementation for Fast-Broadcast for multiple dimensions (mainly 2D, but this version actually works also for 3D scenario, for example scenarios with only drones or with drones and vehicles).

---

**Algorithm 5** Hello message sending procedure for 2D

---

```

1: for each turn do
2:   sendingTime  $\leftarrow$  random(turnSize)
3:   wait(sendingTime)
4:   if  $\neg$  (heardHelloMsg()  $\vee$  heardCollision()) then
5:     helloMsg.declaredMaxRange  $\leftarrow$  max(LMR, CMR)
6:     helloMsg.senderPosition  $\leftarrow$  retrievePosition()
7:     transmit(helloMsg)
8:   end if
9: end for
```

---



---

**Algorithm 6** Hello message receiving procedure for 2D

---

```

1: myPosition  $\leftarrow$  retrievePosition()
2: senderPosition  $\leftarrow$  helloMsg.senderPosition
3: declaredMaxRange  $\leftarrow$  helloMsg.declaredMaxRange
4: d  $\leftarrow$  distance(myPosition, senderPosition)
5: CMR  $\leftarrow$  max(CMR, d, declaredMaxRange)
```

---



---

**Algorithm 7** Alert Message generation procedure for 2D

---

```

1: alertMsg.maxRange  $\leftarrow$  max(LMR, CMR)
2: alertMsg.senderPosition  $\leftarrow$  retrievePosition()
3: alertMsg.originPosition  $\leftarrow$  retrievePosition()
4: transmit(alertMsg)
```

---



---

**Algorithm 8** Alert Message forwarding procedure for 2D

---

```

1: cwnd  $\leftarrow$  computeCwnd()
2: waitTime  $\leftarrow$  random(cwnd)
3: wait(waitTime)
4: if sameBroadcastHeardFromBack() then
5:   exit()
6: else if sameBroadcastHeardFromFront() then
7:   restartBroadcastProcedure()
8: else
9:   alertMsg.maxRange  $\leftarrow$  max(LMR, CMR)
10:  alertMsg.senderPosition  $\leftarrow$  retrievePosition()
11:  transmit(alertMsg)
12: end if
```

---

### 3.3.1 Hello Message Header Structure

The Hello Message header structure is represented in Figure 3.2.

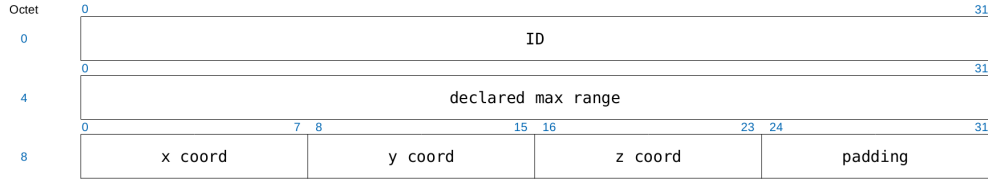


**Figure 3.2:** Fast-Broadcast Hello Message header structure

The fields contained in the Hello Message are the following:

- \* *ID*: unique ID of the Hello Message's sender;
- \* *declared max range*: maximum range detected by the vehicle during Estimation Phase;
- \* *x coord*, *y coord* and *z coord*: coordinates of the Hello Message's sender.

### 3.3.2 Alert Message Header Structure

The Alert Message header structure is represented in Figure 3.3.

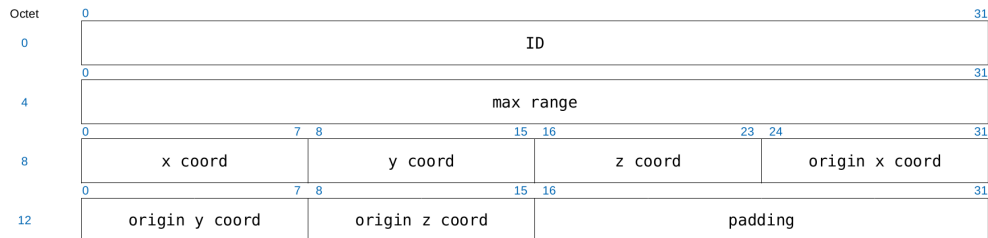


**Figure 3.3:** Fast-Broadcast Alert Message header structure

The fields contained in the Alert Message are the following:

- \* *ID*: unique ID of the Alert Message's sender;
- \* *max range*: maximum range detected by the vehicle during Estimation Phase;
- \* *x coord*, *y coord* and *z coord*: coordinates of the Hello Message's sender;
- \* *origin x*, *origin y* and *origin z coord*: coordinates where the Alert initially originated from.

## 3.4 Smart Junction Fast-Broadcast (SJ-Fast-Broadcast)

This work proposes an extension for Fast-Broadcast which keeps junctions into consideration in order to achieve a greater delivery ratio of Alert Messages. The idea comes from the following observation: whenever buildings block signal propagation

across different roads, the message is relayed only through the road segments inside the forwarder's field of view. This causes the Alert Message propagation to spread:

- \* in one direction, if the forwarder is not inside a junction and the road segment is surrounded by buildings which block the signal;
- \* in three directions, whenever the forwarder lies inside a junction.

Actually the signal travels respectively in two and four directions, but we are not considering the direction where the previous Alert Message is coming from (i.e. we are only considering forwarding towards previously uncovered areas in this analysis). Referring to Figure 3.4, if the message is coming from the top and A and B forwards it, then only vehicles in the north-south road will be reached. Vehicles on the west-east road will be reached by the Alert Message at a later point, if the propagation circles back to them through another road, otherwise they will never be informed about the alert. If C is also forced to forward, then we have coverage across all road segments and the propagation can continue towards all directions. Figure 3.5 shows an example where SJ-Fast-Broadcast is employed and a greater coverage is achieved.



**Figure 3.4:** Usual Fast-Broadcast Alert Message propagation

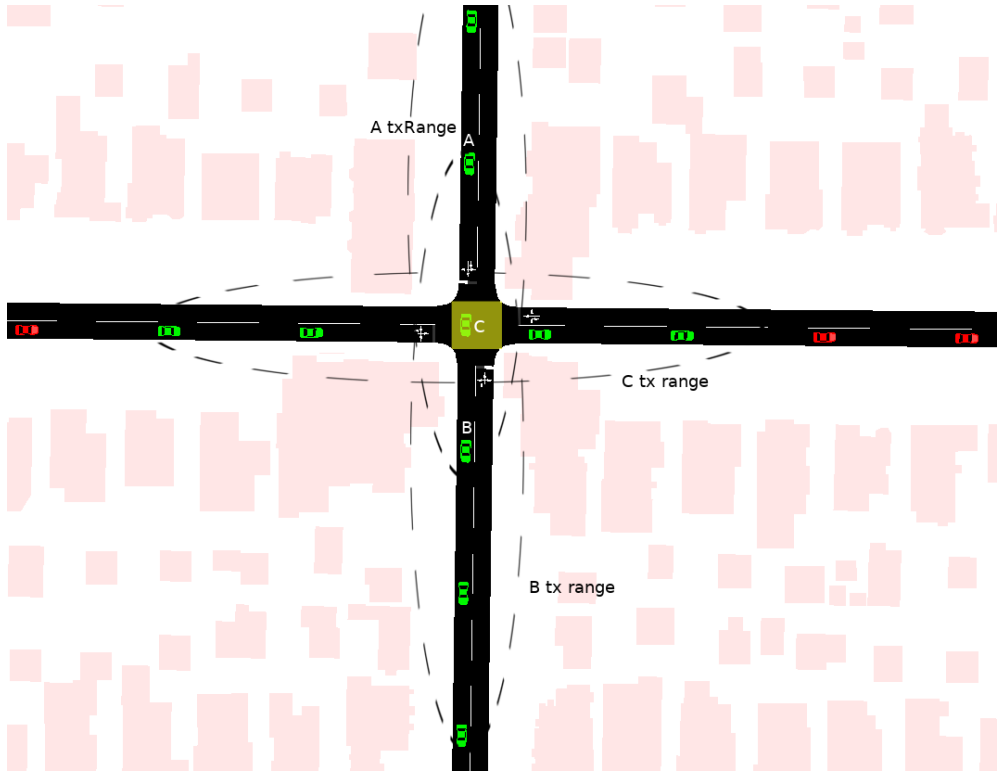


**Figure 3.5:** SJ-Fast-Broadcast Alert Message propagation

The proposed extension works by having nodes inside a junction participate in a second contention with all other vehicles inside the same junction. When the original timer calculated by Fast-Broadcast expires for one of the vehicles inside the junction, it forwards the message. All other vehicles inside the same junction suppress their transmission. This way the propagation can proceed in all directions, while the propagation in the normal direction can proceed without additional delays. Algorithm 9 and 10 show the code for SJ-Fast-Broadcast's Broadcast Phase. Estimation Phase's algorithms remain the same as Algorithm 5 and 6. Line 4 of Algorithm 10 shows that a vehicle suppresses its transmission in one of the following two cases:

- \* if the vehicle has heard the same broadcast coming from the back and is not inside a junction;
- \* if the vehicle has heard the same broadcast coming from the back, is inside a junction with ID  $j$  and the sender is also inside the same junction.

---

**Algorithm 9** SJ-Fast-Broadcast Alert Message generation procedure

---

```

1: alertMsg.maxRange  $\leftarrow \max(\text{LMR}, \text{CMR})$ 
2: alertMsg.senderPosition  $\leftarrow \text{retrievePosition}()$ 
3: alertMsg.originPosition  $\leftarrow \text{retrievePosition}()$ 
4: alertMsg.senderInJunction  $\leftarrow \text{isSenderInJunction}()$ 
5: alertMsg.junctionId  $\leftarrow \text{getJunctionId}()$ 
6: transmit(alertMsg)

```

---

**Algorithm 10** SJ-Fast-Broadcast Alert Message forwarding procedure

---

```

1: cwnd ← computeCwnd()
2: waitTime ← random(cwnd)
3: wait(waitTime)
4: if (sameBroadcastHeardFromBack() ∧ vehicleNotInJunction()) ∨ (sameBroadcastHeardFromBack() ∧ vehicleInJunction(j) ∧ alertMsg.senderInJunction ∧ alertMsg.junctionId == j) then
5:   exit()
6: else if sameBroadcastHeardFromFront() then
7:   restartBroadcastProcedure()
8: else
9:   alertMsg.maxRange ← max(LMBR, CMBR)
10:  alertMsg.senderPosition ← retrievePosition()
11:  transmit(alertMsg)
12: end if

```

---

**3.4.1 Alert Message Header Structure**

The Hello Message header structure is the same as Figure 3.2, hence it is not reported here. The Alert Message header structure is represented in Figure 3.6.

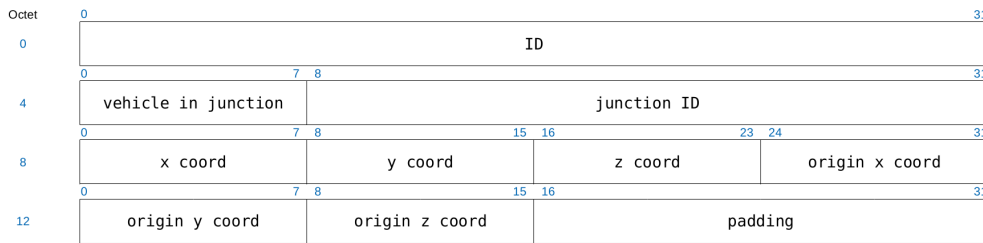


**Figure 3.6:** SJ-Fast-Broadcast Alert Message header structure

The additional fields are the following:

- \* *vehicle in junction*: whether the vehicle which is send this Alert Message is inside a junction;
- \* *junction ID*: the ID of the junction the sender is inside.



# Chapter 4

## ROFF

RObust and Fast Forwarding scheme (ROFF) is a protocol proposed by Hongseok Yoo and Dongkyun Kim in [21]. This chapter will present the two main problems tackled by ROFF already introduced in Section 1.1, namely the perfect suppression of redundant transmissions, which will be explained in 4.1.1 , and the disuniformity and the costant change in spatial vehicle distribution in VANETs, addressed in section 4.1.2.

### 4.1 Forwarder Selection Problem

#### 4.1.1 Collision Analysis

The first problem tackled by ROFF concerns collisions caused by nodes who start to transmit at the same time. This results in a collision in the area resulting from the intersection of the nodes' transmission ranges.

Suppose that  $S_f = \{f_i | 0 < i \leq N, i \in \mathbb{N}\}$  is the set of PFCs ordered in ascending order by the distance between the previous forwarder and the PFC, where  $N$  is the number of PFCs and  $f_n$  is the FFC. We define  $f_0$  as the previous forwarder. Based on the most common idea in existing protocols, ideally a PFC  $f_i$  suppresses its scheduled transmission whenever it receives the transmission from  $f_N$ . In order to achieve suppression, vehicles from  $f_i$  to  $f_i - 1$  should wait until they receive the transmission from  $f_N$  before forwarding. If a vehicle forwards the message before having received the transmission from  $f_N$ , then a collision will occur. As stated in Section 1.1, existing protocols employ a strategy for waiting time assignment by which each PFC calculates its waiting time based on the distance between itself and the previous forwarder (that is  $distance = d_{f_i, f_0}$ ). As a consequence, successful suppression of all PFCs ( $f_1$  to  $f_{N-1}$ ,  $f_{N-1}$  included) can be achieved only if the timer of  $f_{N-1}$  is long enough to detect the transmission from  $f_N$ . The authors define  $minDiff$  as the minimum time difference between  $f_N$  and  $f_{N-1}$  to prevent  $f_{N-1}$  from forwarding.

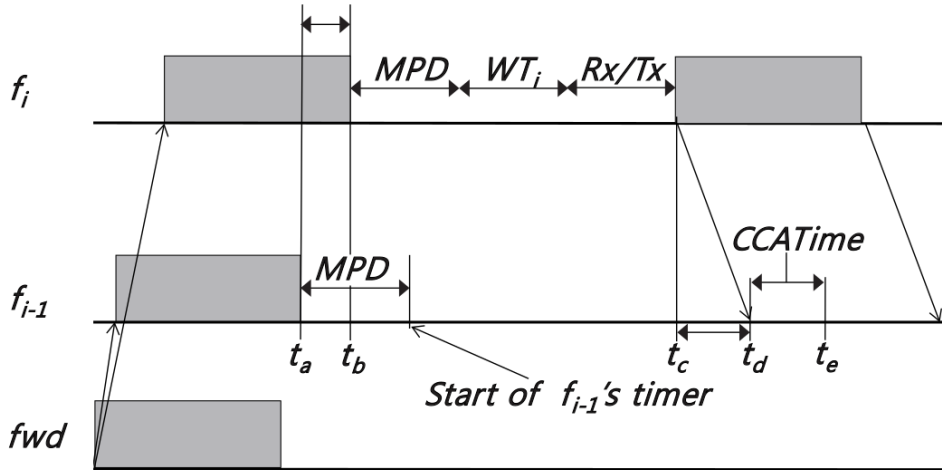


**Figure 4.1:** Definition of  $minDiff$  between  $f_N$  and  $f_{N-1}$  ([21])

Figure 4.1 depicts a situation where  $fwd$  is the forwarder and  $f_i$  (farther from  $fwd$  than  $f_{i-1}$ ) relays the message before  $f_{i-1}$ . The two vehicles  $f_i$  and  $f_{i-1}$  complete receiving the message at different times ( $t_a$  and  $t_b$ ) due to propagation delay (calculated as  $pd = d/s$ , where  $d$  is the distance between two points in space and  $s$  is the wave propagation speed of the medium, i.e.  $s = c$ , the speed of light, in wireless communication). After reception we have additional amount of time in order to process and retransmit the message:

- \* each PFC spends MAC Processing Delay (MPD) to process the message and then waits for  $WT_i$  calculated according to whichever multi-hop algorithm is being used. As explained previously, this waiting time is inversely proportional to the distance between the PFC and  $fwd$ ;
- \* after timer expiration, each PFC wait for Rx/Tx turnaround time ( $Rx/Tx$ ), in order to switch their interface from reception to transmission mode.

After  $f_i$  has forwarded the message,  $f_{i-1}$  starts receiving it at  $t_d$ ,  $t_d - t_c$  being equal to  $pd_{f_{i-1}, f_i}$ . The time between the PHY module of  $f_{i-1}$  starts reception and the MAC module of the same vehicle is aware of reception is called  $CCATime$ . Hence, if  $f_{i-1}$ 's timer expires between  $t_a$  and  $t_e$ ,  $f_{i-1}$ 's transmission will collide with  $f_i$ 's. In order to accomplish successful suppression,  $f_{i-1}$ 's timer should not expire before  $t_e$ .

Given the fact that propagation delay is not controllable and MPD,  $Rx/Tx$  and  $CCATime$  are usually standard-defined parameters, an algorithm can only manage the difference between waiting times of  $f_i$  and  $f_{i-1}$  (represented by  $WT_i$  and  $WT_{i-1}$  respectively in the following formula). To achieve successful suppression,  $f_{i-1}$  should wait until the forwarding from  $f_i$  is detected by  $f_{i-1}$ 's MAC layer, so  $MPD + WT_{i-1}$  should be greater than  $t_e - t_a$ . Hence, the formula for  $minDiff$  is the following:

$$minDiff = (pd_{fwd, f_i} - pd_{fwd, f_{i-1}}) + pd_{f_i, f_{i-1}} + Rx/Tx + CCATime \quad (4.1)$$

#### 4.1.2 Latency Analysis

The second problem ROFF tries to overcome is the effect of empty space in vehicle distribution on forwarding latency.

The region where PFCs are placed can be defined as *naive forwarding area* (NFA) and is defined as the intersection between:

- \* the transmission range of a forwarder  $fwd$ ;
- \* the area in the opposite movement direction of the same forwarder  $fwd$ .

The distribution of vehicle inside NFA can vary in time; moreover, vehicles are not usually placed at the same distance, so empty spaces of various sizes exist inside the area.

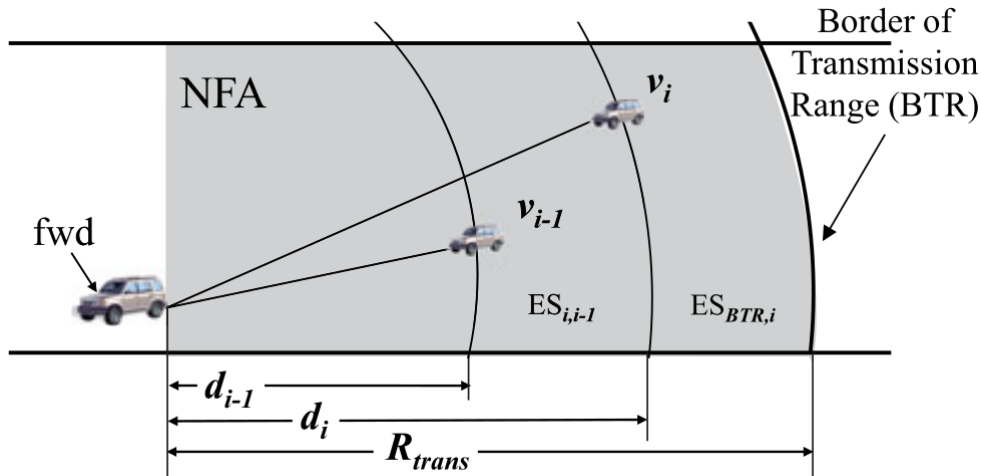


**Figure 4.2:** Definition of empty space ([21])

Suppose that  $S_v = \{v_i | 0 < i \leq M\}$  is a set of  $M$  vehicles inside NFA with vehicles ordered by distance between the vehicle and the previous forwarder in ascending order. Referring to Figure 4.2, the empty space  $ES_{i,i-1}$  between  $v_i$  and  $v_{i-1}$  is the segment within the two circles centered in  $fwd$  with radius  $d_{i-1}$  and  $d_i$  respectively. Hence, the size of  $ES_{i,i-1}$  is equal to  $d_i - d_{i-1}$ .

Large empty spaces have a negative effect on forwarding latency. There is no guarantee that the farthest vehicle from the previous forwarder become the FFC: lossy channel environments, shadowing and other phenomena can make any vehicle within NFA become the forwarder. Suppose that  $fwd$  is the previous forwarder and there are two vehicles,  $A$  and  $B$ , inside NFA where  $A$  is farther from  $fwd$  than  $B$ ,  $A$  has not received the transmission from  $fwd$  while  $B$  has. The empty space  $ES_{A,B}$  between  $A$  and  $B$  influences the forwarding latency:

- \* if  $ES_{A,B}$  is small,  $B$  relays the message after a short waiting time;
- \* if  $ES_{A,B}$  is large,  $B$  waits needlessly (since there is no other vehicle farther from  $fwd$  which has received the message) a large amount of time.

ROFF aims at resolving the effect of empty spaces by allowing vehicles to choose waiting time inversely proportional to their *unique forwarding priority* proportional to the distance between the vehicle and the previous forwarder, instead of using directly such distance in the waiting time computation.

## 4.2 ROFF Algorithm

The ROFF algorithm works under the following two assumptions:

1. each vehicle has access to a GPS system and a digital map;
2. vehicles periodically (e.g. every 100 milliseconds) broadcast a Hello message containing various information, such as its position, velocity, etc. The period between each Hello message broadcast is called *Beacon Interval*.

The algorithm is composed of three components, as depicted in Figure 4.3.

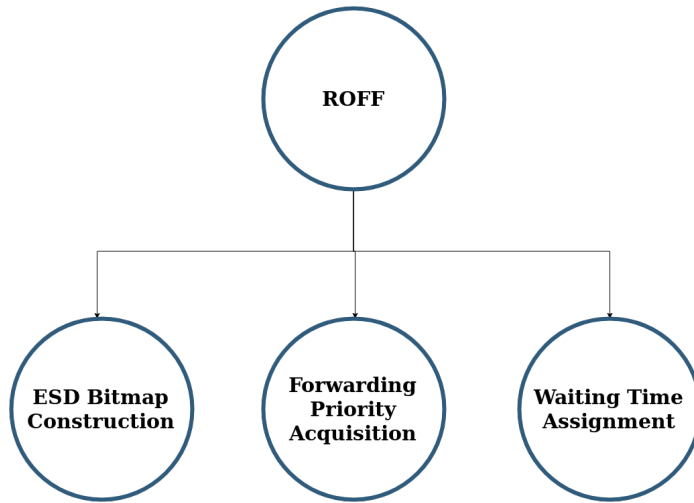


**Figure 4.3:** Components of ROFF algorithm

The algorithm in short works as follows (additional information will be given in the following sections):

- \* when a forwarder relays an Alert Message, it also broadcasts a special structure called ESD Bitmap which describe the empty space distribution within the forwarders' NFA;
- \* PFCs which receive the Alert Message and the ESD Bitmap decide whether they are eligible for contention based on the ESD Bitmap;
- \* Eligible PFCs contend by choosing different waiting times based on a unique forwarding priority.

### 4.2.1 ESD Bitmap Construction

Upon Hello Message reception, each vehicle uses the data within the message in order to update and maintain a structure called Neighbor Table (NBT) which monitors its local view (i.e. all the vehicles in the neighborhood of said vehicle). Each entry of the NBT contains:

- \* the ID of the neighbor;
- \* the position of the neighbor;

- \* the reception time of the Hello Message to verify the freshness of information and remove outdated entries.

An example of Neighbor Table of node with ID 0 is represented in Picture 4.4.

ID	Position	Reception time
1	(150, 120, 0)	13:25:31
2	(130, 145, 0)	13:25:32
3	(180, 200, 0)	13:25:31

**Figure 4.4:** Example of Neighbor Table of node with ID 0

Thanks to the NBT, the forwarder can advertise its neighborhood to other vehicles. We can define the set of neighbors detected by the forwarder as its *local view*. If a vehicle who receives an Alert Message is not present inside the local view of the forwarder, then that vehicle cannot participate in contention.

The NBT could be piggybacked as-is on the Alert Message, but the authors of ROFF identified some problems with this solution, such as the great overhead caused by the size of IDs. Hence, the proposed solution consists in compressing the NBT in a bitmap-like structure called ESD Bitmap.

In order to build the ESD Bitmap, first of all the forwarder measures the distance between itself and each of its neighbors listed in the NBT. Due to GPS granularity, distances are expressed at meter-level and can be represented with non-negative integers.

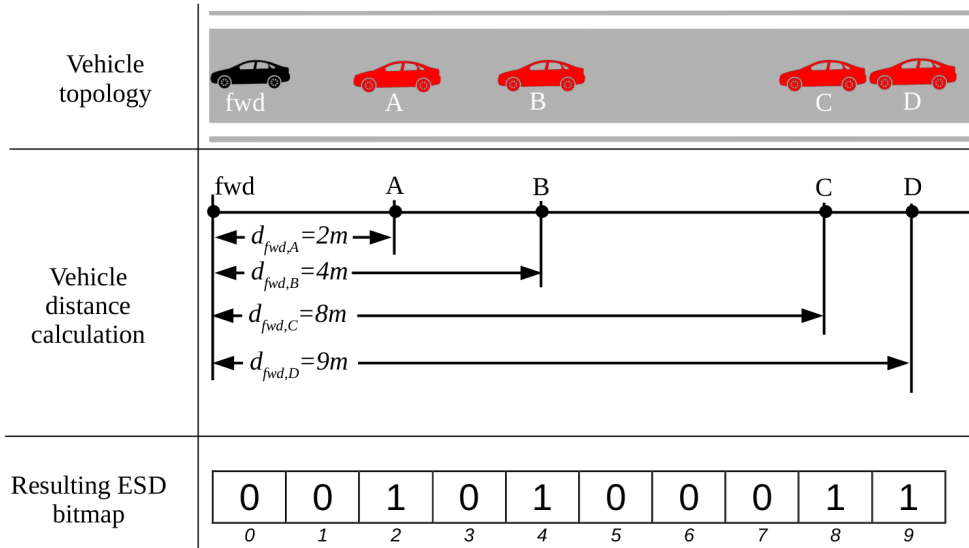


**Figure 4.5:** ESD Bitmap construction with  $k = 1$

After distance measurement, *fwd* builds a bitmap to represent the measured distances by setting the  $i$ -th bit to either:

- \* 1 if there is a PFC distant  $d$  from *fwd* such that  $k * i \leq d \leq k * (i + 1) - 1$ ;

\* 0 otherwise.

The parameter  $k$ , called *distance range*, identifies how many distances can be identified by the same bit in the ESD Bitmap. This parameter can be controlled to manage the compression level and the accuracy of the Bitmap. Increasing  $k$  decreases the number of bits of the Bitmap, but every bit will identify  $k$  different distances, hence losing precision. Picture 4.5 shows the construction of an ESD Bitmap using  $k = 1$ .

An ESD Bitmap using  $k = 2$  is show in Figure 4.6. It is possible to see that the bit in position 4 represents distances  $d$  such that  $8 \leq d \leq 9$ .

<b>0</b>	<b>1</b>	<b>1</b>	<b>0</b>	<b>1</b>
0	1	2	3	4

**Figure 4.6:** Resulting ESD Bitmap with  $k = 2$

#### 4.2.2 Forwarding Priority Acquisition

Whenever a PFC  $f_i$  receives the Alert Message with included the ESD Bitmap from  $fwd$ , it checks whether the distance between itself and the previous forwarder is listed inside the bitmap (i.e.  $f_i$  checks whether the bit in position  $d(fwd, f_i)$  in the bitmap is equal to 1, assuming  $k = 1$ ). If so,  $f_i$  can participate in contention since it is inside the *local view* of  $fwd$ . Otherwise, is cannot participate in contention to forward the Alert Message.

After  $f_i$  has entered contention, it can calculate its own forwarding priority based on the distances express by the ESD Bitmap. These distances are the distances of every other PFC which can participate in contention. Assuming that  $L_{dist}$  is the list of distances ordered in ascending order and  $distance = d(fwd, f_i)$ ,  $f_i$ 's forwarding priority is set as the rank of  $distance$  inside  $L_{dist}$ . This way PFCs that are farther away from  $fwd$  are assigned a higher forwarding priority, while PFCs nearer  $fwd$  are assigned a lower forwarding priority.

ROFF avoids assigning the same priority to two different PFCs by a technique called *ID-based contention*. Using this technique, whenever a PFC  $f_i$  receives an Alert Message it checks whether its NBT contains another vehicle  $f_j$  whose distance from  $fwd$  is the same as  $f_i$ 's (hence the distance is identified by the same bit in the bitmap). If so,  $f_i$  participates in contention only if its ID is higher than the ID of  $f_j$ . In other words, if inside  $f_i$ 's NBT there exists an entry for  $f_j$  such that  $d(fwd, f_i) = d(fwd, f_j)$  and  $ID_{f_j} > ID_{f_i}$ , then  $f_i$  defers its transmission. Figure 4.7 depicts a scenario where node A does not participate in contention due to ID-based contention.

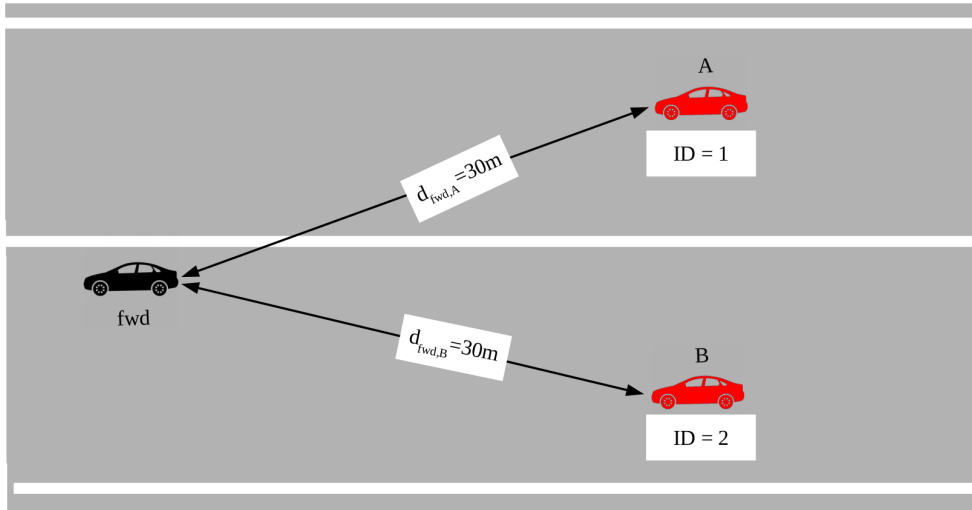


**Figure 4.7:** ID-based contention: node A defers its transmission

#### 4.2.3 Waiting Time Assignment

Once forwarding priorities are determined, ROFF assigns a waiting time to each vehicle that is inversely proportional to the priority. Letting  $PFC(i)$  be the PFC with forwarding priority  $i$  and  $WT_p$  the waiting time of PFC  $p$ , in order to achieve successful suppression of transmission by  $PFC(i-1)$ , the waiting time of  $PFC(i-1)$  should be at least longer by  $\text{minDiff}_{PFC(i),PFC(i-1)}$  than waiting time of  $PFC(i)$  (i.e.  $WT_{PFC(i-1)} \geq WT_{PFC(i)} + \text{minDiff}_{PFC(i),PFC(i-1)}$ ). Hence, the waiting time of  $PFC(k)$  is the sum of  $\text{minDiffs}$  (calculated using Equation 4.1) between PFCs with forwarding priorities lower than  $k$ , as shown in Equation 4.2. PFC with top priority (being equal to 1) broadcasts immediately and does not have to wait any time.

$$WT_{PFC(k)} = \sum_{i=2}^k \text{minDiff}_{PFC(i),PFC(i-1)} \quad (k \geq 2) \quad (4.2)$$

Figure 4.8 shows the application of 4.2 in the scenario represented in Figure 4.5.

PFC	Priority	Waiting time
D	1	0
C	2	$\text{minDiff}(C, D)$
B	3	$\text{minDiff}(B, C) + \text{minDiff}(C, D)$
A	4	$\text{minDiff}(A, B) + \text{minDiff}(B, C) + \text{minDiff}(C, D)$

**Figure 4.8:** Waiting time assignment based on vehicle distribution depicted in Figure 4.5

When calculating  $minDiff$  as explained in Section 4.1.1, , MPD, Rx/Tx and CCATime are fixed system parameters; the only variables are propagation delays between vehicles, which are dependent on distance. Since coordinates are not included in the ESD Bitmap (only distances are), each PFC needs to identify the coordinates of the previous forwarder's neighbors. In other words, whenever a PFC  $f_i$  receives the ESD Bitmap from  $fwd$  and calculates its own waiting time, it checks for each distance  $dist$  in  $L_{dist}$  whether there is a vehicle  $f_j$  distant  $dist$  from  $fwd$  (i.e.  $d(fwd, f_j) = dist$ ). If such vehicle exists, then  $f_i$  uses  $f_j$  coordinates in the propagation delay (hence  $minDiff$ ) calculation, otherwise it disregards  $dist$  in the computation since possibly there is no vehicle distant  $dist$  from  $fwd$  in  $f_i$ 's local view.

### 4.3 Multiple dimensions extension

In the original work [21], ROFF has been implemented in the network simulator ns-2. Since retrieval of the original code has proven to be impossible, part of this thesis concerned the implementation of ROFF in ns-3. Moreover, the original article focuses only on 1D message propagation along a strip-shaped area. This work proposes a 2D and 3D extension of ROFF based on the idea of Fast-Broadcast presented in Section 3.3. The main addition to the original algorithms consists in the suppression of scheduled transmissions only when an Alert Message is heard coming from a vehicle farther from the initial sender than the current vehicle. More in detail, if  $fwd$  is the origin of the Alert Message,  $A$  is the previous forwarder and  $B$  is a PFC with a scheduled transmission.  $B$  will suppress its transmission only if it hears an Alert Message coming from  $D$  such that  $d_{fwd,D} > d_{fwd,B}$ . Algorithm 11, 12, 13 and 14 show ROFF's phases in detail.

---

**Algorithm 11** Hello message sending procedure for 2D

---

```

1: for each beaconInterval do
2:   helloMsg.ID ← retrieveID()
3:   helloMsg.senderPosition ← retrievePosition()
4:   transmit(helloMsg)
5: end for
```

---



---

**Algorithm 12** Hello message receiving procedure for 2D

---

```

1: id ← helloMsg.ID
2: sp ← helloMsg.senderPosition
3: time ← currentTime()
4: addNBTEEntry(id, sp, time)
```

---



---

**Algorithm 13** Alert Message generation procedure for 2D

---

```

1: esdBitmap ← createEsdBitmap(NBT)
2: alertMsg.esdBitmapSize ← esdBitmap.size
3: alertMsg.esdBitmap ← esdBitmap
4: alertMsg.senderPosition ← retrievePosition()
5: alertMsg.originPosition ← retrievePosition()
6: transmit(alertMsg)
```

---

**Algorithm 14** Alert Message forwarding procedure for 2D

---

```

1: esdBitmap ← alertMsg.esdBitmap
2: if vehicleNotPresentInEsd() ∨ lostIDContention() then
3:   exit()
4: else
5:   listOfDistances ← computeListOfDistances(esdBitmap)
6:   myPosition ← retrievePosition()
7:   senderPosition ← alertMsg.senderPosition
8:   dist ← distance(myPosition, senderPosition)
9:   myRank ← getRank(dist, listOfDistances)
10:  wait ← computeWaitTime(myRank)
11:  if sameBroadcastHeardFromBack() then
12:    exit()
13:  else if sameBroadcastHeardFromFront() then
14:    restartBroadcastProcedure()
15:  else
16:    esdBitmap ← createEsdBitmap(NBT)
17:    alertMsg.esdBitmapSize ← esdBitmap.size
18:    alertMsg.esdBitmap ← esdBitmap
19:    alertMsg.senderPosition ← retrievePosition()
20:    transmit(alertMsg)
21:  end if
22: end if

```

---

**4.3.1 Hello Message Header Structure**

The Hello Message header structure is represented in Figure 4.9.

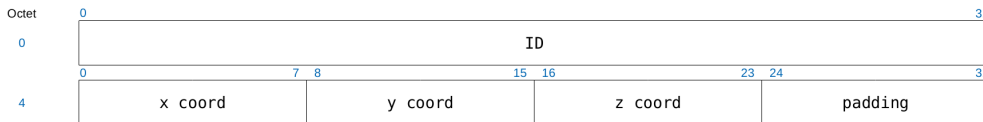


**Figure 4.9:** ROFF Hello Message header structure

The fields contained in the Hello Message are the following:

- \* *ID*: unique ID of the Hello Message's sender;
- \* *x coord*, *y coord* and *z coord*: coordinates of the Hello Message's sender.

**4.3.2 Alert Message Header Structure**

The Alert Message header structure is represented in Figure 4.10.

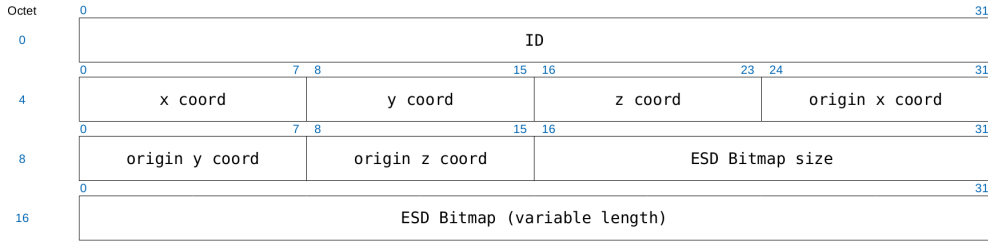


**Figure 4.10:** ROFF Alert Message header structure

The fields contained in the Alert Message are the following:

- \* *ID*: unique ID of the Alert Message's sender (or forwarder);
- \* *x coord*, *y coord* and *z coord*: coordinates of the Alert Message's forwarder;
- \* *origin x*, *origin y* and *origin z coord*: coordinates where the Alert initially originated from;
- \* *ESD Bitmap size*: field which indicates how many bytes the ESD Bitmap occupies;
- \* *ESD Bitmap*: the ESD Bitmap itself, with variable length.

#### 4.4 Smart Junction ROFF (SJ-ROFF)

Since ROFF does not consider junctions in the default algorithm, the proposal explained in Section 3.4 could also bring benefits to it. Hence, we have implemented a Smart Junction variant of ROFF (called SJ-ROFF) following the logic of SJ-Fast-Broadcast. The modifications to the base algorithm are fairly simple: two fields have been added to the Alert Message Header to indicate whether the sender is inside a junction (and the ID of the junction, if it is). Algorithm ?? and 16 show the updated functionalities of Alert Message creation and forwarding. Hello Message algorithms are unchanged.

---

##### Algorithm 15 Alert Message generation procedure for 2D

---

```

1: esdBitmap ← createEsdBitmap(NBT)
2: alertMsg.esdBitmapSize ← esdBitmap.size
3: alertMsg.esdBitmap ← esdBitmap
4: alertMsg.senderPosition ← retrievePosition()
5: alertMsg.originPosition ← retrievePosition()
6: alertMsg.senderInJunction ← isSenderInJunction()
7: alertMsg.junctionId ← getJunctionId()
8: transmit(alertMsg)

```

---

**Algorithm 16** Alert Message forwarding procedure for 2D

---

```

1: esdBitmap ← alertMsg.esdBitmap
2: if vehicleNotPresentInEsd() ∨ lostIDContention() then
3:   exit()
4: else
5:   listOfDistances ← computeListOfDistances(esdBitmap)
6:   myPosition ← retrievePosition()
7:   senderPosition ← alertMsg.senderPosition
8:   dist ← distance(myPosition, senderPosition)
9:   myRank ← getRank(dist, listOfDistances)
10:  wait ← computeWaitTime(myRank)
11:  if (sameBroadcastHeardFromBack() ∧ vehicleNotInJunction()) ∨ (sameBroadcastHeardFromBack() ∧ vehicleInJunction(j) ∧ alertMsg.senderInJunction ∧ alertMsg.junctionId == j) then
12:    exit()
13:  else if sameBroadcastHeardFromFront() then
14:    restartBroadcastProcedure()
15:  else
16:    esdBitmap ← createEsdBitmap(NBT)
17:    alertMsg.esdBitmapSize ← esdBitmap.size
18:    alertMsg.esdBitmap ← esdBitmap
19:    alertMsg.senderPosition ← retrievePosition()
20:    transmit(alertMsg)
21:  end if
22: end if

```

---

#### 4.4.1 Alert Message Header Structure

The Hello Message header structure is the same as Figure 4.9, hence it is not reported here. The Alert Message header structure is represented in Figure 4.11.

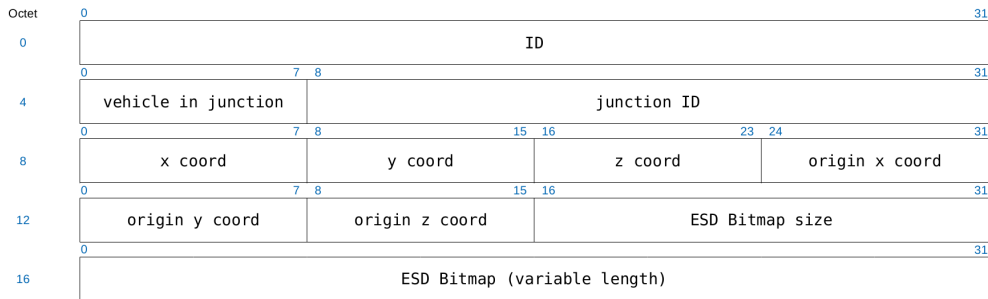


**Figure 4.11:** SJ-ROFF Alert Message header structure

The additional fields are the following:

- \* *vehicle in junction*: whether the vehicle which has forwarded this Alert Message is inside a junction;
- \* *junction ID*: the ID of the junction the sender is inside.



# Chapter 5

## Tools and applications

### 5.1 Network Simulator 3

Network Simulator 3 (ns-3) is a discrete-event network simulator for Internet systems, targeted primarily for research and educational use. ns-3 is free software, licensed under the GNU GPLv2 license, and is publicly available for research, development, and use.

ns-3 development began in 2006 by a team lead by Tom Henderson, George Riley, Sally Floyd and Sumit Roy. Its first version was released on June 30, 2008.

ns-3 is the successor of ns-2, released in 1989. The fact that the former was built from scratch makes it impossible to have backward compatibility. In fact, ns-2 used oTCL scripting language to describe network topologies and C++ to write the core of the simulation. This choice was due to avoid the very time consuming C++ code recompilation, exploiting the interpreted language oTCL. ns-2 mixed the “fast to run, slow to change” C++ with the “slow to run, fast to change” oTCL language. Since compilation time was not an issue with modern computing capabilities, ns-3 developers chose to utilize exclusively C++ code (and optional Python bindings) to develop simulations.

#### 5.1.1 Modules and module structure

ns-3 is composed of various modules, which are groups of classes, examples and tests each related to a certain feature. The components of a module work in a cohesive way in order to offer APIs to other modules and users. Some examples of built-in modules are:

- \* WiFi;
- \* AODV;
- \* CSMA.

The obstacle shadowing propagation loss model and the Fast Broadcast algorithm have been implemented as modules too.

Modules follow a prototypical structure in order to promote clarity and offer built-in documentation. [Figure 5.1](#) shows the typical module structure.

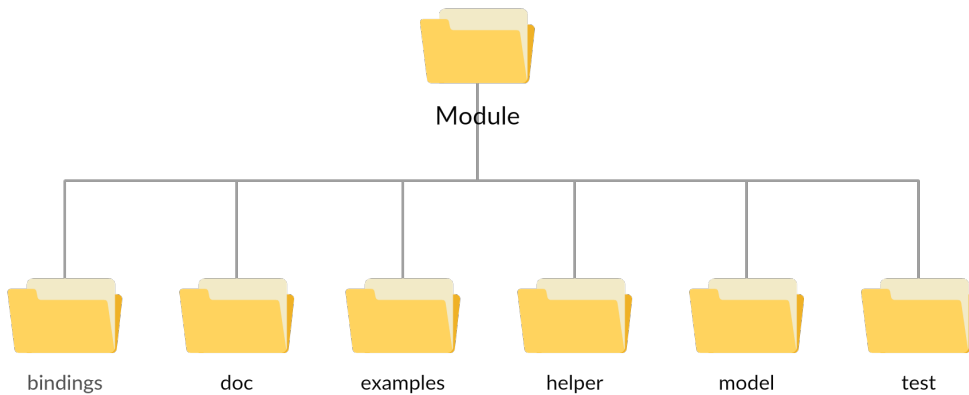


**Figure 5.1:** ns-3 module structure

The following directories can be found inside a module's root directory:

- \* **bindings:** Python bindings used to make the module's API compatible with Python;
- \* **doc:** documentation of the module;
- \* **examples:** examples and proof of concepts of what can be done using the module;
- \* **helper:** higher level APIs to make the module easier to use;
- \* **model:** headers and source files which implement the module's logic;
- \* **test:** test suite and test cases to test the module.

### 5.1.2 Key elements

The element at the base of ns-3 is called *node*, instance of `ns3::Node`. A node can be thought of as a shell of a computer. Various other elements can be added to nodes, such as:

- \* NetDevices (e.g. `NICs`, which enable nodes to communicate over *channels*);
- \* protocols;
- \* applications.

The applications implement the logic of a simulation. For example, the `UdoEchoClientApplication` and `UdpEchoServerApplication` can be used to implement a client/server application which exchange and print the packets' content over the network. The Fast Broadcast protocol has been implemented as an application as well.

The *channels* model various type of transmission media, such as the wired and the wireless ones.

### 5.1.3 Structure of a simulation

A simulation can be implemented in many ways, but in most cases the following steps are executed:

- \* manage command line arguments (e.g. number of nodes to consider in the simulation, transmission range, etc.);
- \* initialize all the necessary fields in classes;
- \* create nodes;
- \* set up physical and MAC layers;
- \* set up link layer, routing protocols and addresses;
- \* configure and install applications on nodes;
- \* position nodes and (optionally) give them a mobility model;
- \* schedule user defined events, such as transmissions of packets;
- \* start the simulation;
- \* collect and manage output data.

### 5.1.4 NetAnim

Netanim is an offline animator tool based on the Qt toolkit. It collects an XML tracefile during the execution of a simulation and can be used to animate the simulation, analyzing packet transmissions and contents.

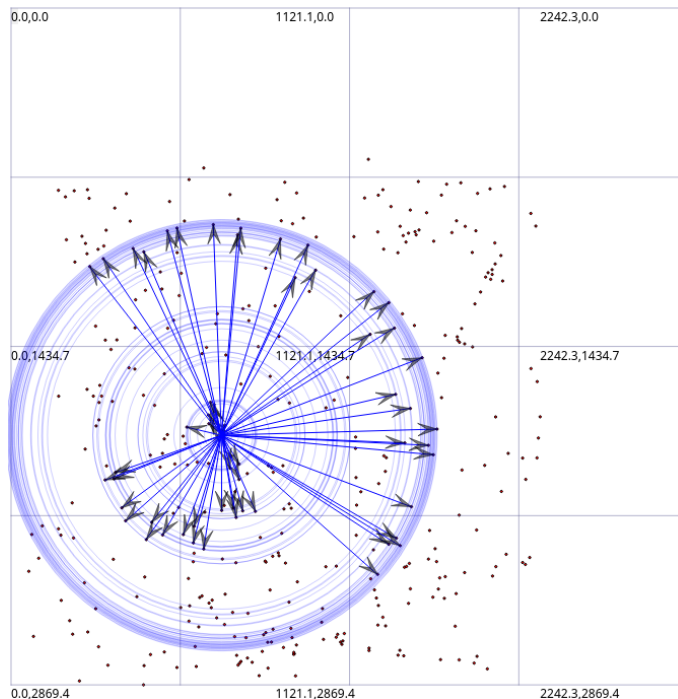


**Figure 5.2:** Packet transmission in NetAnim

## 5.2 Simulation of Urban MObility

Simulation of Urban MObility is an open-source road traffic simulation package. It is written in C++ and licensed under GPLv3.

It offers different tools to analyze and manage real maps from the urban mobility point of view, including pedestrian movement and various types of vehicles.

The original work, starting from real maps obtained from OpenStreetMap (OSM), [19] utilized SUMO to produce two files:

1. a `.poly` file using the SUMO tool *Polyconvert*. This file contains information about all the obstacles, such as buildings, useful for the Obstacle Shadowing module;
2. a `.ns2mobility` file using the SUMO tool *TraceExporter*. This file contains information about the vehicles and their positioning.

The process of generating these two files necessary for ns-3 simulations requires some intermediate steps. The full process is represented in Figure 5.3.

The original work considered a only a distance of 25 meters between vehicles; this work considers various distances, ranging from 15 to 45 meters. Figure 5.4 shows the same scenario (Padua) with different distances between vehicles.

One of the intermediate results, the `.net` file which describes the road infrastructure using a graph resulting from *Netconvert*, has been utilized for junction modeling, as explained in Section 2.2.

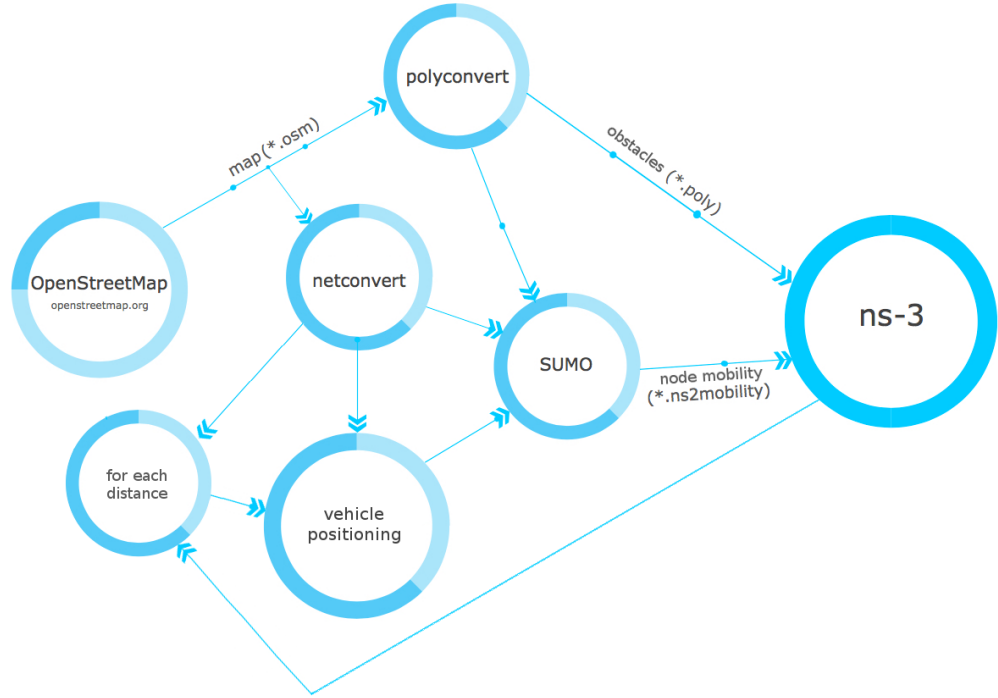


**Figure 5.3:** Steps to generate necessary files using SUMO ([19])



**Figure 5.4:** Padua scenario with vehicle distance equals to 15 meters (top) and 45 meters (bottom)



# Chapter 6

## Simulations

After the protocols under consideration have been presented in Chapters 3 and 4, this Chapter will contain the results of the simulation carried out through various scenario of increasing complexity. Numeric results in every chart will be coupled with their 95% confidence interval.

### 6.1 Metrics

Before proceeding with the presentation of simulation results, metrics used to evaluate the protocol's performances will be presented in this section.

#### 6.1.1 Total Delivery Ratio (TDR)

This metric is used to detect how many vehicles have received the Alert Message in total. Ideally, broadcasting protocols should be able to reach all the reachable nodes in the scenario in order to warn them of the danger. The metric is calculated as follows:

$$TDR = \frac{\text{no. of vehicles successfully receiving the Alert Message}}{\text{no. of vehicles in the scenario}} \quad (6.1)$$

All scenarios are created in a way such that every node can be reached by multi-hop propagation regardless of the source of the Alert Message. In other words, from graph theory point of view, the graph resulting from vehicle distribution where two nodes are connected only if they are within transmission range of each other is a connected graph. This way, the term at the denominator of Equation 6.1 is equivalent to the number of vehicles reachable by pure flooding.

#### 6.1.2 Total Delivery Ratio On Circumference (TDROC)

This metric is used to detect how many vehicles on the circumference have received the Alert Message. The circumference is built starting from the source of the Alert Message. The way it is built depends on scenario topology (e.g. 1D, 2D, etc) and will be explained more thoroughly in the following Sections. The main idea behind the circumference consists in considering only vehicles far from the source of the AM. The metric is calculated as follows:

$$TDROC = \frac{\text{no. of vehicles on circ. successfully receiving the Alert Message}}{\text{no. of vehicles on circ.}} \quad (6.2)$$

The same consideration about vehicles and reachability by pure flooding presented in Section 6.1.1 is also valid for Equation 6.2.

### 6.1.3 Number Of Hops (NOH)

This metric is used to measure the mean number of hops required in order to propagate the Alert Message from the source to all vehicles reached on the circumference. This value is obviously dependent on the paths taken by forwarder Alert Messages from the source to all destinations. We have that  $ONOH$  is always greater than or equal to the *Optimal Number of Hops*  $BNOH$  (i.e.  $ONOH \leq NOH$ ).  $BNOH$  is calculated using the following formula:

$$BNOH = \frac{\text{Circumference Radius}}{\text{Transmission Range}}$$

The Number Of Hops metric can be calculated as:

$$NOH = \frac{\sum_{p \in RC} \text{no. of hops from source to } p}{\text{no. of vehicles on circ}} \quad (6.3)$$

where  $RC$  is the set of vehicles which have successfully received the message on the circumference.

The  $NOH$  metric (whose value should be as close as possible to  $BNOH$ ) is an important indicator of the effectiveness of the multi-hop protocol in choosing the farthest forwarder during contention.

Figure 6.1 can be used as an example to calculate  $NOH$ . Using Equation 6.3, the mean number of hops is equal to 3.

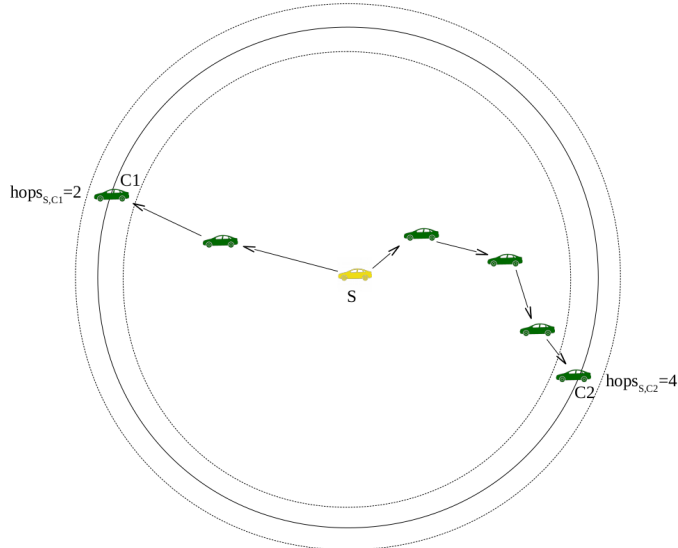


**Figure 6.1:** Example of  $NOH$  calculation with Alert Message starting from node S

### 6.1.4 Number Of Slots (NOS)

This metric is used to measure the number of slots required in order to propagate the Alert Message from the source to all vehicles reached on the circumference. High values of this metric means that the multi-hop protocol introduces a lot of waiting time before each forwarding, hence increasing end-to-end delay and hurting the timeliness of the emergency message propagation.

$$NOH = \frac{\sum_{p \in RC} \text{no. of slots waited along path from source to } p}{\text{no. of vehicles on circ}} \quad (6.4)$$

where  $RC$  is the set of vehicles which have successfully received the message on the circumference. The number of slots along the path from node  $a$  to  $b$  at the numerator of Equation 6.4 is the sum of the slots waited by each forwarder before relaying the Alert Message.

Based on the scenario represented in Figure 6.2 and Equation 6.4, the mean number of slots from source S to nodes on the circumference is 100.

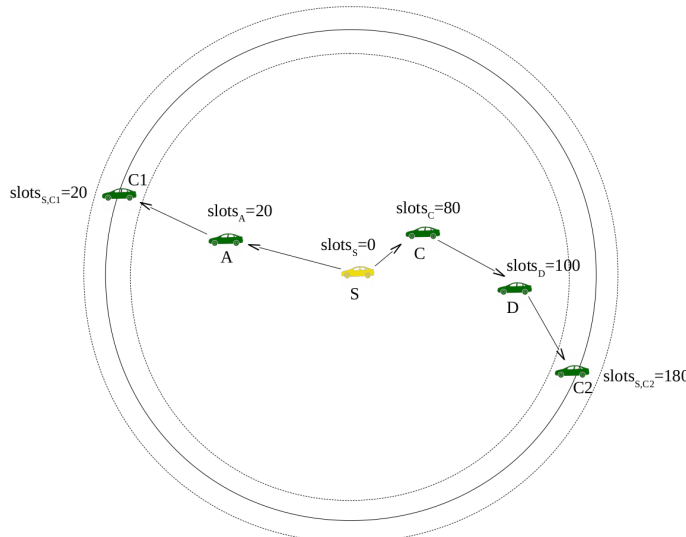


**Figure 6.2:** Example of NOS calculation with Alert Message starting from node S

### 6.1.5 Forwarding Node Number (FNN)

This metric is used to measure the number of vehicles which forward the Alert Message. The value of this metric is an indicator of the effectiveness of the multi-hop protocol in successfully suppressing scheduled transmissions from PFCs after the FFC has relayed the message. The metric is calculated as follows:

$$FNN = \text{no. of vehicles forwarding the Alert Message} \quad (6.5)$$

## 6.2 Platoon scenario

The first scenario taken into consideration is a simple platoon scenario, where vehicles are placed in a strip-like area 15 kilometers long. Vehicles are 25 meters distant from each other. Transmission ranges of 100, 300 and 500 has been employed during simulations. Parameters for this scenario are included in Table ??.

Parameter	Value	
Scenario configuration		
Road length	15000	m
Distance between vehicles	25	m
Circumference radius	14000	m
Number of vehicles	600	
Source of alert message position	Left of platoon	
Mobility model	ns3::ConstantPosition	
Network configuration		
Packet size	100	byte
Transmission standard	802.11b	
Frequency	2.4	GHz
Channel bandwidth	22	MHz
Transmission speed	11	Mbps
Transmission powers	-7.0, 4.6, 13.4	dBm
Transmission range	100, 300, 500	m
Modulation	DSSS	
Propagation loss model	ns3::TwoRayGround	
Shadowing model	No	
Propagation delay model	ns3::ConstantSpeed	
Junction modeling	No	
Protocols configuration		
FB contention window	[32, 1024]	slot
ROFF distance range ( $k$ parameter)	1	
Number of simulations per configuration	1000	

**Table 6.2:** Platoon scenario configuration

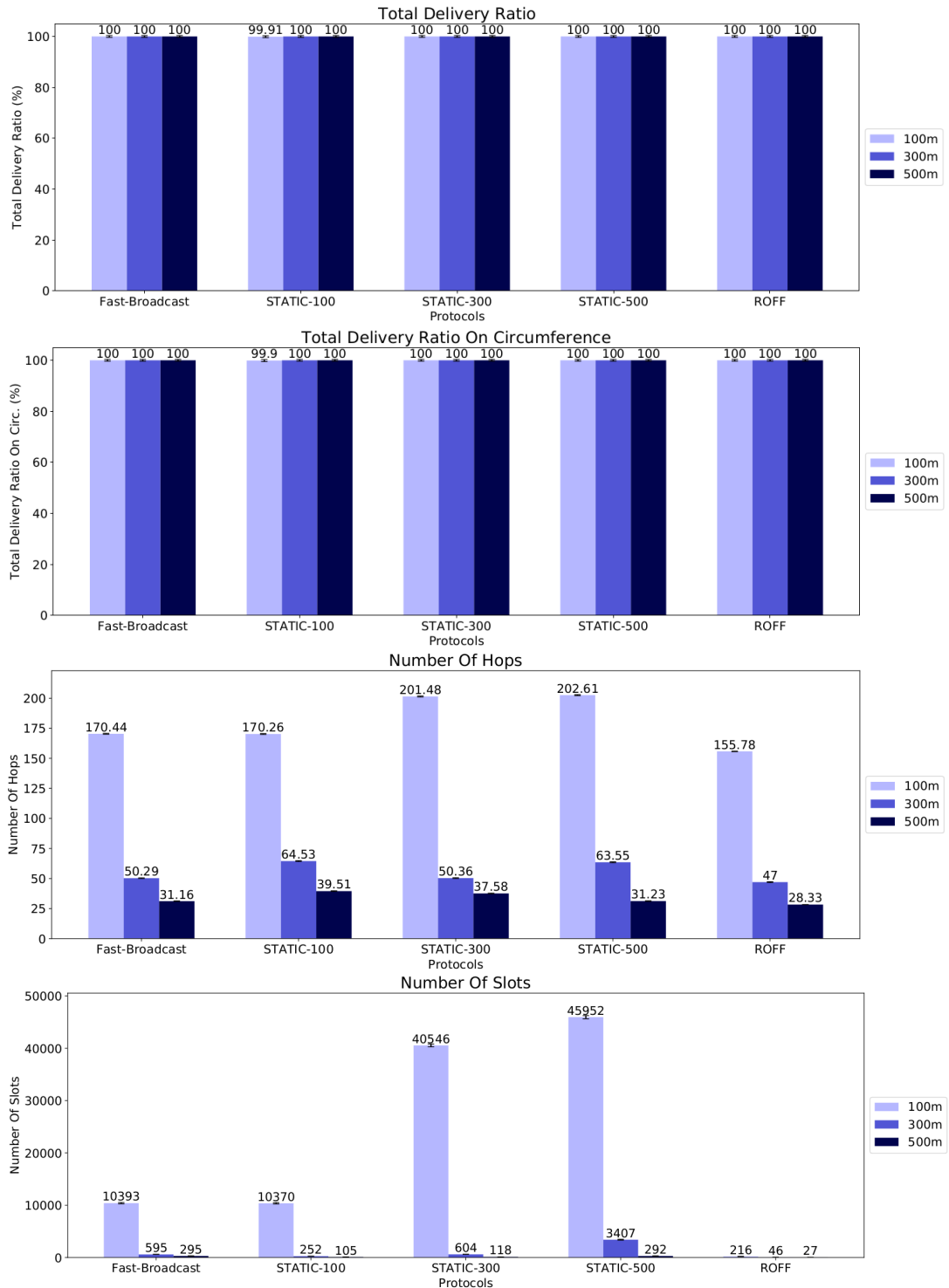


**Figure 6.3:** TDR, TDROC, NOH and NOS metrics for Platoon scenario

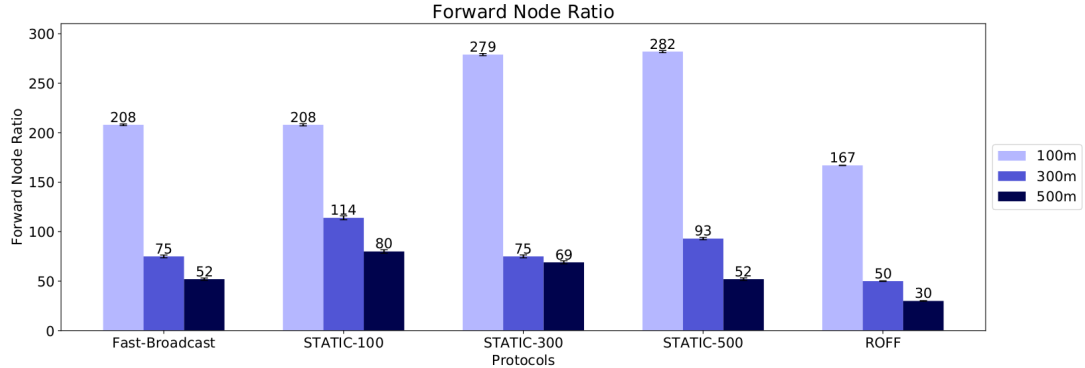


**Figure 6.4:** FNN metric for Platoon scenario

Since this scenario is one-dimensional, the circumference simply consists in vehicles distant  $14.000 \pm 12$  meters from the source of Alert Message. Both metrics about Delivery Ratio (global and on circumference) are close to 100%, so the algorithms successfully propagate the AM until the end of the platoon.

Considering the Number Of Hops, ROFF's results are 11,76%, 6,54% and 9,08% lower than Fast-Broadcast's results respectively for 100, 300 and 500 meters transmission range. ROFF's results are close to the optimal number of hops, respectively 140, 46,6 and 28 for the same transmission ranges as above. This means that the forwarder selection algorithms based on ESD Bitmap works better in choosing the farthest vehicle from the previous forwarder compared to the contention window approach for 1D scenarios. Considering STATIC variants of Fast-Broadcast, it is possible to observe that the STATIC- $tx$  variant produces comparable results with Fast-Broadcast with  $tx$  transmission range (e.g. STATIC-100 value is comparable to Fast-Broadcast with 100 meters transmission range), as expected. The STATIC protocol performs worse (hence the Number of Hops increases) whenever the transmission range is underestimated (e.g. STATIC-100 with 300 meters transmission range, compared to Fast-Broadcast with the same transmission range) or overestimated (e.g. STATIC-500 with 100 meters transmission range, compared to Fast-Broadcast with the same transmission range). This behaviour is expected, as reported in [30].

Regarding the Number of Slots, ROFF's performs much better than Fast-Broadcast. The metric's value is decreased respectively by 97,92%, 92,27% and 90,85% using ROFF. The waiting time calculation, based on unique forwarding priority instead of distance, guarantees a much lower wait compared to Fast-Broadcast contention window approach. As before, STATIC approaches produce results comparable with Fast-Broadcast when the transmission range estimation is correct. Instead, the Number of Slots greatly increases when the transmission range is underestimated and decreases when the transmission range is overestimated. In this last case, the decrease in NOS comes with an increase in Number Of Hops reported in the previous paragraph, so an overestimation of transmission range is not desirable.

Lastly, it is possible to see that ROFF's achieves a better suppression of redundant transmissions, guaranteeing a decrease of 19,71%, 33,33% and 42,31% respectively for each one of the transmission ranges considered.

### 6.3 Grid scenario

After tests on the 1D Platoon scenario have been carried out, the next step consisted in testing the algorithms' performances in a 2D Grid scenario, employing also the shadowing model introduced in 2.1. Parameters for this scenario are included in Table 6.4.

Parameter	Value	
Scenario configuration		
Road length	4800	m
Distance between roads	300	m
Road width	10	m
Number of roads (vertical)	17	
Number of roads (horizontal)	17	
Distance between vehicles	25	m
Circumference radius	2000	m
Number of vehicles	6528	
Source of alert message position	Center	
Mobility model	ns3::ConstantPosition	
Edge of buildings	290	m
Number of buildings	255	m
Network configuration		
Shadowing model	Obstacle Shadowing	
Junction modeling	No	
Number of simulations per configuration	1000	

Table 6.4: Grid scenario configuration

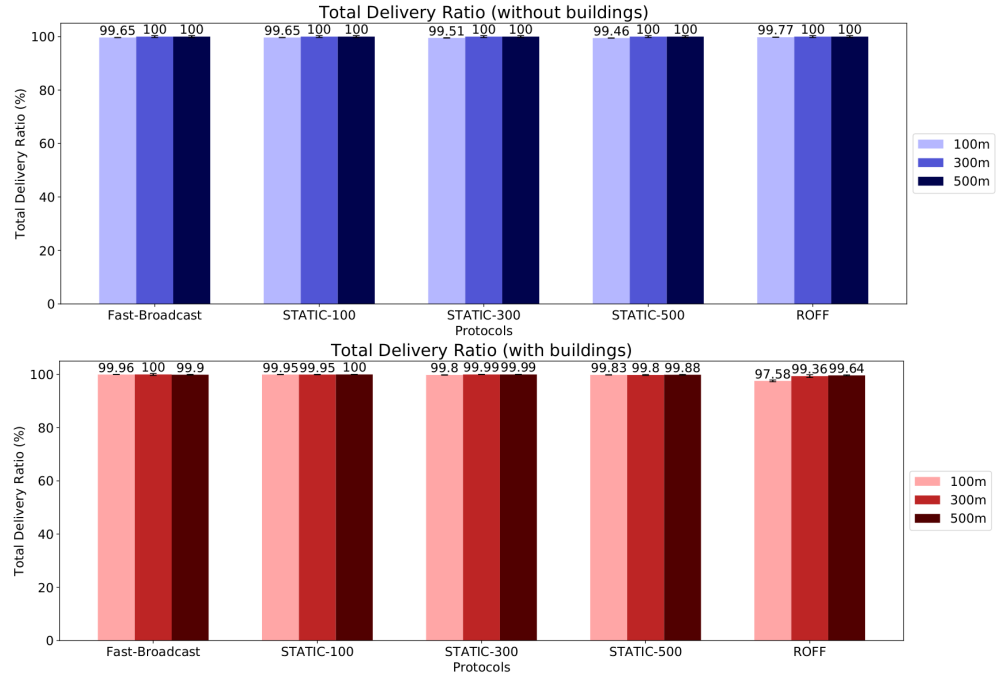


**Figure 6.5:** TDR without buildings (top) and with buildings (bottom) for Grid scenario

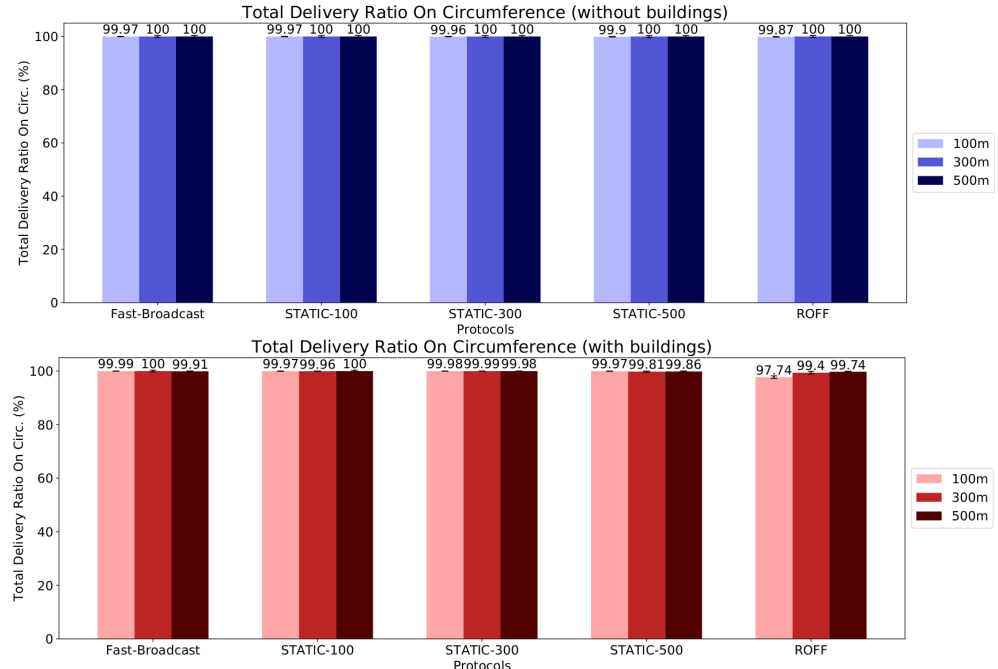


**Figure 6.6:** TDROC without buildings (top) and with buildings (bottom) for Grid scenario

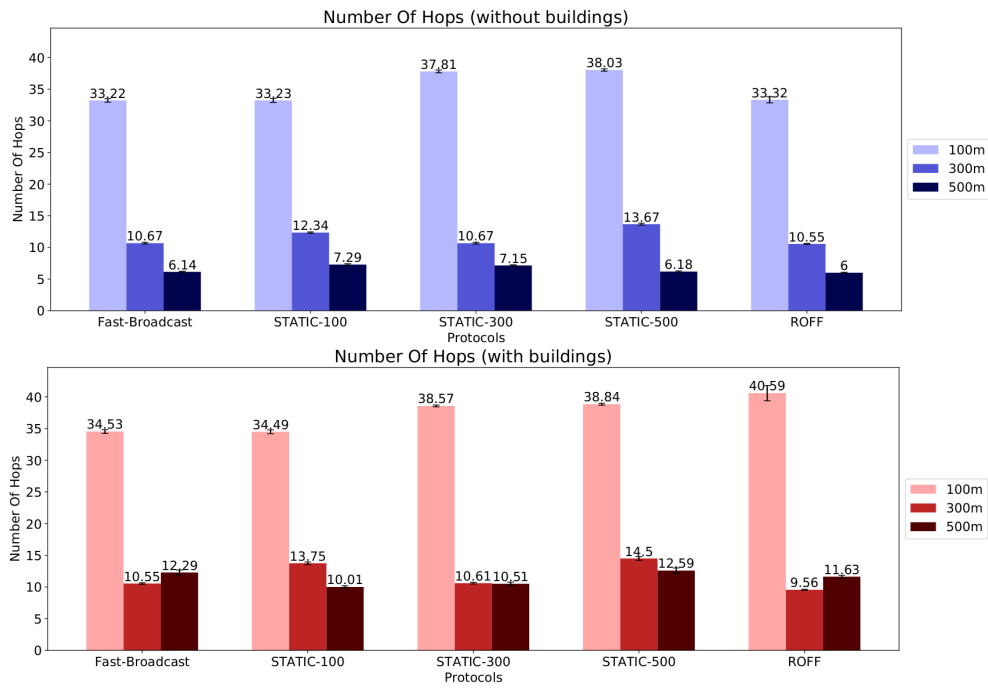


**Figure 6.7:** NOH without buildings (top) and with buildings (bottom) for Grid scenario

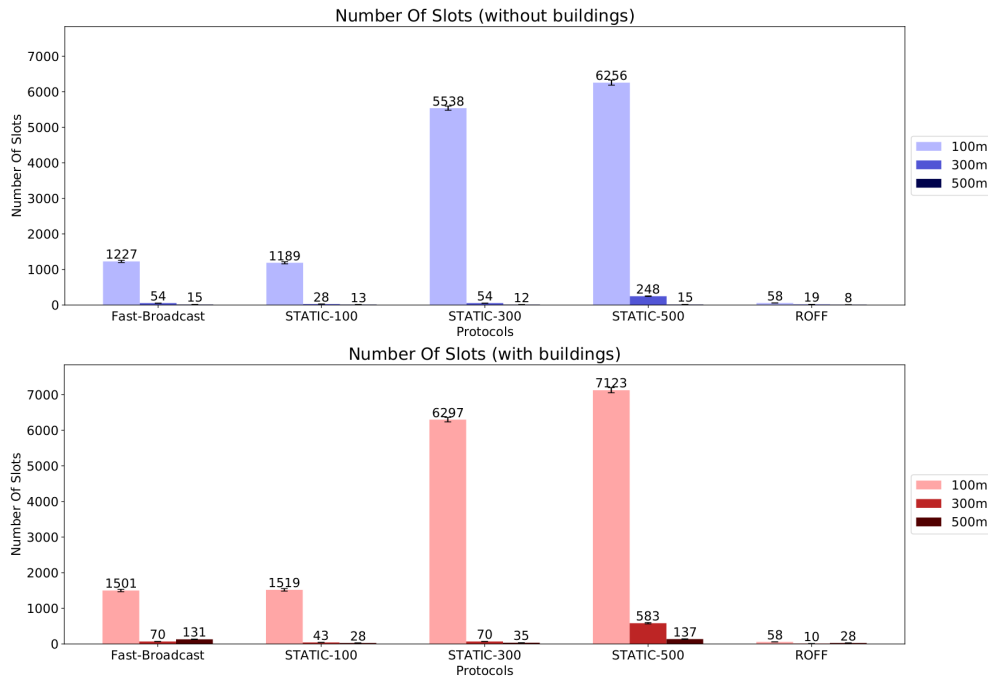


**Figure 6.8:** NOS without buildings (top) and with buildings (bottom) for Grid scenario

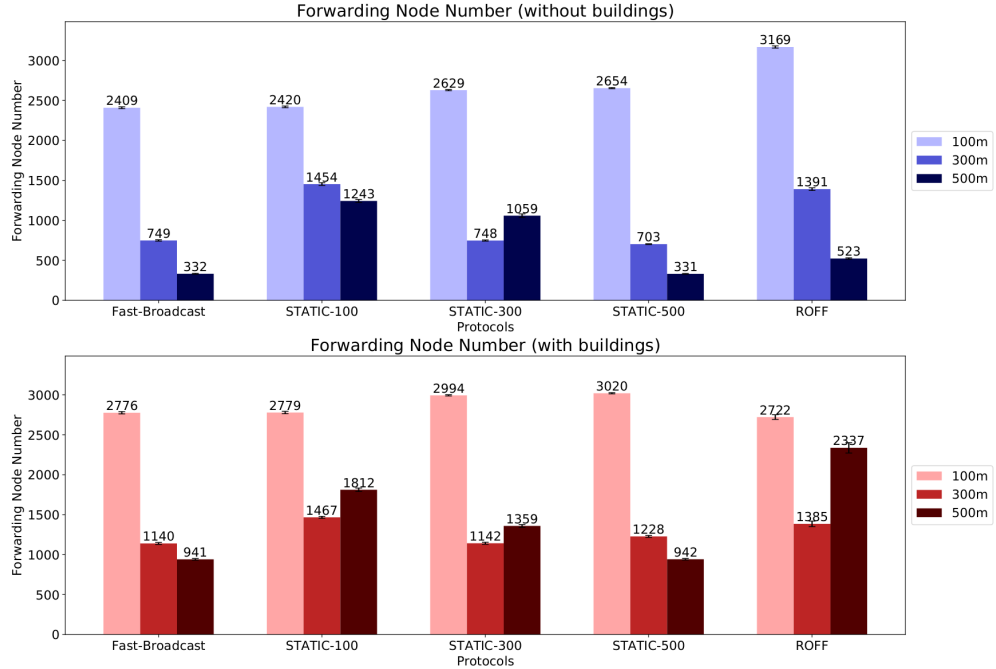


**Figure 6.9:** FNN without buildings (top) and with buildings (bottom) for Grid scenario

All the algorithms perform well as far as delivery ratios are concerned (Figure 6.5 and 6.6), both for scenarios with and without buildings. This means that the shadowing caused by the Obstacle Model does not create no-reach zones, and the signal manages to find its way to almost all of the vehicles. The regular pattern by which vehicles are placed may help with that: further testing where this hypothesis is removed will be presented in the next sections. Even though delivery ratios are unchanged, the effect of the Obstacle model can be observed qualitatively comparing Figure 6.10 and 6.11 for Fast-Broadcast, and Figure 6.12 and 6.13 for ROFF. The effects of obstacles on propagation cause the signal to travel only through roads segments where line of sight is possible. Instead, without obstacles the signal can be propagated freely in all directions.

Moreover, Fast-Broadcast and ROFF can be compared with each other by looking at Figure 6.10 and 6.12 for the scenario without buildings, and Figure 6.11 and 6.13 for the scenario with buildings. In both cases, ROFF designates the furthest PFC as the next forwarder much more reliably than Fast-Broadcast thanks to the Neighbor Table mechanism. Instead, Fast-Broadcast relies on a random choice of waiting time, so the next designated forwarder is sometimes not one of the farthest vehicles from the previous forwarder. Based on this observation, we can expect a much lower NOH value for ROFF. Quantitative analysis of this and other metrics will be reported in the next paragraphs of this section.

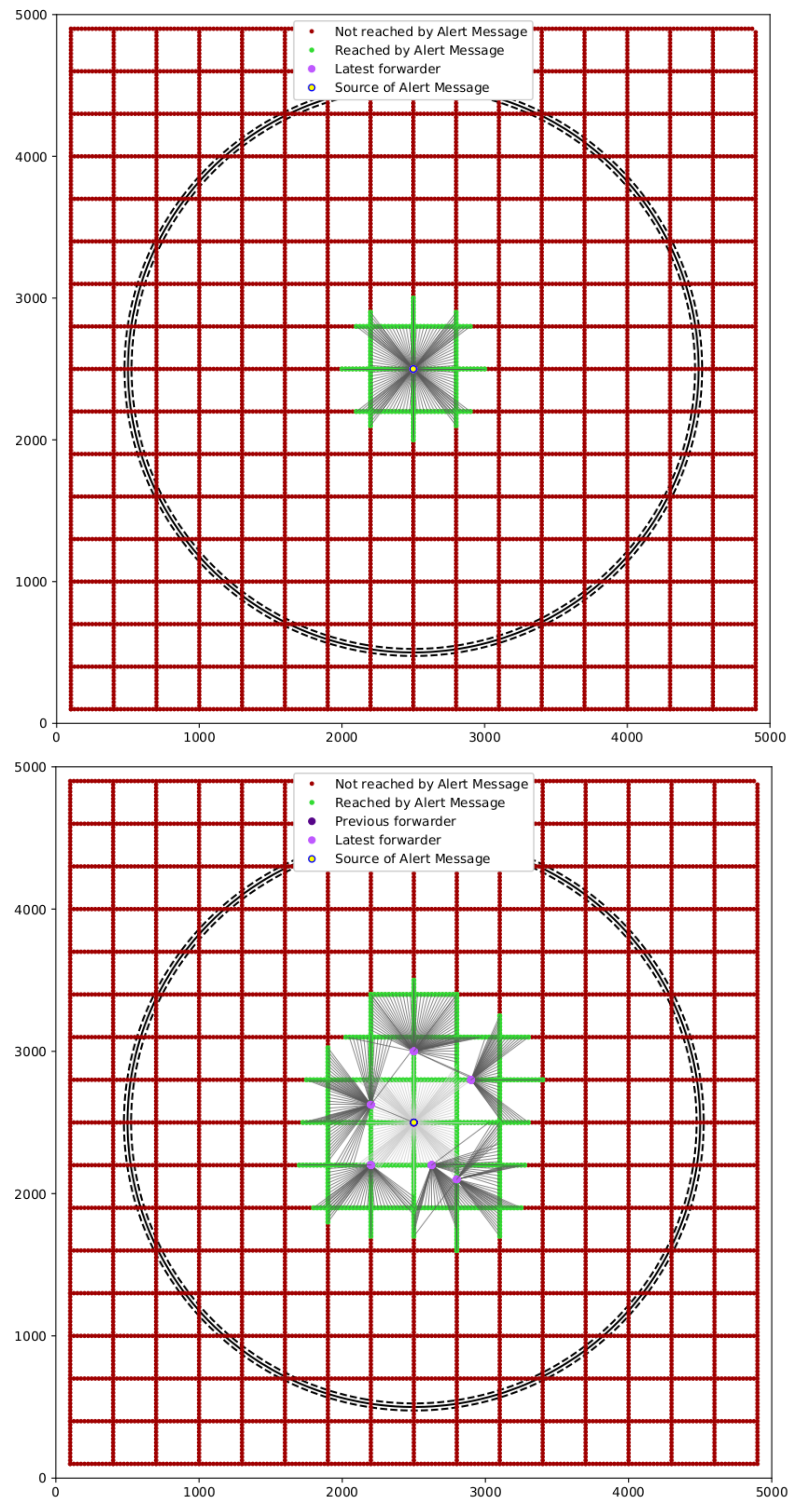


**Figure 6.10:** Fast-Broadcast after 1 hop (top) and 2 hops (bottom) in Grid scenario with 500 meters transmission range and without the Obstacle model

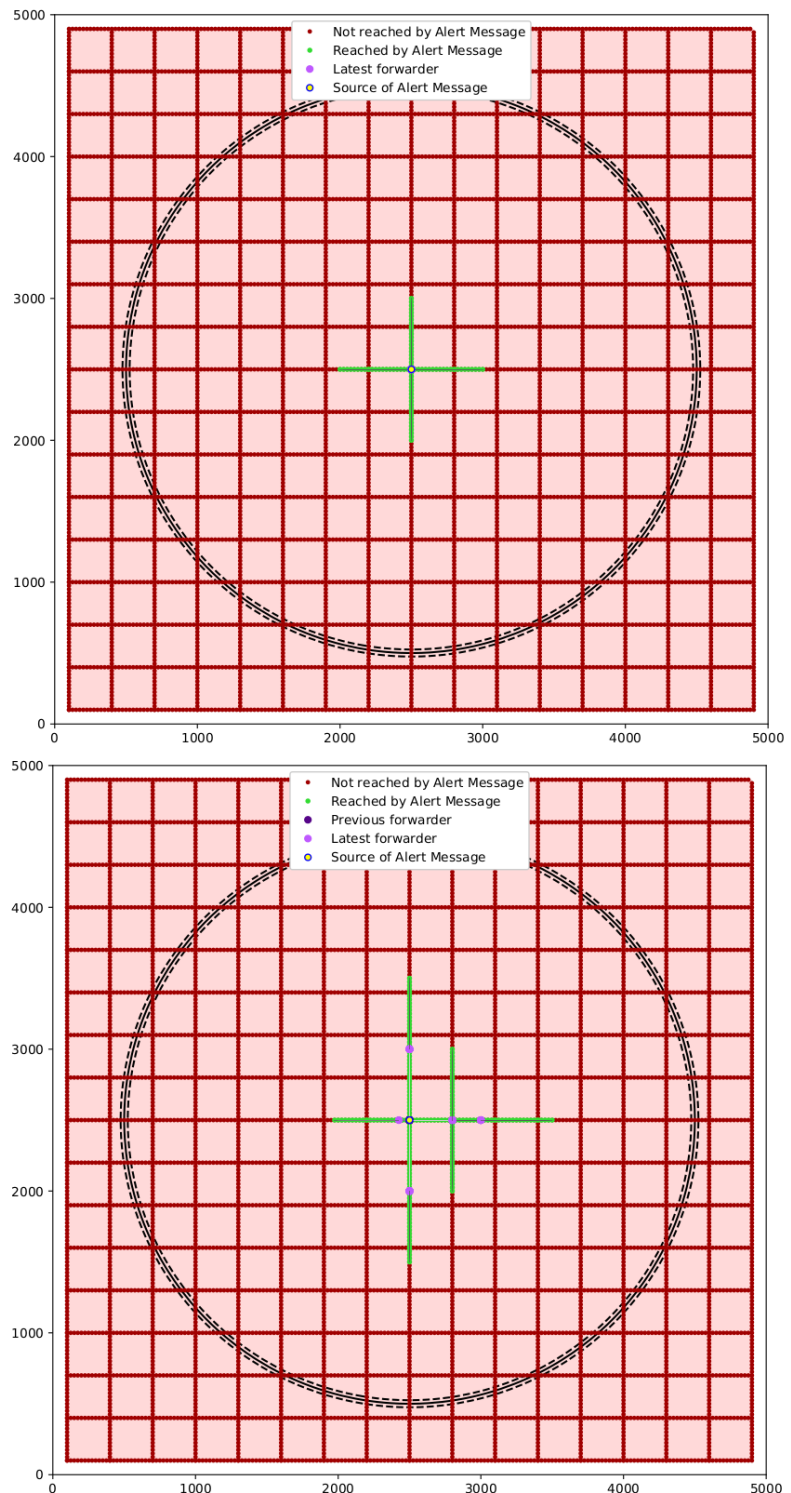


**Figure 6.11:** Fast-Broadcast after 1 hop (top) and 2 hops (bottom) in Grid scenario with 500 meters transmission range and with the Obstacle model

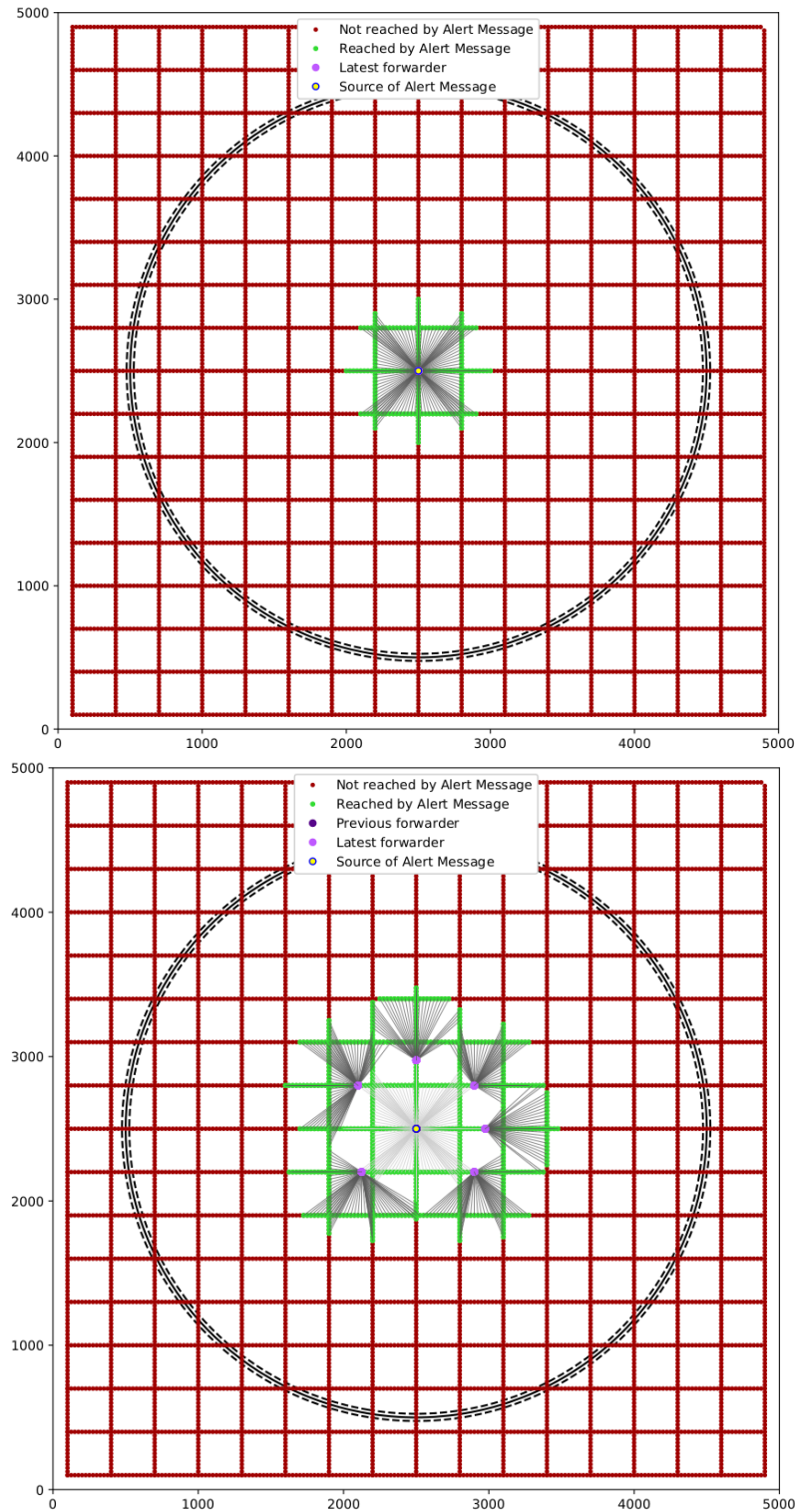


**Figure 6.12:** ROFF after 1 hop (top) and 2 hops (bottom) in Grid scenario with 500 meters transmission range and without the Obstacle model

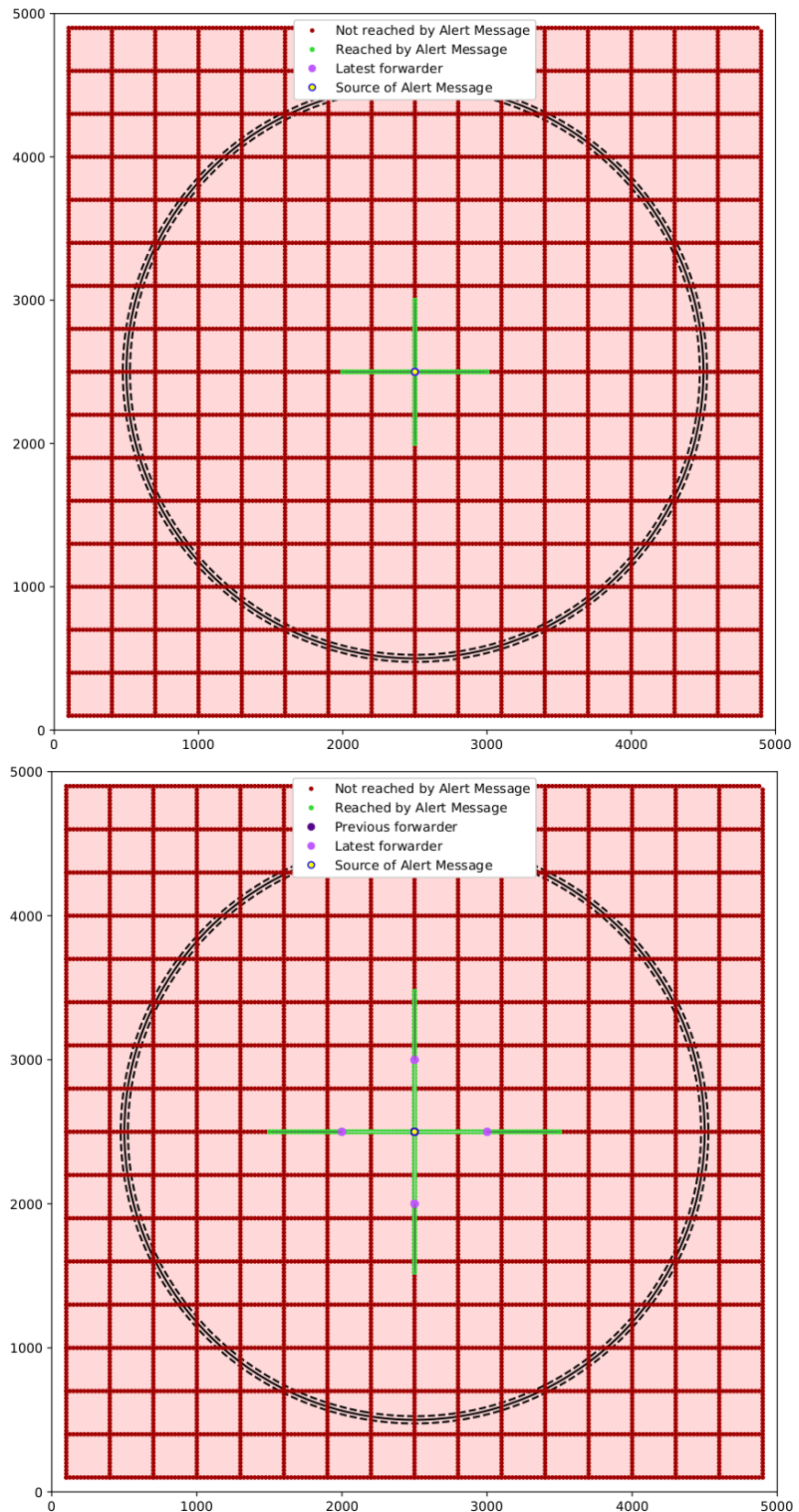


**Figure 6.13:** ROFF after 1 hop (top) and 2 hops (bottom) in Grid scenario with 500 meters transmission range and with the Obstacle model

If we focus on the Number Of Hops (Figure 6.7), we notice that the introduction of buildings causes the number of hops to increases for transmission ranges of 100 and 500 meters, while decreases for 300 meters transmission range. This is probably due to the fact that the distance between roads is also 300 meters and the starting vehicle is inside a junction. This means that the effect of buildings causes the signal to travel along roads, hopping from junction to junction, and reaching the circumference much faster. Another unusual observation consists in ROFF with 100 meters transmission range, where the value increases by a lot. This case needs further examination in order to be explained. Apart from this case, ROFF achieves better results than Fast-Broadcast, with results 9% and 3.47% better for 300 and 500 meters transmission range respectively.

The analysis of the Number Of Slots (Figure 6.8) shows similar results: the shadowing model causes the metric's value to rise in all configurations except for ROFF with 300 meters transmission range. ROFF continues to outperform Fast-Broadcast with results similar to those observed in the Platoon scenario.

Considering the Forwarding Node Number (Figure 6.9), the situation is much different than the previous scenario. It is possible to see in both graphs that ROFF's values are higher than Fast-Broadcast's across all configurations. Despite the almost-perfect suppression of redundant transmission works in a 1D scenario, as observer in the previous section, the mechanism does not seem to have much of an effect in a 2D scenario, regardless of the presence of buildings. A possible explanation of this phenomenon might be the one reported in Figure 6.14, which indicates a possible Alert Message propagation process. Suppose that S is the previous forwarder: the other nodes on the circumference (distant txRange from S) are the elected FFCs which win the contention and relay the message. Due to how ROFF works, those nodes send the message at the same time, hence if we focus on A and B we have a collision area (the red area in Figure 6.14). The nodes inside that collision area receive the forwarding from A and B at the same time and a collision occurs. As a consequence, they are not aware that the message has already been forwarded and some of them will fire their transmission. This process is repeated for every forward (and also for other FFCs other than A and B in the example) and so this could cause the increase in the FNN value. In other words, ROFF is guaranteed to cause the collision area shown in the example due to the exact waiting time calculation for nodes at the same distance from S. Fast-Broadcast is less affected by this problem since the waiting time calculation is not deterministic (the waiting time is chosen randomly from the interval [1...CW] where CW is calculated using Formula 3.1).

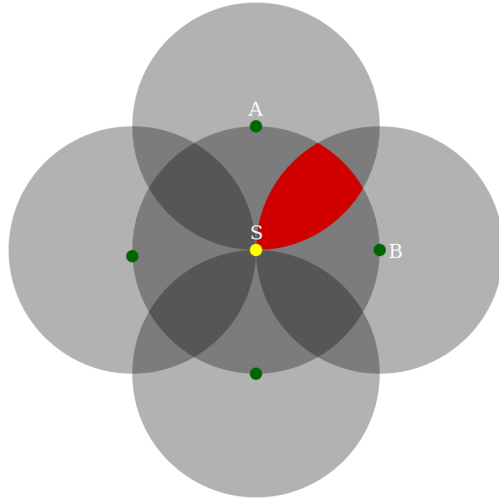


**Figure 6.14:** Collision area in 2D ROFF

## 6.4 Los Angeles urban scenario

The next step consisted in expanding the 2D scenario with realistic urban data taken from OpenStreetMap and processed by SUMO as explained in Section 5.2. In addition to the shadowing model, in this scenario (and also in the urban scenario regarding Padua, which will be presented in the next section), a *smart junction* variant of the algorithms has been introduced in order to try to increase the delivery ratios.

Figure 6.15 depicts the scenario with vehicles (green dots), buildings (purple polygons) and junctions (yellow polygons).

All configurations are reported in Figure 6.16. In order to facilitate the understanding of the various configurations, the following graphs will utilize shades of color similar to those in Figure 6.16 (e.g. graphs with shades of blue will represent a scenario without buildings and without junctions, while shades of orange will represent a scenario with buildings and with junctions). Parameters for this scenario are included in Table 6.6.

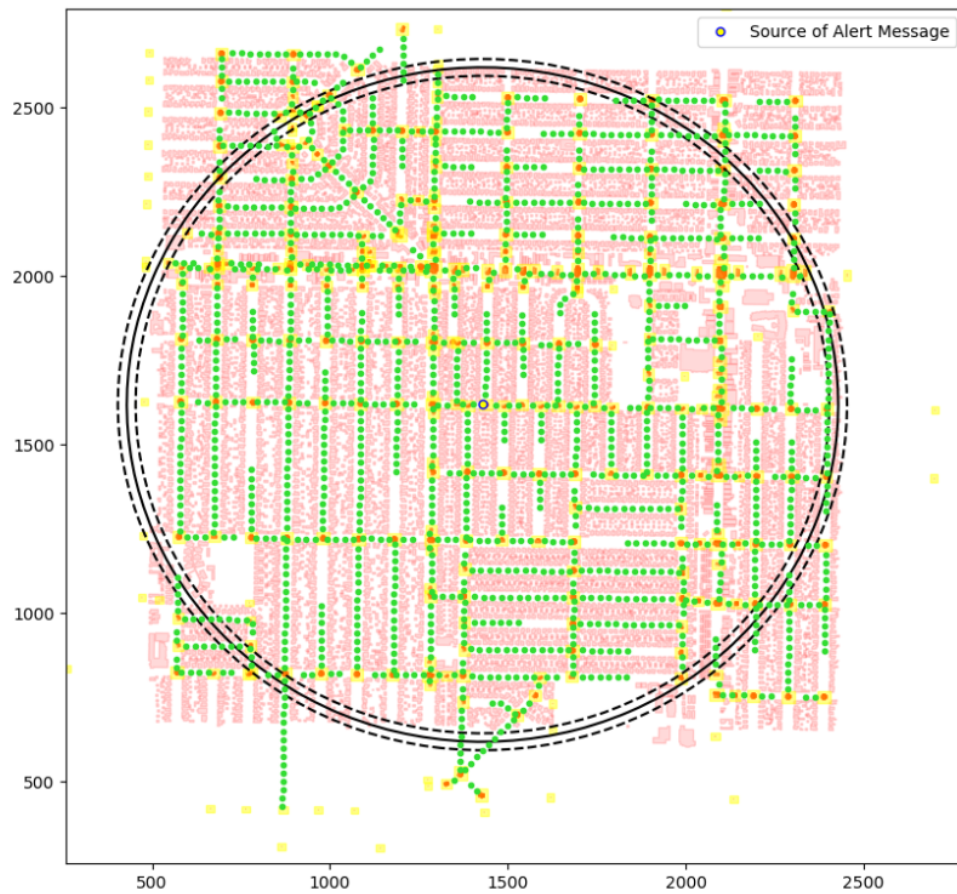


Figure 6.15: Los Angeles urban scenario depiction

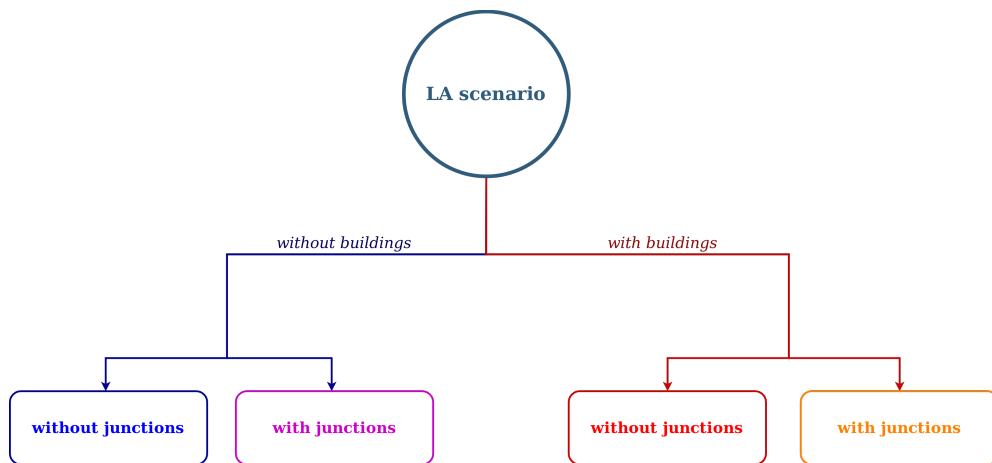
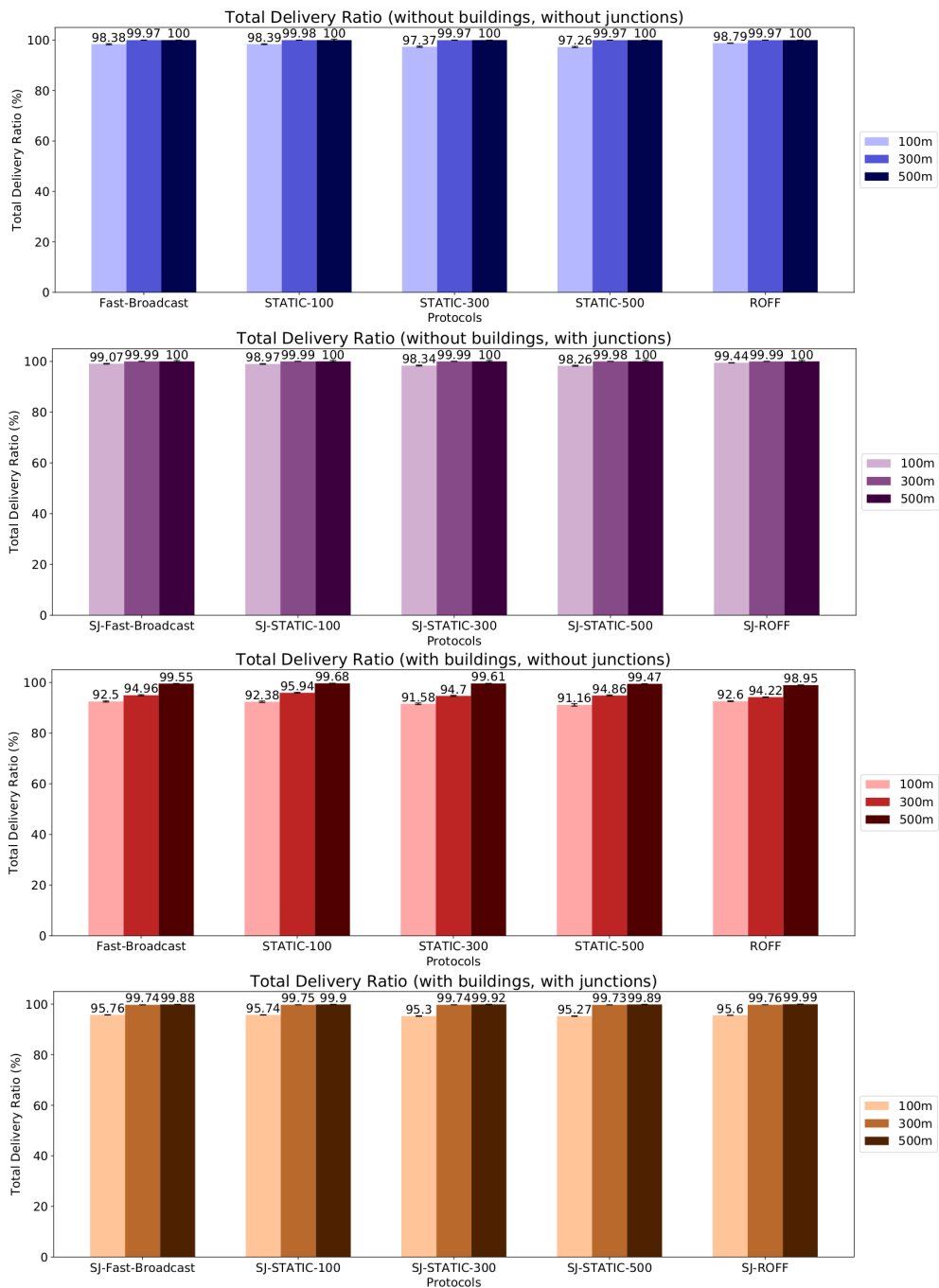


Figure 6.16: Los Angeles urban scenario test overview

Parameter	Value
Scenario configuration	
Latitude N	33.9654 °
Latitude S	33.9478 °
Longitude W	-118.3260 °
Longitude E	-118.3055 °
Road length	1200 m
Distance between vehicles	25 m
Circumference radius	1000 m
Number of vehicles	1465
Source of alert message position	Center
Number of buildings	8241
Mobility model	ns3::ConstantPosition
Number of junctions	1288
Network configuration	
Shadowing model	Obstacle Shadowing
Junction modeling	Yes
Number of simulations per configuration	5000

**Table 6.6:** Los Angeles urban scenario configuration

**Figure 6.17:** TDR for Los Angeles urban scenario

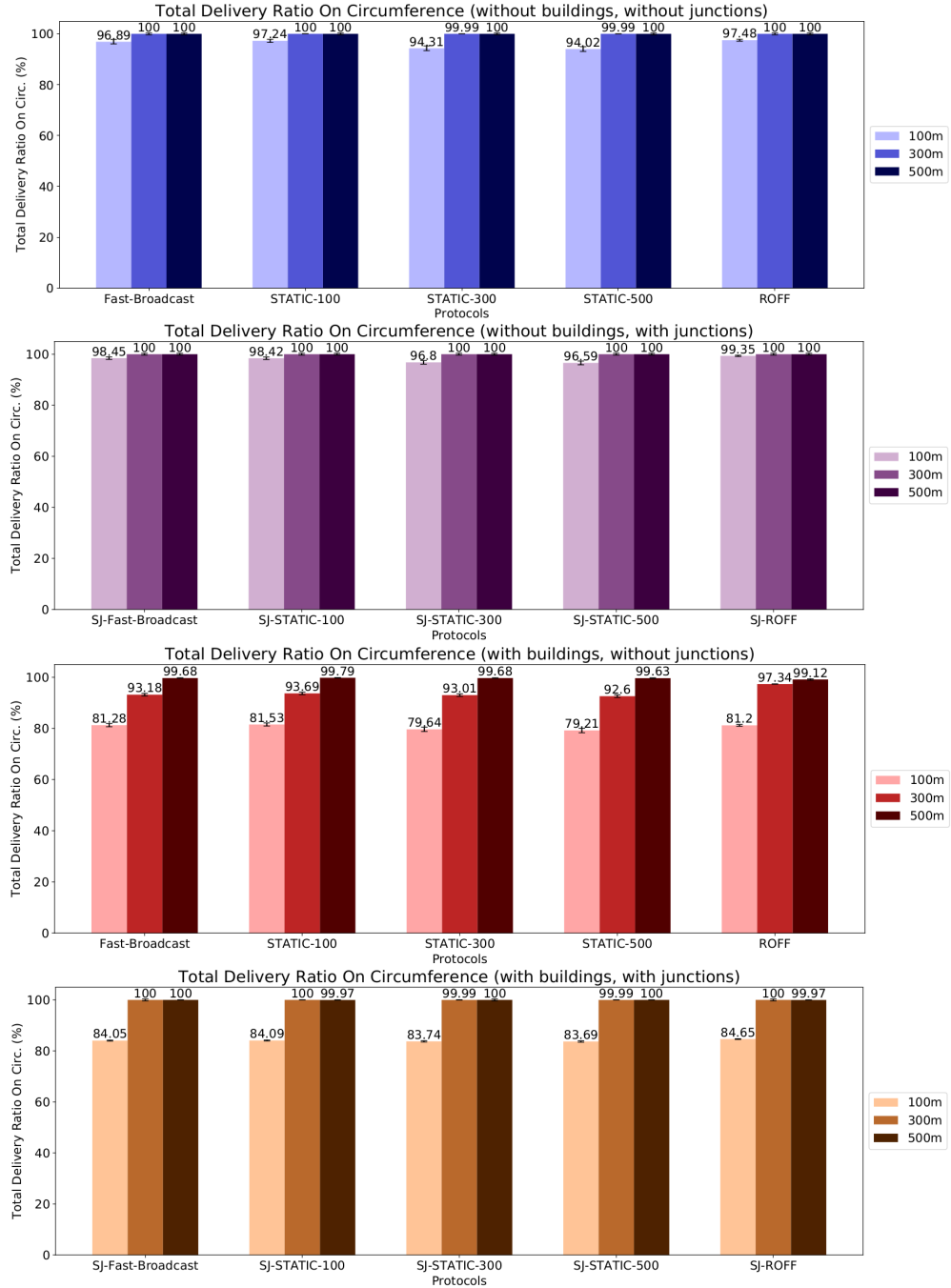
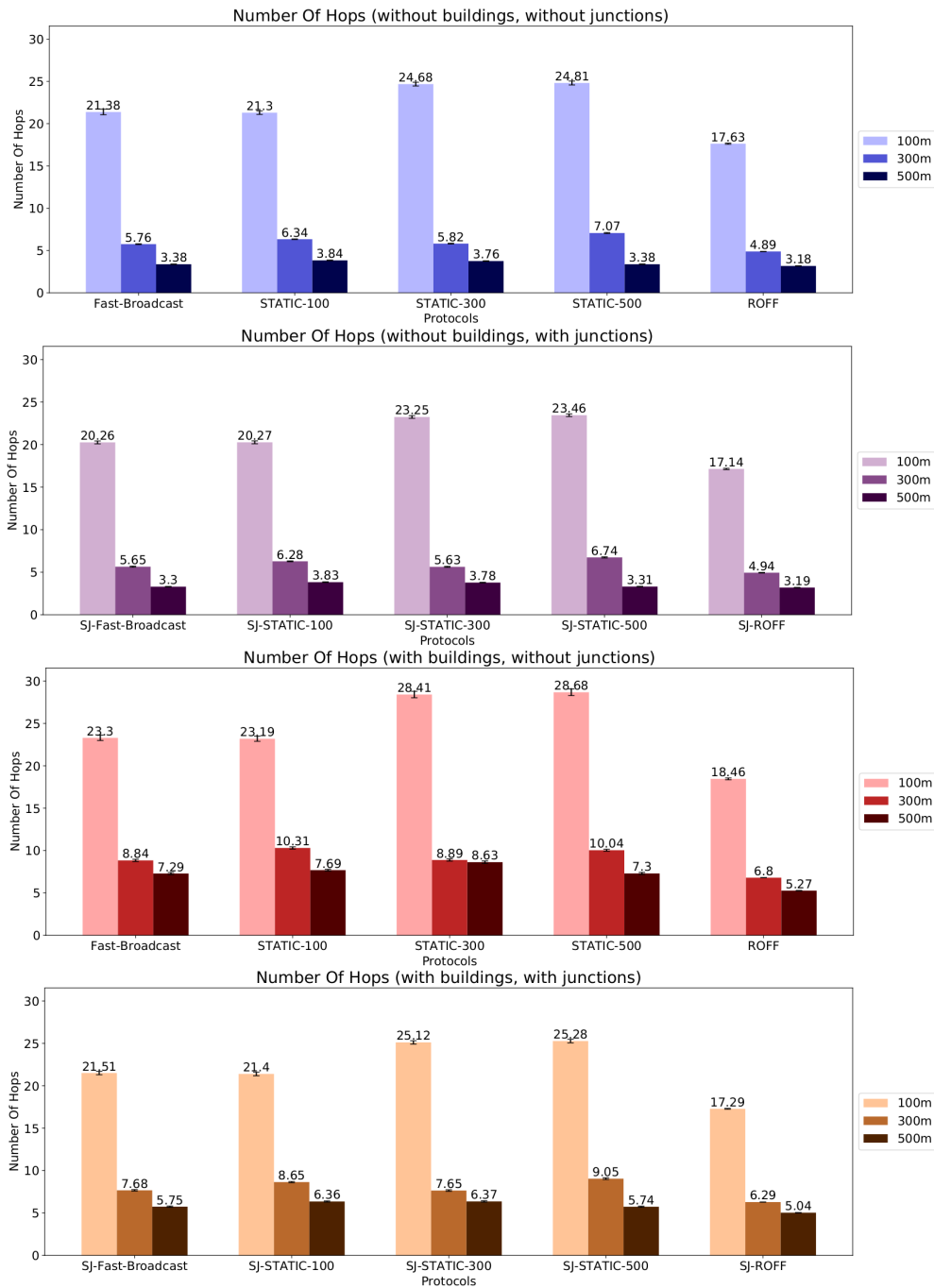
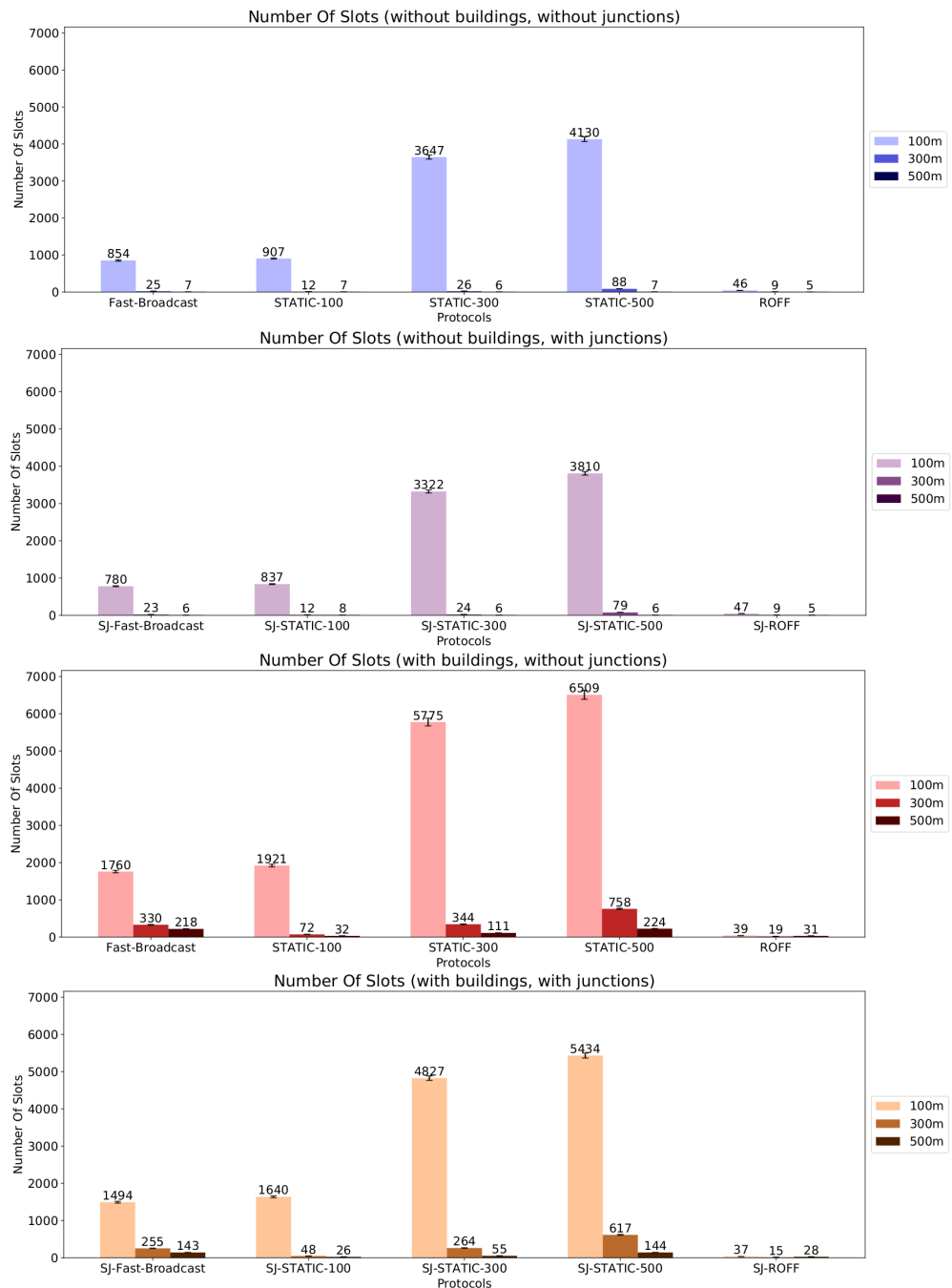


Figure 6.18: TDROC for Los Angeles urban scenario

**Figure 6.19:** NOH for Los Angeles urban scenario



**Figure 6.20:** NOS for Los Angeles urban scenario

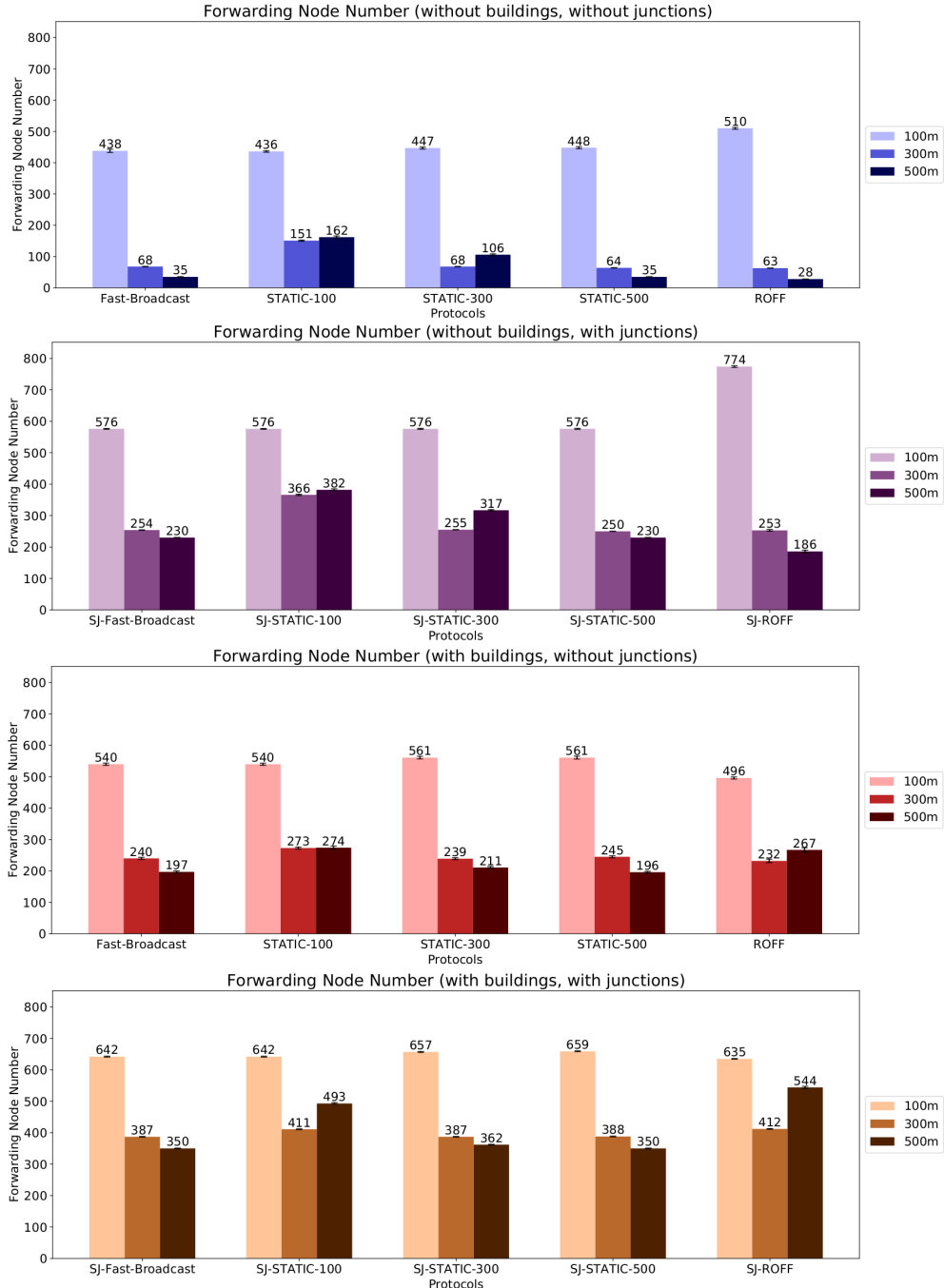
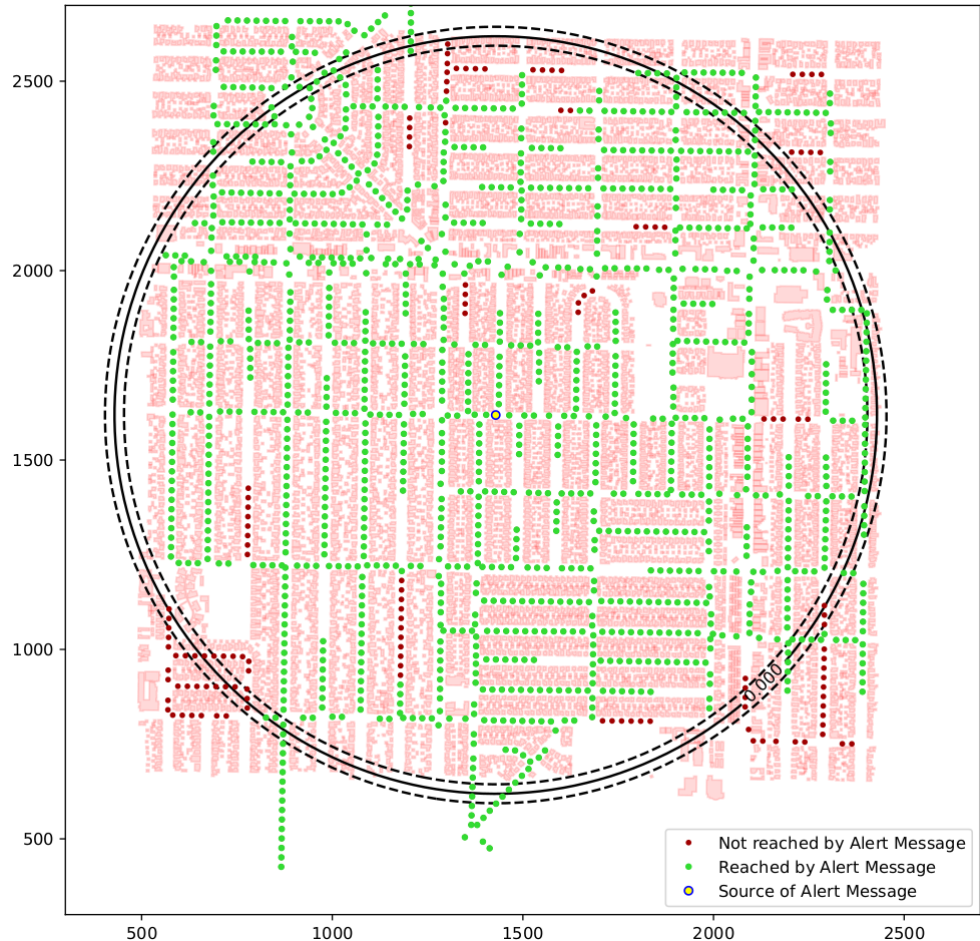


Figure 6.21: FNN for Los Angeles urban scenario

It is possible to observe the effects of the Obstacle Shadowing model on *Total Delivery Ratio* and *Total Delivery Ratio On Circumference*. The effects are pretty mild across all configurations, but are more noticeable with lower transmission ranges (100 and 300 meters). For example, introducing the shadowing model without considering junctions leads to a decrease of 5.97% (98.38 to 92.5) in *TDR* (Figure 6.17) with a transmission

range of 100 meters and a decrease of 5% (99.96 to 94.96) with transmission range of 300 meters for Fast-Broadcast. Results for ROFF are comparable, with decreases of 6.28% and 5.73% respectively.

The decrease in *TDROC* (Figure 6.17) is much more noticeable, especially for the 100 meters transmission range. The value decrease by 16.11% for Fast-Broadcast and 16.74% for ROFF. This means that introducing building shadowing leads to more problems when the Alert Message has to reach further distances. This phenomenon can be seen in Figure 6.22. Vehicles not reached by the Alert Message are more concentrated towards the circumference instead of the center.



**Figure 6.22:** Alert Message delivery for Los Angeles scenario with buildings and without junctions (Fast-Broadcast with 100 meters transmission range)

The introduction of the smart junction variants of the algorithms proves to be fairly effective, increasing *TDR* by 3.52% and 5.03% when employing SJ-Fast-Broadcast instead of Fast-Broadcast for the scenario with buildings and transmission range of 100 and 300 meters respectively. Increases of the same magnitude can be noticed when utilizing SJ-ROFF instead of ROFF. With regards to *TDROC*, both SJ-Fast-Broadcast and SJ-ROFF reach 100% for 300 and 500 meters transmission ranges, while having a

mild increase of around 3,40% for 100 meters transmission range.

Considering the Number Of Hops to reach the circumference (6.19), we can observe that the introduction of the shadowing model leads to an increase in the metric's value across all algorithms. Comparing the first and third configuration,  $NOH$  rises by 8.98, 53,74 and 115,68% for Fast-Broadcast, and by 3.85, 36.27 and 64.69% for ROFF, for the three increasing transmission ranges. We notice that:

1. the rise increases with the increase in transmission range;
2. Fast-Broadcast is affected in a greater way by the shadowing model compared to ROFF.

The first point is expected, since the one-hop progress is greater in a scenario with a higher transmission range. This leads to a greater probability for the signal to run into a building. In a scenario with a lower transmission range, transmissions have a lower probability to run into a building and follow more closely the road segment even without the effects of buildings. Hence, they are less likely to be influenced by the model. The second point may be due to the fact that the Neighbor Table continues to work well to identify the FFC along the road segment, leading to a smaller increase in the number of hops.

SJ-Fast-Broadcast and SJ-ROFF need less hops in order to reach the circumference than their counterparts which do not take junctions into consideration. This holds true for both scenarios with and without buildings. This is probably due to the additional transmissions inside junctions, which help to propagate the signal along road segments in a linear way, hence covering more space with each hop. SJ-ROFF performs better than SJ-Fast-Broadcast with regards to  $NOH$ . The difference between the two algorithms decreases as the transmission range increases.

Regarding  $NOS$  (Figure 6.20), Fast-Broadcast results increase by 106.09, 1220 and 3014% while ROFF's ones increase by 111.11 and 520% for 300 and 500 meters transmission range, and decrease by 4.44% for 100 meters transmission range, when going from a building-less scenario to a scenario with buildings. Moreover, Fast-Broadcast's values are 4412.82, 1636.84 and 603.23% higher than ROFF's values in the scenario with buildings. This goes to show the effect of empty space distribution on waiting times (here represented by the number of slots waited): when the distance between the FFC and the previous forwarder is close to the estimated transmission range, then Fast-Broadcast's waiting slots are pretty close to the minimum. But when obstacles are introduced, there might not be any PFC close to the estimated transmission range. Hence, the FFC will wait a very long time. ROFF is not affected by this phenomenon thanks to the forwarding priority acquisition, as introduced in Chapter 4. Comparing the third and fourth image in Figure 6.20, we can see that the introduction of junctions is beneficial for both algorithms, leading to a decrease in  $NOS$ . This is a consequence of the abovementioned decrease in Number Of Hops.

Concerning the Forwarding Node Number (Figure 6.21), the value increases when the shadowing model is introduced. ROFF with 100 meters transmission range is the only configuration where the values decreases. This configuration needs further testing in order to be explained. The introduction of junctions brings about an increase in the number of forwardings for all algorithms, as expected. Focusing on the fourth image of Figure 6.21, SJ-ROFF is affected greatly by this increase, almost equalling SJ-Fast-Broadcast with 100 meters transmission range, and with  $FNN$  much greater values in 300 and 500 meters transmission range configurations. This might be caused by the introduction of transmissions inside junctions, which exacerbate the collision

problem already reported in the previous section (Figure 6.14), leading to an imperfect suppression of scheduled transmissions. The problem is not as severe as in the Grid scenario since the node distribution is less regular, but overall Fast-Broadcast performs slightly better in terms of FNN.

## 6.5 Padua urban scenario

As reported in the previous section the Los Angeles scenario, despite being realistic, still had a certain degree of regularity for what concerns vehicle distribution and scenario topology. In fact, roads and sidewalks are pretty large and the overall road positioning resembles a Grid scenario. The next step in testing consisted in employing the algorithms in a more difficult scenario, with narrower roads and intersections, smaller (if any) sidewalks and pedestrian zones where no traffic is allowed. The chosen scenario is located in Padua and, as the previous one, data about the scenario have been retrieved by OSM and processed through SUMO. The scenario is depicted in Figure 6.23, while its configuration is reported in Table 6.8.

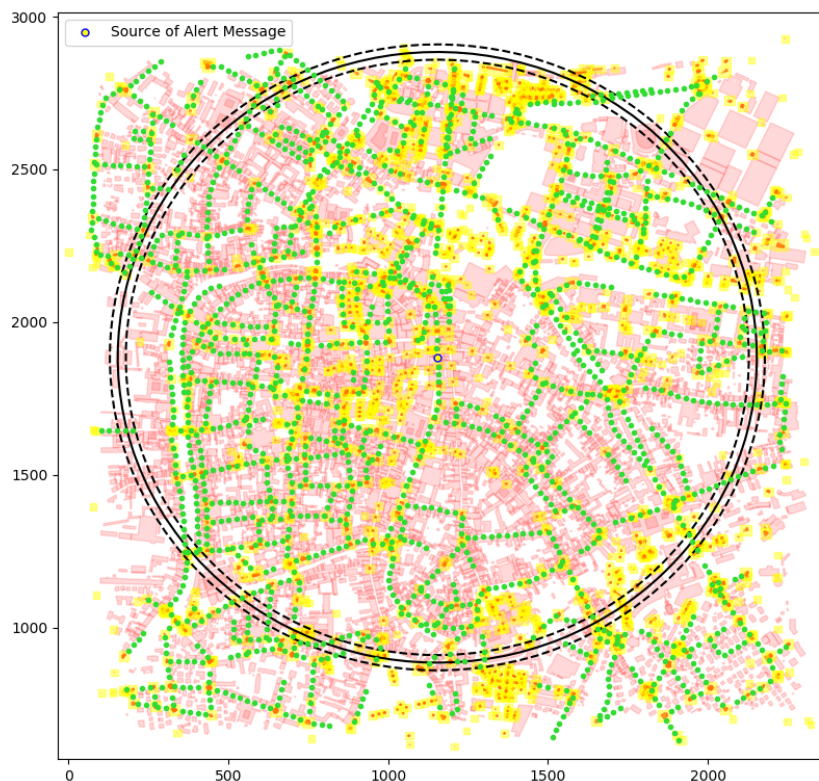


**Figure 6.23:** Padua urban scenario depiction

Parameter	Value
Scenario configuration	
Latitude N	45.4171 °
Latitude S	45.3981 °
Longitude W	11.8654 °
Longitude E	11.8923 °
Road length	1200 m
Distance between vehicles	25 m
Circumference radius	1000 m
Number of vehicles	1775
Source of alert message position	Center
Number of buildings	6322
Mobility model	ns3::ConstantPosition
Number of junctions	3231
Network configuration	
Shadowing model	Obstacle Shadowing
Junction modeling	Yes
Number of simulations per configuration	5000

**Table 6.8:** Los Angeles urban scenario configuration

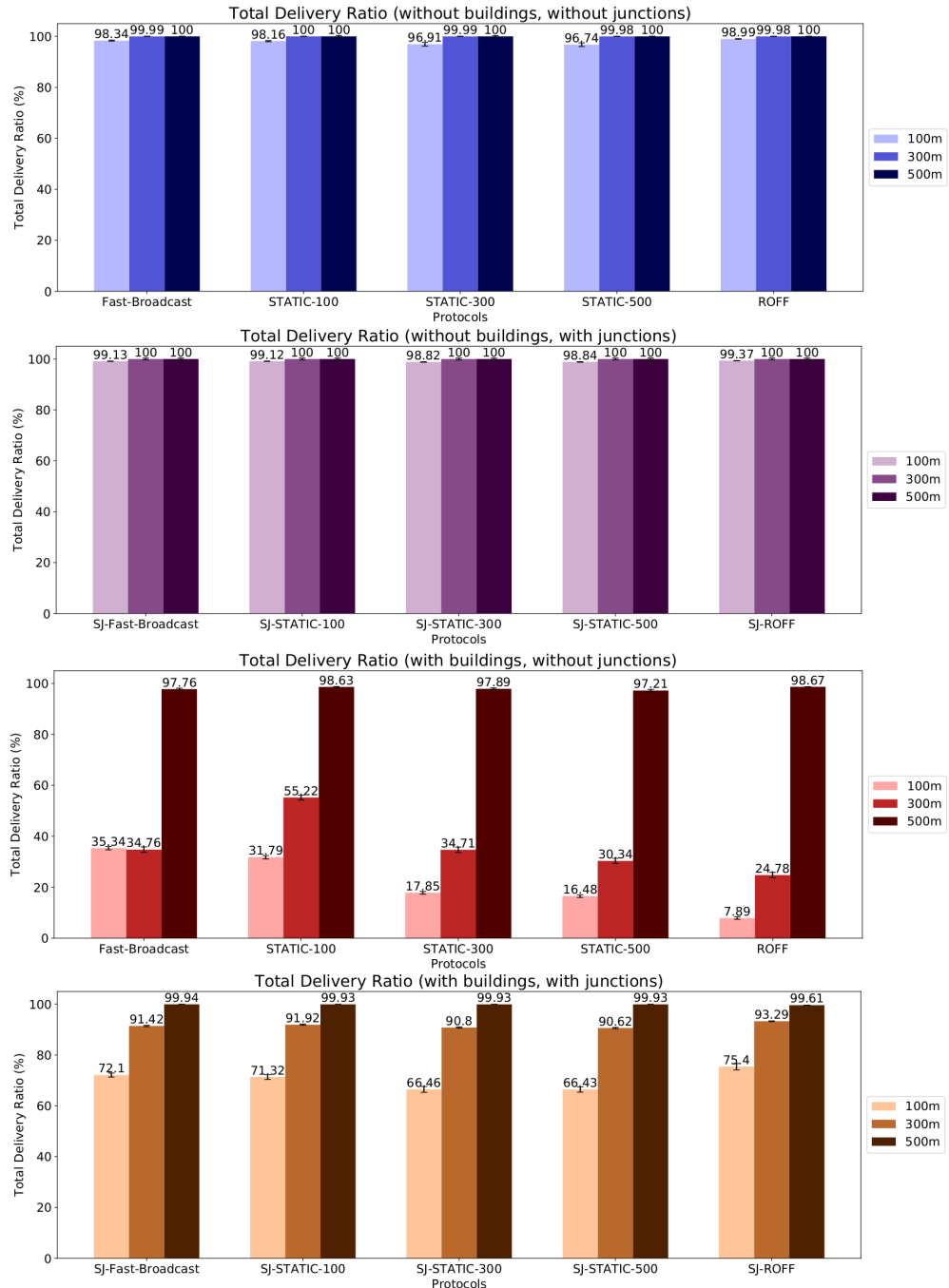


Figure 6.24: TDR for Padua urban scenario

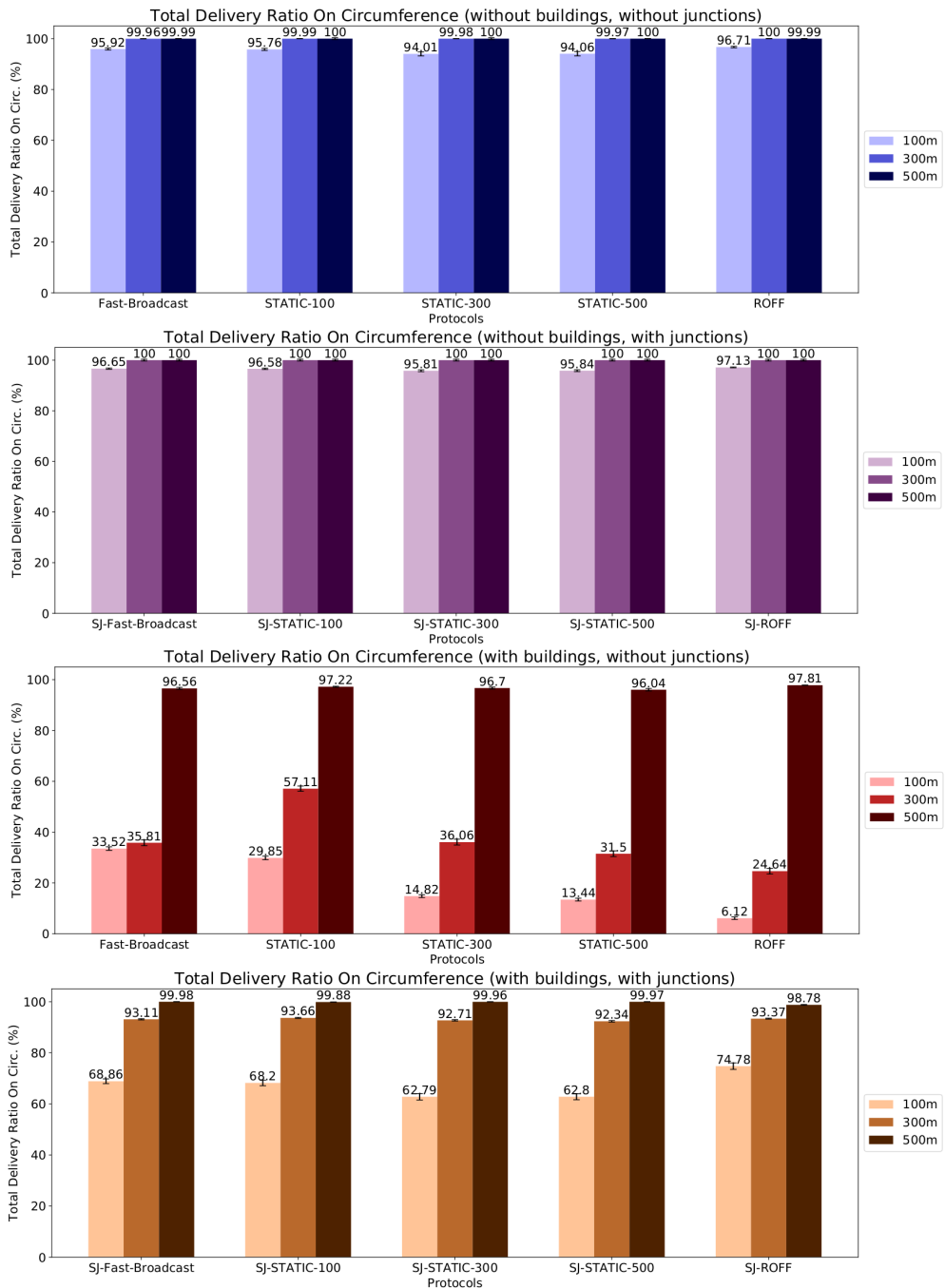


Figure 6.25: TDROC for Padua urban scenario

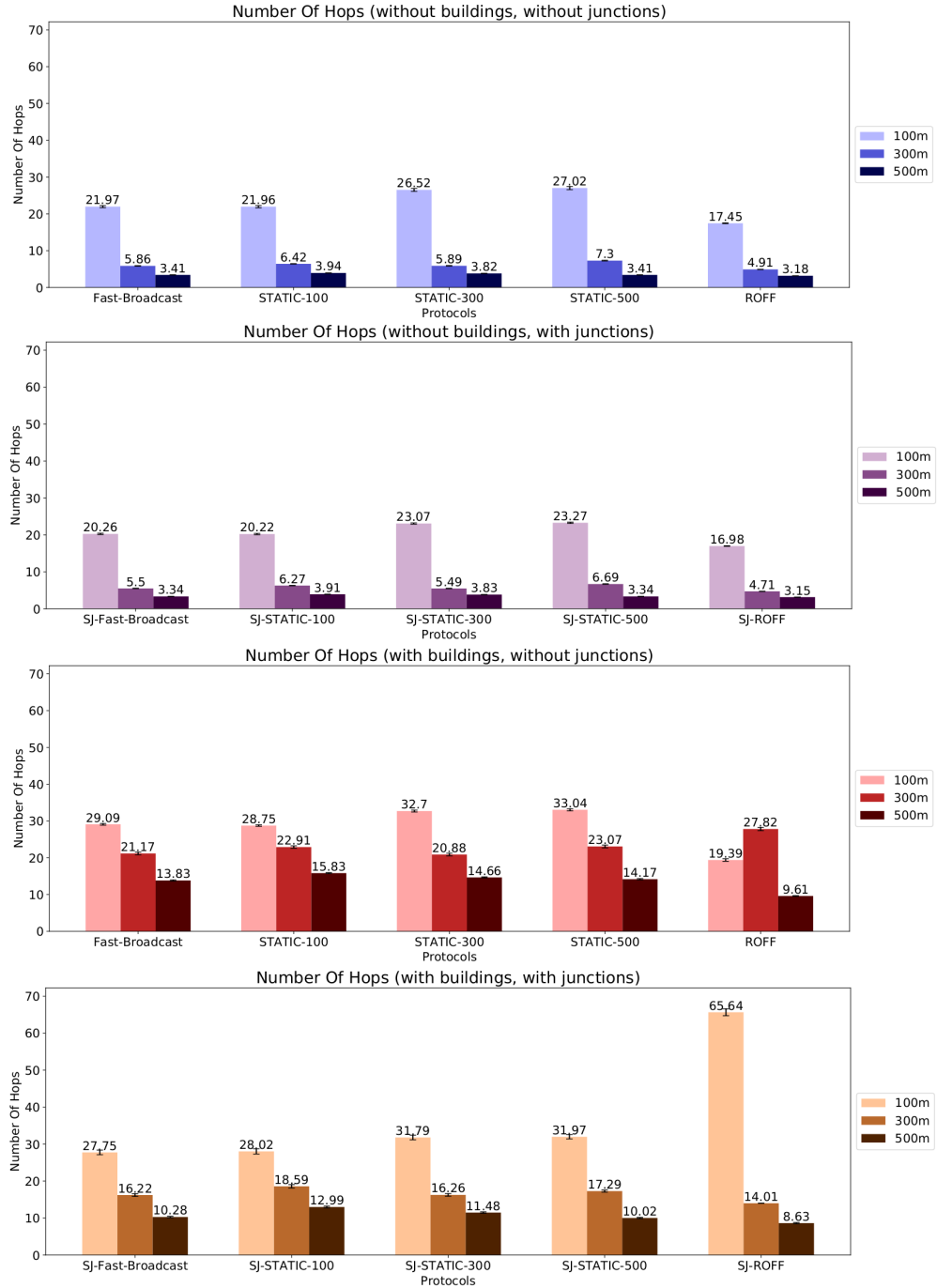
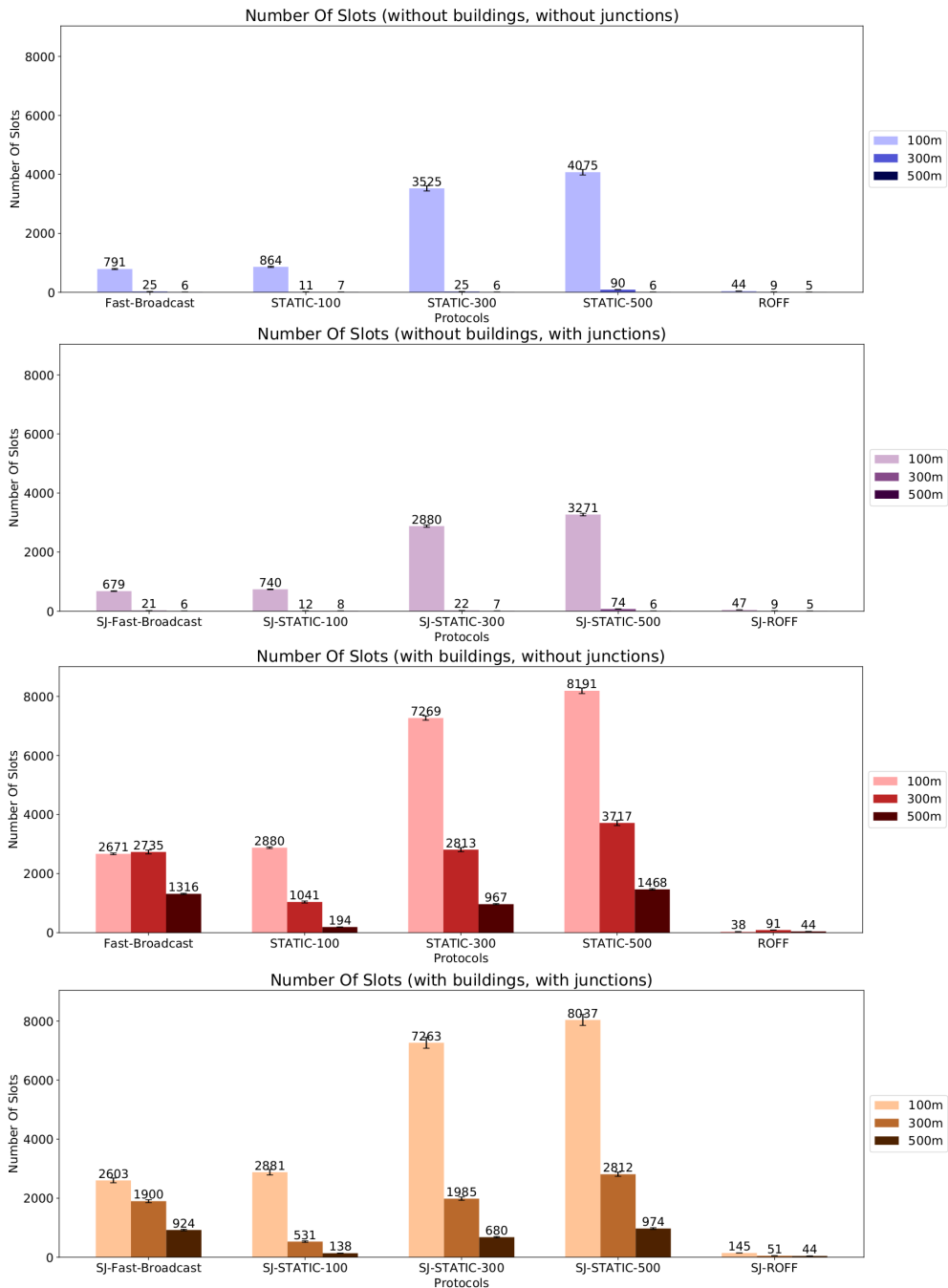
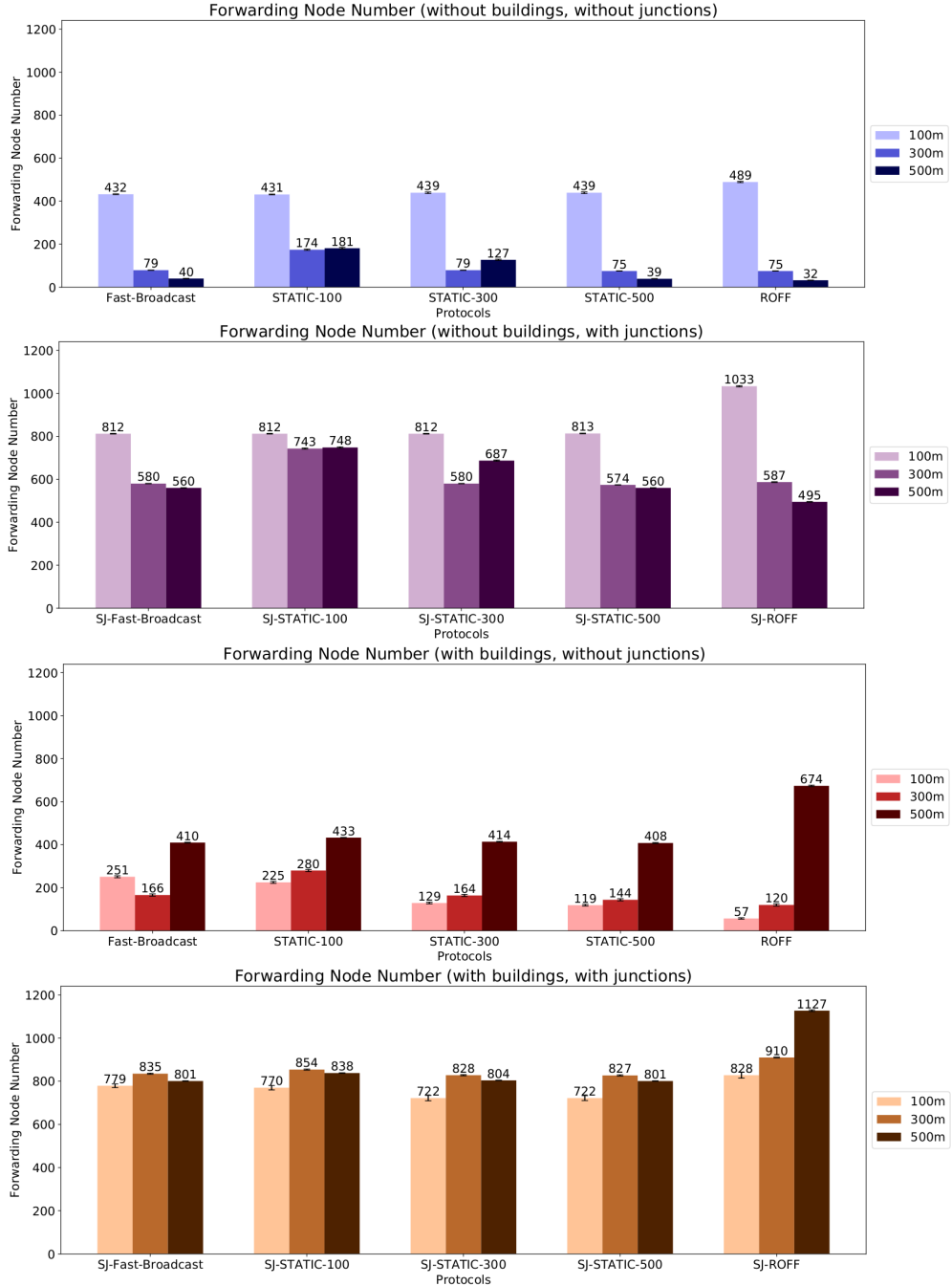


Figure 6.26: NOH for Padua urban scenario

**Figure 6.27:** NOS for Padua urban scenario



**Figure 6.28:** FNN for Padua urban scenario

In this scenario the effects of obstacle shadowing on delivery ratios is quite large, especially for the 300 and 500 meters cases, for all algorithms. We have a decrease in *TDR* (Figure 6.24 of around 65% for Fast-Broadcast in both transmission ranges when introducing buildings (first and third images), which results in quite poor performances. The Smart Junction variants of Fast-Broadcast manages to reach pretty good results

in total delivery ratio (fourth image), with 72.1% and 91.42% for the two transmission ranges. ROFF's results are even worse before the introduction of junctions, with  $TDR$  below 10% for the lowest transmission range. Even in this case, SJ-ROFF manages to improve the values, overcoming Fast-Broadcast's results.

The same observations hold true even for  $TDROC$  (6.24). Hence, the benefits of junctions are twofold even for this scenario regarding delivery ratios.

Concerning  $NOS$ , the increase due to the obstacle model is even more pronounced than the previous scenario for both algorithms. Due to the lower coverage, it is possible that the few messages who reach the circumference go through a very irregular path with and the one-hop progress is quite low. The introduction of junctions, as in the Los Angeles scenario, causes a decrease in  $NOH$ . One anomalous result is ROFF with 100 meters transmission range, whose values shoots up by more than 232\$ when comparing it with SJ-ROFF, and is much higher than SJ-Fast-Broadcast under the same conditions. This phenomenon might be due to the harsher vehicle distribution, obstacle and junction positioning which cause the signal to follow very long paths from the source to the circumference. With the other two transmission ranges, SJ-ROFF outperforms SJ-Fast-Broadcast.

Results for  $NOH$  and  $FNN$  are comparable with the one observed in previous scenarios.

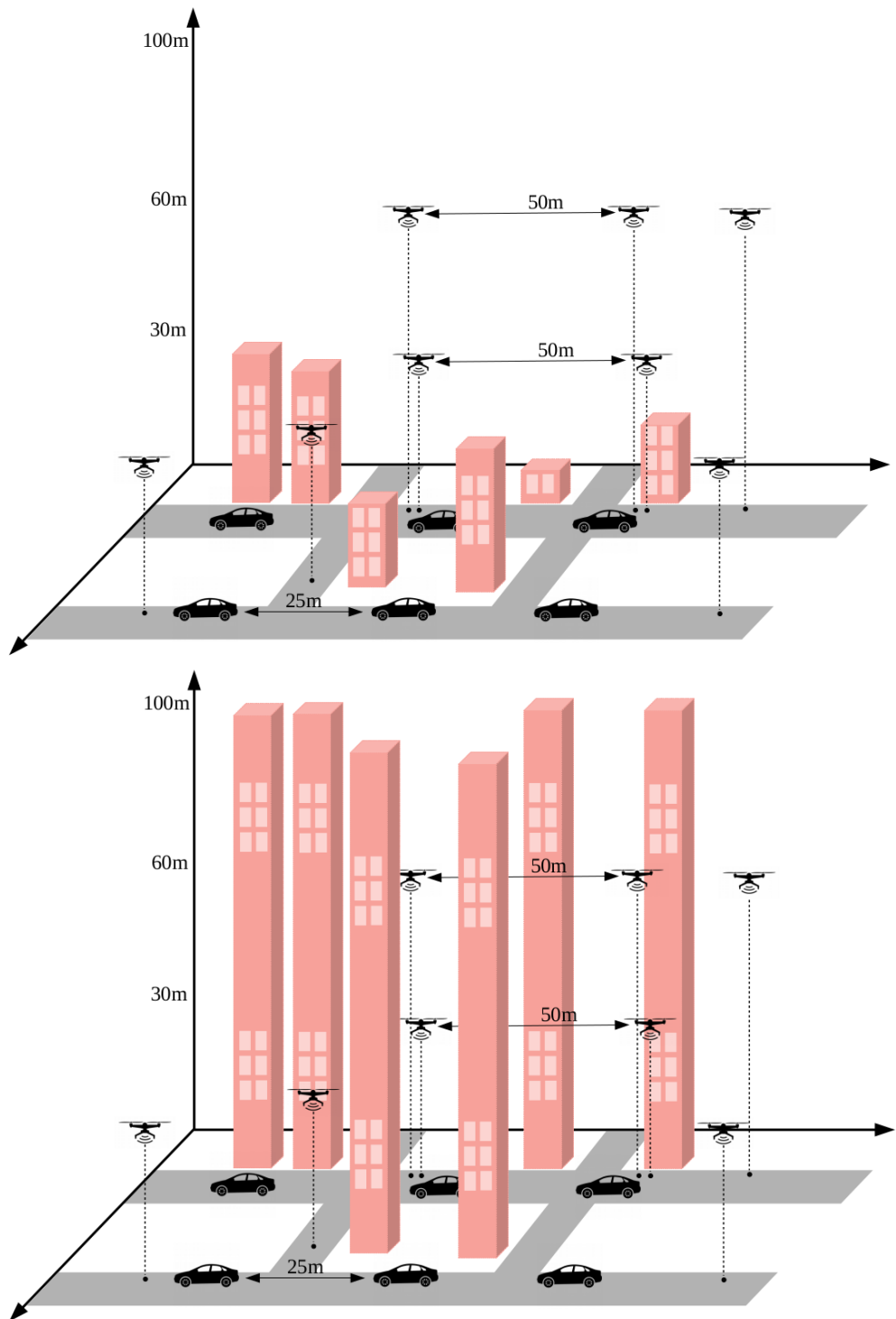
## 6.6 Los Angeles smart city scenario

After the comparison of the algorithms in 2D scenarios, we wanted to test them in a mixed 2D-3D scenario, where drones were also employed. Drones are utilized in many military and civil applications, such as agriculture, environmental protection and traffic flow control. It is foreseeable that they will also be a part of the development of the so called "smart cities", defined as "the use of discrete new technology applications such as RFID and Internet Of Things through more holistic conception of intelligent, integrated working that is closely linked to the concept of living and user generated services"[31]. One of the possible applications of drones in a urban scenario could make them help vehicles in Emergency Message Dissemination in order to exploit their greater field of view and bypass the effects of ground level shadowing and obstacles.

This scenario is built upon the Los Angeles urban scenario presented in Section 6.4. Two layers of drones were added to the ground level of vehicles:

- \* the first layer is situated at a height of 30 meters from ground level and employs 732 drones;
- \* the second layer, employing the same number of drones, is situated at a height of 60 meters.

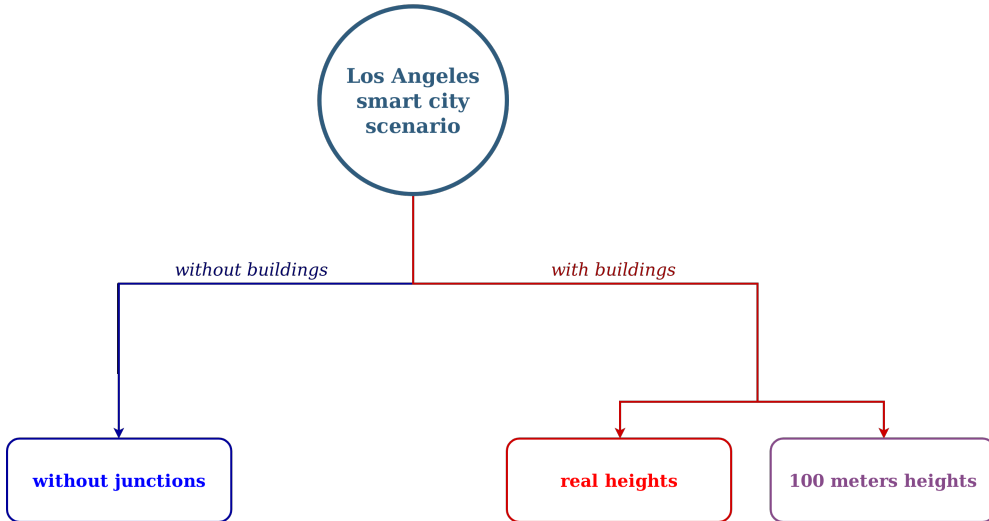
Drones are more spaced from one another than vehicles, with an average distance of 50 meters. We also wanted to test the effects of the Obstacle Model on drones in this scenario. Since the maximum height of a building in the data retrieved from OpenStreetMap is 21.9 meters, drones would not have their line of sight affected by the obstacles. Hence, as an additional configuration of this scenario, all buildings have been heightened to be taller than the second layer of drones (e.g. every building is high 100 meters). Figure 6.29 shows a representation of the two scenarios with buildings.



**Figure 6.29:** Los Angeles smart city scenario with real height buildings (top) and very high buildings (bottom)

The *TDR* metric considers delivery to all entities in the scenario (both vehicles and drones), while the circumference relative to the area of interest continues to be defined in the same way as the 2D Los Angeles urban scenario, hence TDROC concerns exclusively vehicles.

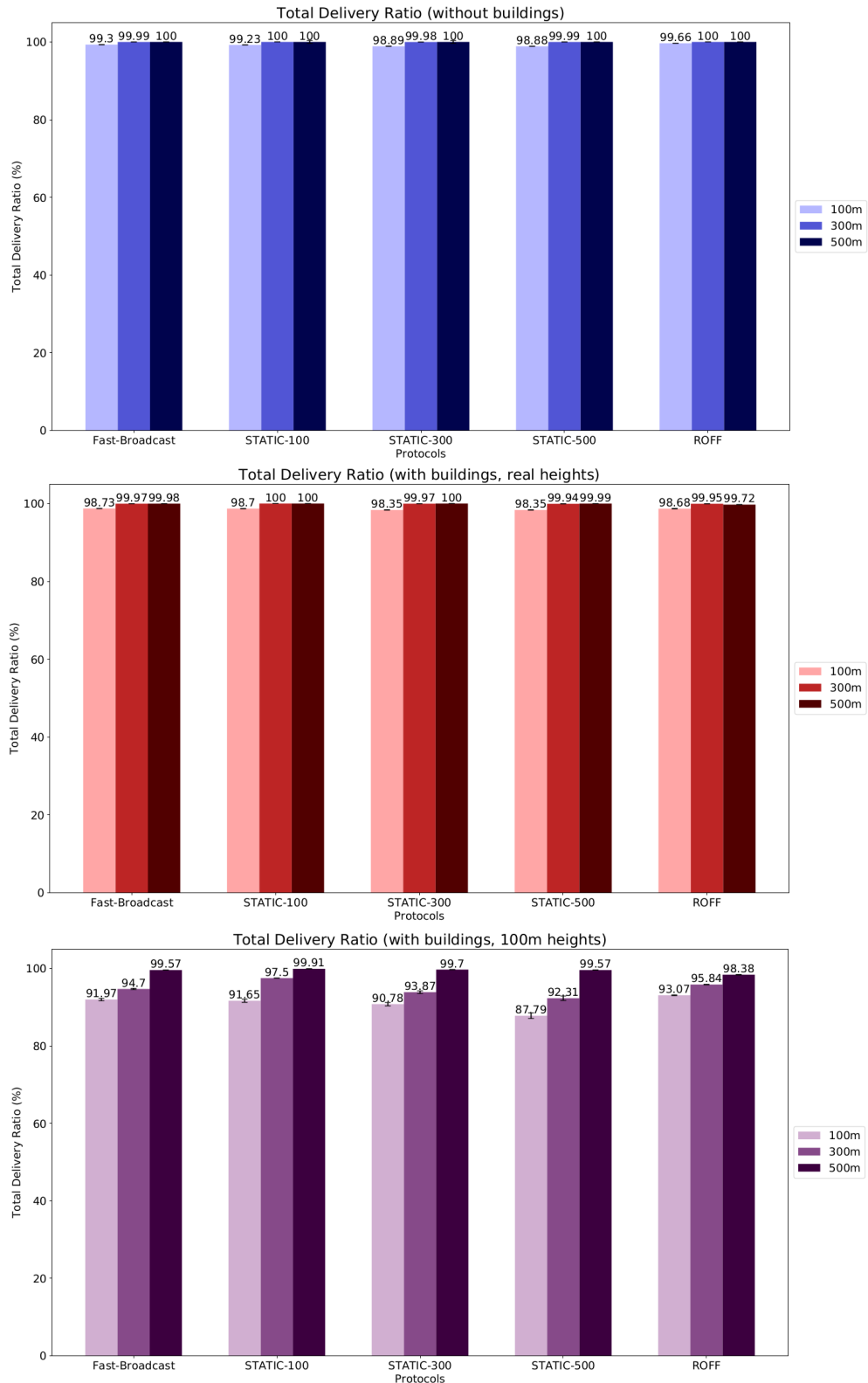
All configurations are reported in Figure 6.30, whose colors will guide the following graph results. Table 6.10 reports all the scenario settings.



**Figure 6.30:** Test overview of Los Angeles smart city scenario

Parameter	Value
Scenario configuration	
Circumference radius	1000 m
Number of vehicles	1465
Distance between vehicles	25 m
Source of alert message position	Center
Number of drone layers	2
Height of first drone layer	30 m
Number of drones in first layer	732
Height of second drone layer	60 m
Number of drones in second layer	732
Distance between drones (average)	50 m
Number of buildings	8241
Building heights	Real, 100 m
Mobility model	ns3::ConstantPosition
Network configuration	
Shadowing model	Obstacle Shadowing
Junction modeling	No
Number of simulations per configuration	5000

**Table 6.10:** Los Angeles urban scenario configuration

**Figure 6.31:** TDR for Los angeles smart city scenario

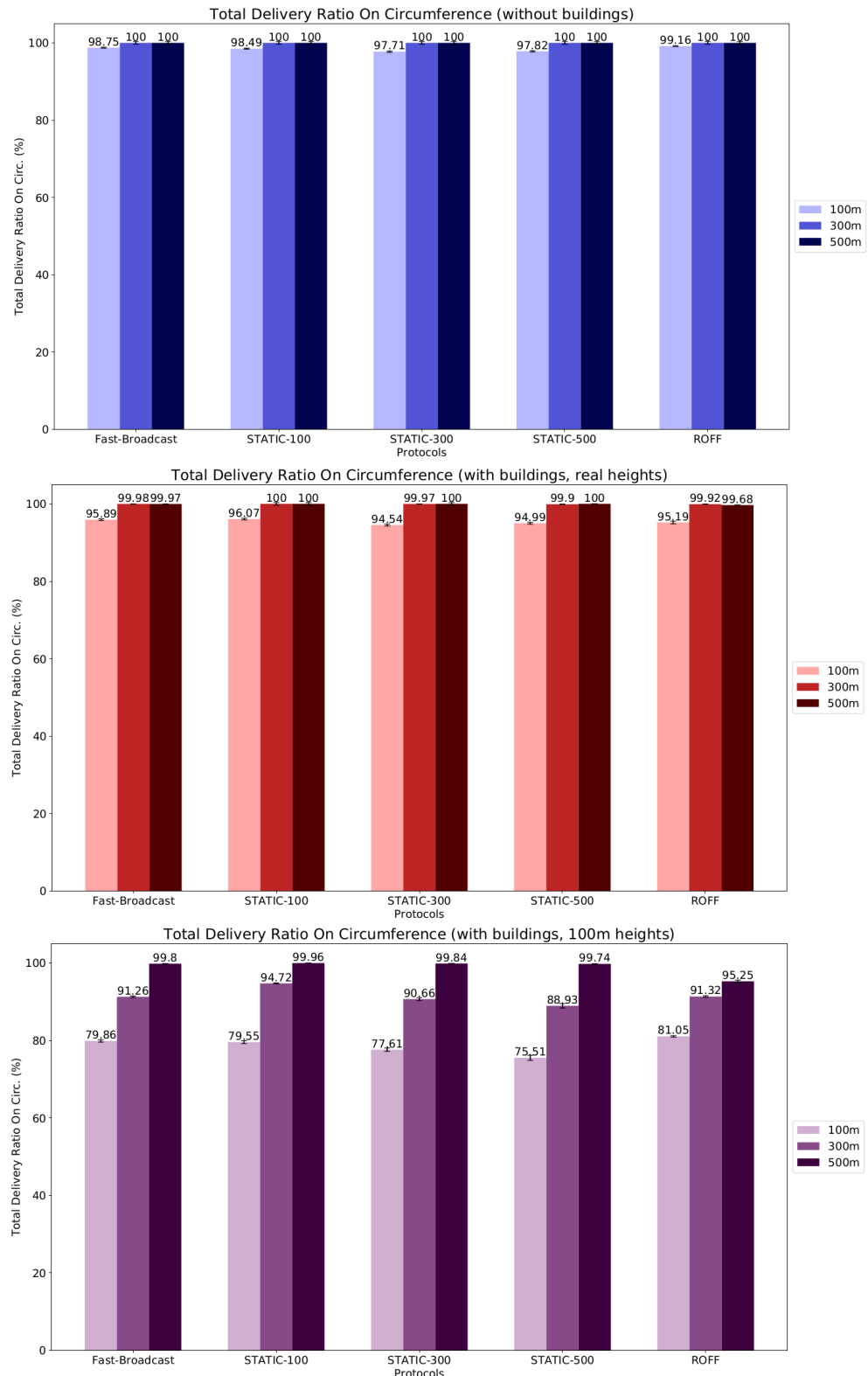
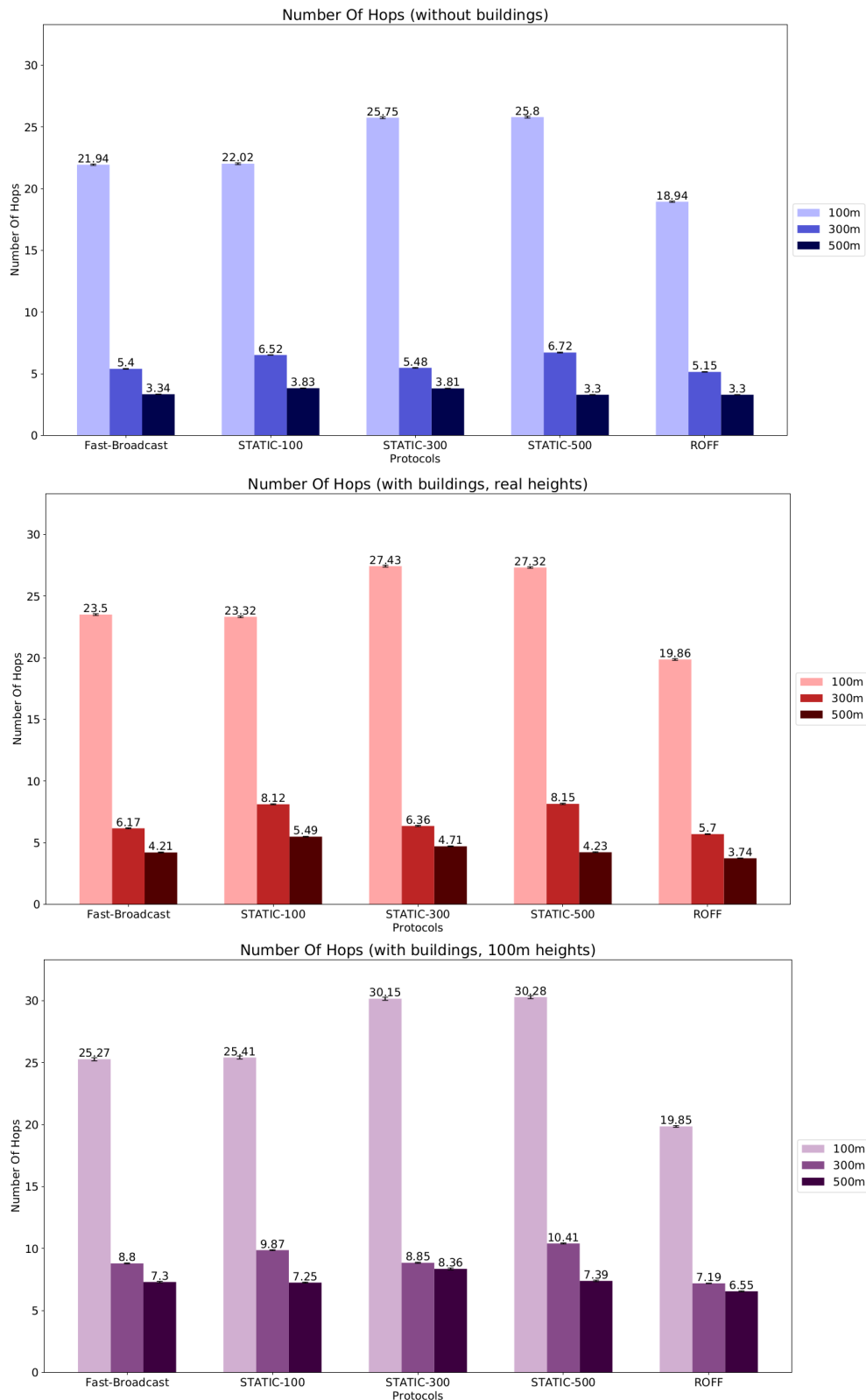


Figure 6.32: TDROC for Los angeles smart city scenario

**Figure 6.33:** NOH for Los angeles smart city scenario

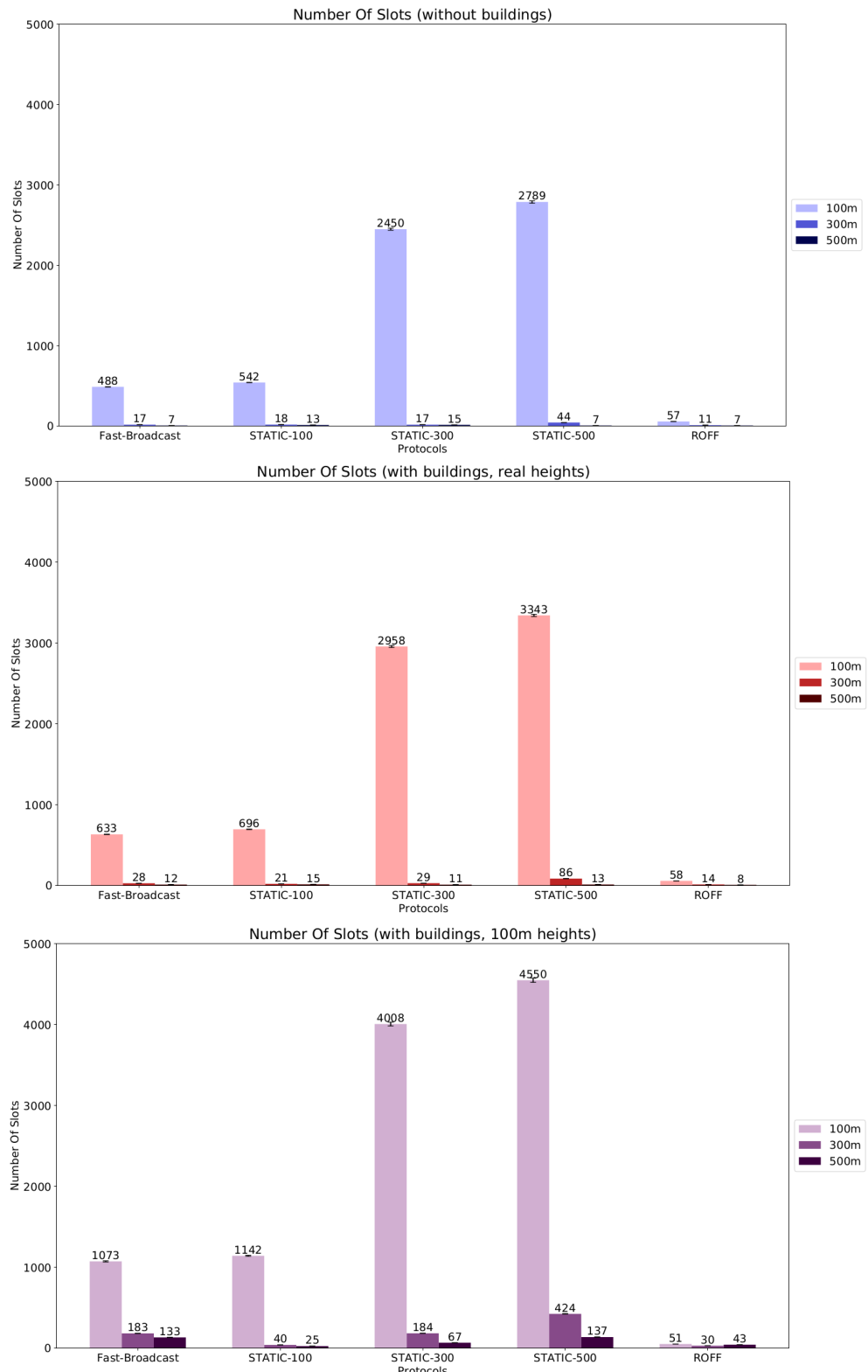
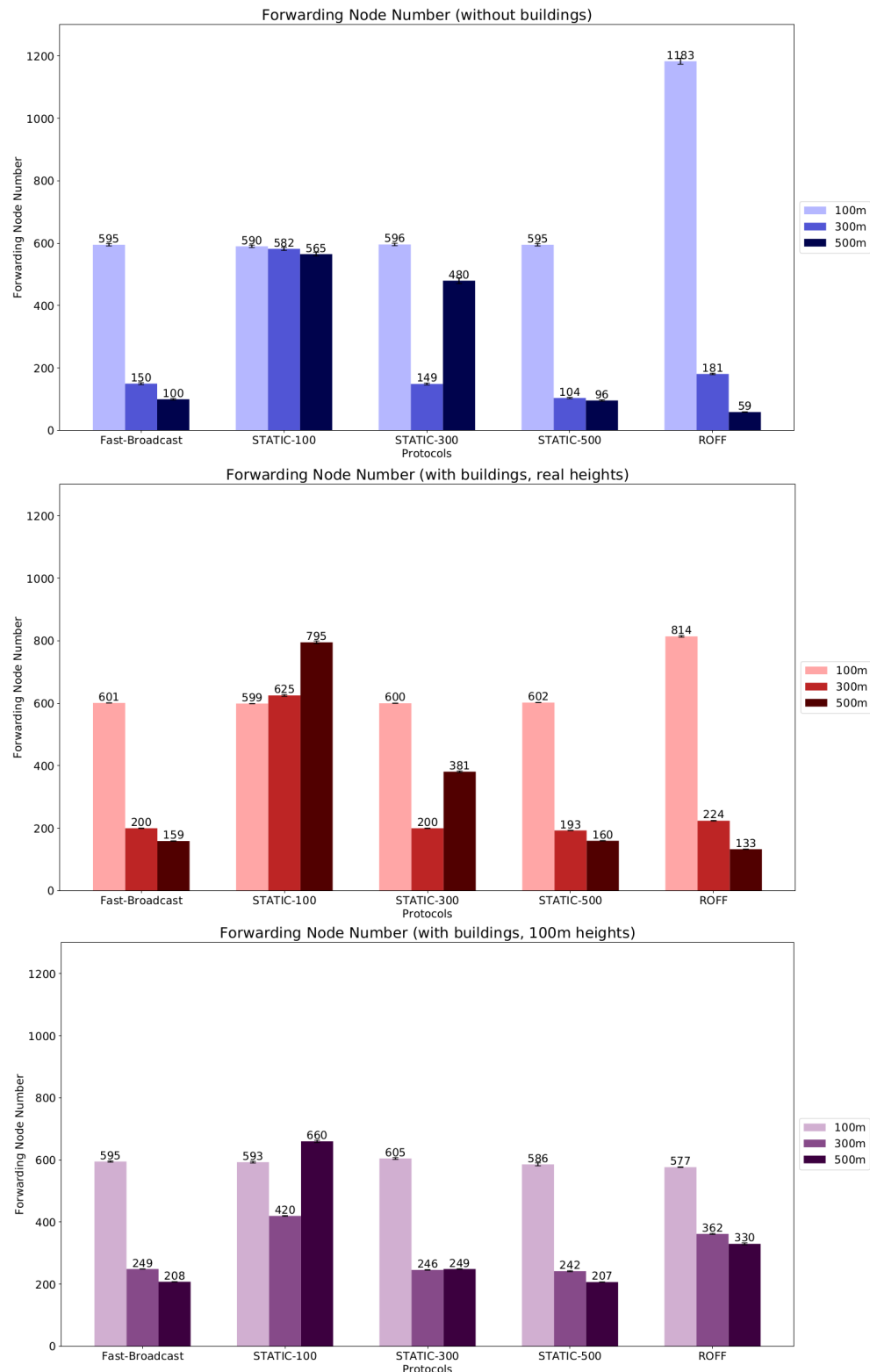


Figure 6.34: NOS for Los angeles smart city scenario

**Figure 6.35:** FNN for Los angeles smart city scenario

Judging by the results shown in Figure 6.31 6.32, drones seem to help a lot in signal propagation thanks to their altitude. In fact, the scenario without buildings and with real-height buildings yield comparable results. In the third scenario, when the obstacles's heights exceed the second drone layer's height, the shadowing effect is more pronounced for lower transmission range configurations. Overall the total delivery ratio is still acceptable, with neither Fast-Broadcast or ROFF falling under 90%. *TDROC* in configurations with 100 meters transmission range is affected in a greater way. In fact, as specified above, in this scenario the *TDROC* metric is only about vehicles on the ground, so the greater shadowing due to high buildings yields the expected results.

The effects of obstacles on *NOH* (Figure 6.33) are consistent with those observed in previous scenarios. The metric's value further increases with high buildings, since the signal probably propagates more often on the ground instead of covering larger distances thanks to inter-street drone to vehicle communications. With high buildings the propagation is restrained inside the road, hence the effects of drones are much more limited.

Concerning *NOS* (Figure 6.34, we can notice that the increase is much higher when going from obstacles with real heights to 100 meters high obstacles. For example, focusing on the 300 meters transmission range configuration, for Fast-Broadcast we have an increase of 64.71% from the first to the second image and of 553.57% from the second to the third. For ROFF those values are 27.27% and 114.29%. Once again, this phenomenon could be due to the same effect explained in the previous paragraph: with inter-street communication heavily impeded and the increase in *NOH*, *NOS* increases as a consequence.

Focusing on the 300 and 500 meters transmission range configurations, *FNN* (Figure 6.35) increases for Fast-Broadcast and ROFF, both when going from the first image to the second and from the second to the third. This is expected, since in both cases the shadowing effects are increased and a greater number of forwarders is necessary to cover the same area. For the 100 meters case, we can notice some anomalous results: Fast-Broadcast's value stays around the same number, while ROFF's decreases considerably the last two scenarios. The same observation about collision areas in ROFF introduced in Section 6.3 might explain this behaviour, but it would affect in a similar way also the 300 and 500 meters configurations. Hence, this phenomenon needs more thorough testing in order to be explained.

## 6.7 Hello Message forging scenario

During our analysis we wanted to test how vulnerable the algorithms were to attacks where some malicious attacker tries to increase the end to end delay (the *NOS* metric in our case). The attack consists in sending fake Hello Messages to vehicles during the Estimation Phase in order to mess with their estimations. We tested two different levels of severity on the attack: a low severity one, reported in Section 6.7.1, and a high severity one, reported in Section 6.7.2. Several percentages of affected vehicles (i.e. the vehicles which receive the forged hello message bursts) ranging from 0 to 50% have been tested. Both tests were carried out using the Los Angeles urban scenario without the effect of the Obstacle model. Only Fast-Broadcast and ROFF algorithms (and their Smart Junction variants) were tested.

### 6.7.1 Low severity attack

In the low severity attack the effect of 100 different forged Hello Messages was tested. Each forged message reports a fake position such that the detected distances by the affected node (the receiver) ranges from 301 ( $txRange + 1$ ) to 40 ( $txRange + 100$ ). Parameters for this scenario are reported in Table 6.12.

Parameter	Value
Scenario configuration	
Vehicles affected by forging	0, 10, 20, 30, 40, 50 %
Number of forged messages	100
Forged distances	301, 302,...,400
Network configuration	
Transmission power	4.6 dBm
Transmission range	300
Shadowing model	No
Junction modeling	No
Number of simulations per configuration	1000

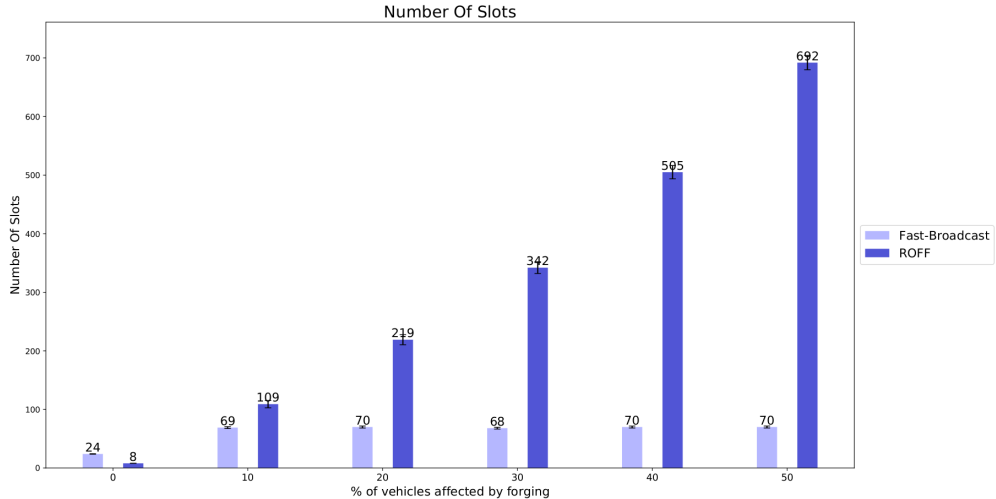
**Table 6.12:** Low severity forging attack scenario configuration based on Los Angeles urban scenario

### 6.7.2 High severity attack

In the high severity attack the number of forged Hello Messages was increased to 1000. Moreover, even the fake positions included in the messages have been increased in a way such that the receivers detected distances ranging from 301 to 1300 meters. Parameters for this scenario are reported in Table 6.14.

Parameter	Value
Scenario configuration	
Vehicles affected by forging	0, 10, 20, 30, 40, 50 %
Number of forged messages	1000
Forged distances	301, 302,...,1300
Network configuration	
Transmission power	4.6 dBm
Transmission range	300
Shadowing model	No
Junction modeling	No
Number of simulations per configuration	1000

**Table 6.14:** High severity forging attack scenario configuration based on Los Angeles urban scenario



In this case it is possible to observe that ROFF is affected a lot more than Fast-Broadcast. Even when jumping from 0% to only 10% of affected nodes, ROFF's *NOS* increases more than tenfold, with a value 57.97% higher than Fast-Broadcast under the same conditions. Fast-Broadcast is affected as well when going from 0% to 10%, but the increase is much lower. Higher percentages of affected vehicles increase the Number Of Slots even more for ROFF, while Fast-Broadcast caps out after 10% and its metric's value does not increase.

## 6.8 Different vehicle density scenario

The previous scenarios all employed a distance between vehicles equal to 25 meters. Real vehicle distributions are obviously different than this idealistic scenario. Moreover,

good broadcasting algorithms should work well regardless of vehicle distribution and density. Hence, in this section different vehicle distribution (generated by different distances between vehicles) have been tested. The scenario is based on the Padua urban scenario (Section 6.5, with vehicle distances ranges from 5 to 45 meters. Parameters are reported in Table 6.16.

Parameter	Value
Scenario configuration	
Distance between vehicles	5, 15, 25, 35, 45
Number of vehicles	4975, 2856, 1776, 1318, 1072
Network configuration	
Transmission powers	-7.0, 4.6, 13.4
Transmission range	100, 300, 500
Shadowing model	No
Junction modeling	No
Protocols configuration	
FB contention window	[32, 1024]
ROFF distance range ( $k$ parameter)	1
Number of simulations per configuration	1200

**Table 6.16:** Different vehicle densities scenario configuration based on Padua urban scenario

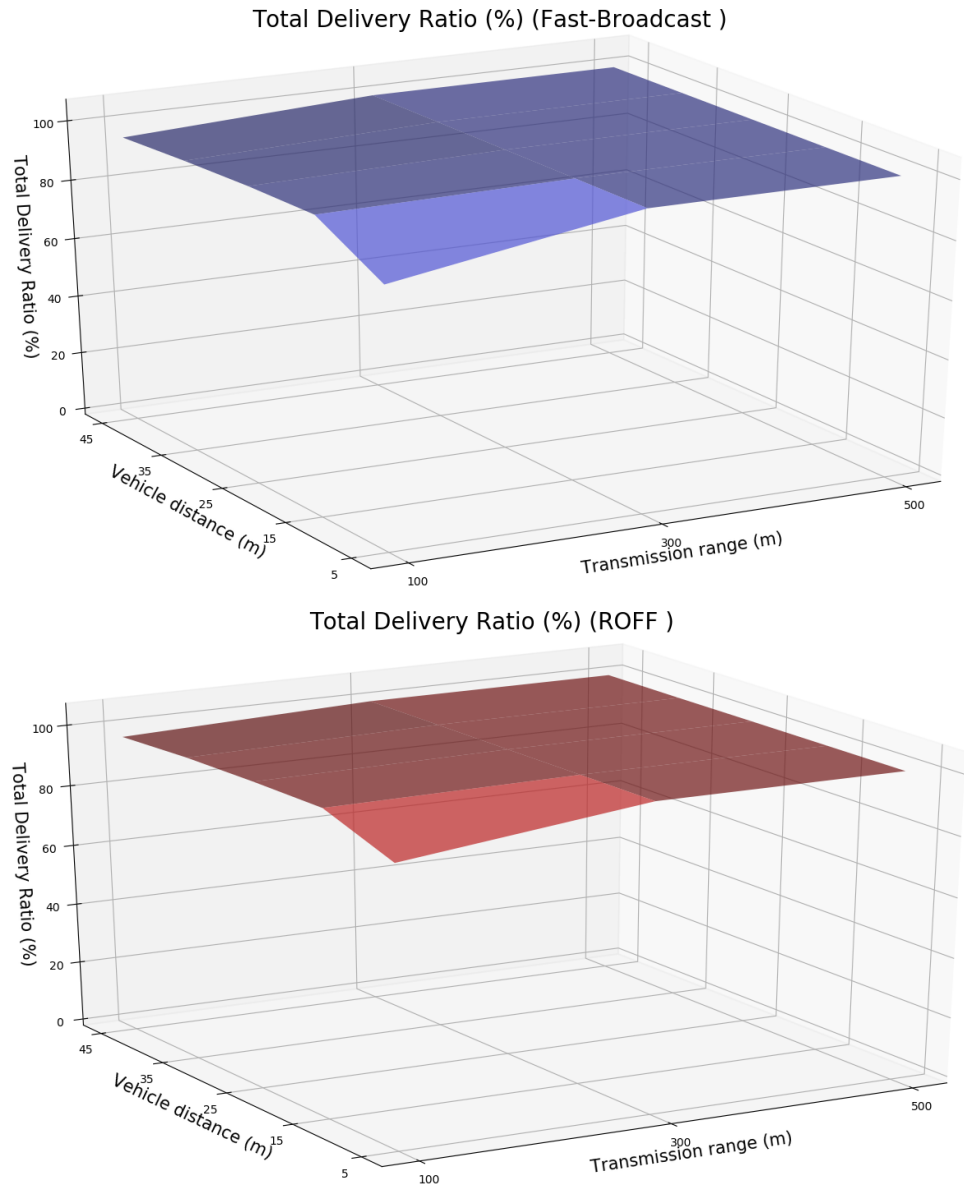


**Figure 6.36:** TDR for Fast-Broadcast (top) and ROFF (bottom) with different distance between vehicles and transmission ranges

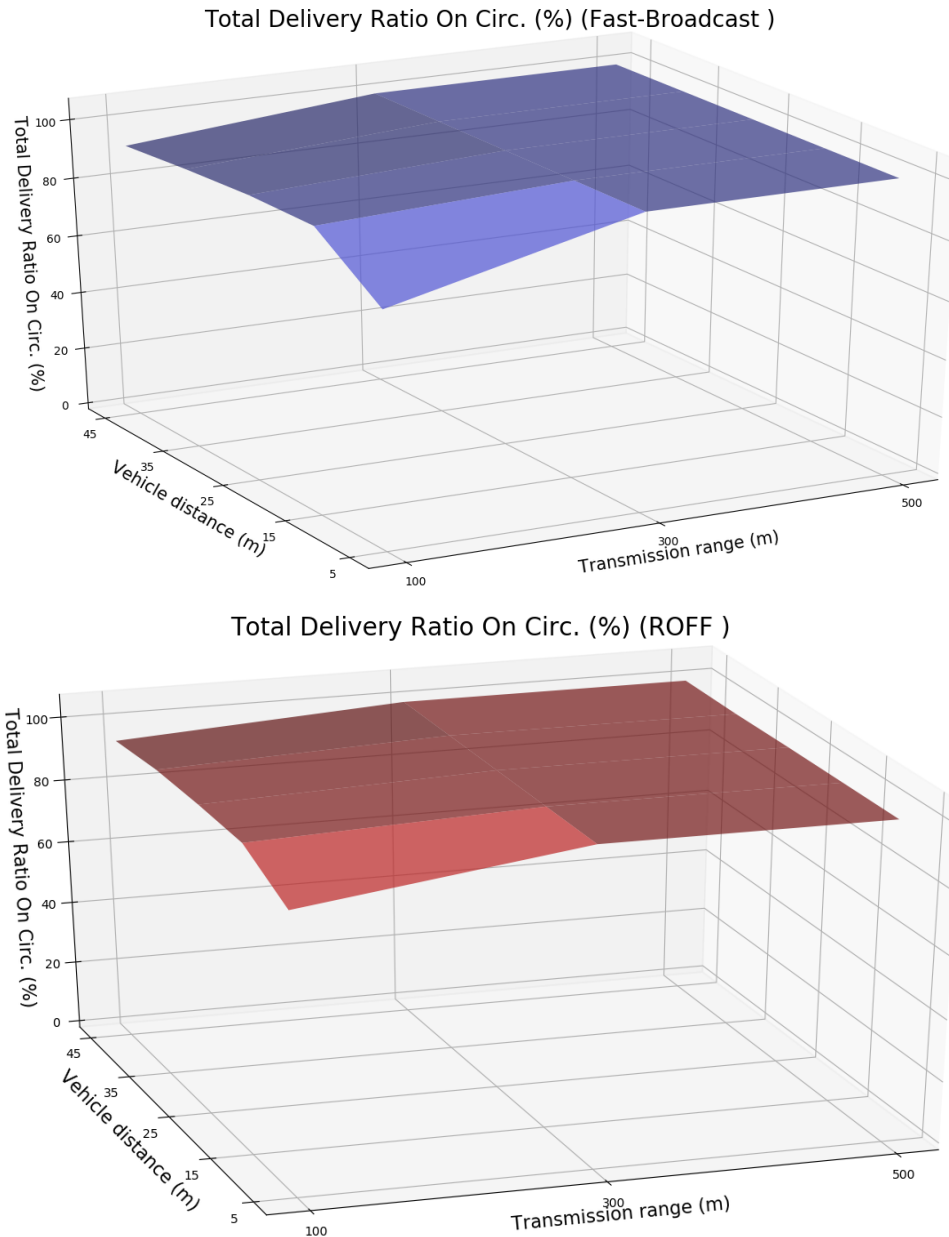


**Figure 6.37:** TDROC for Fast-Broadcast (top) and ROFF (bottom) with different distance between vehicles and transmission ranges

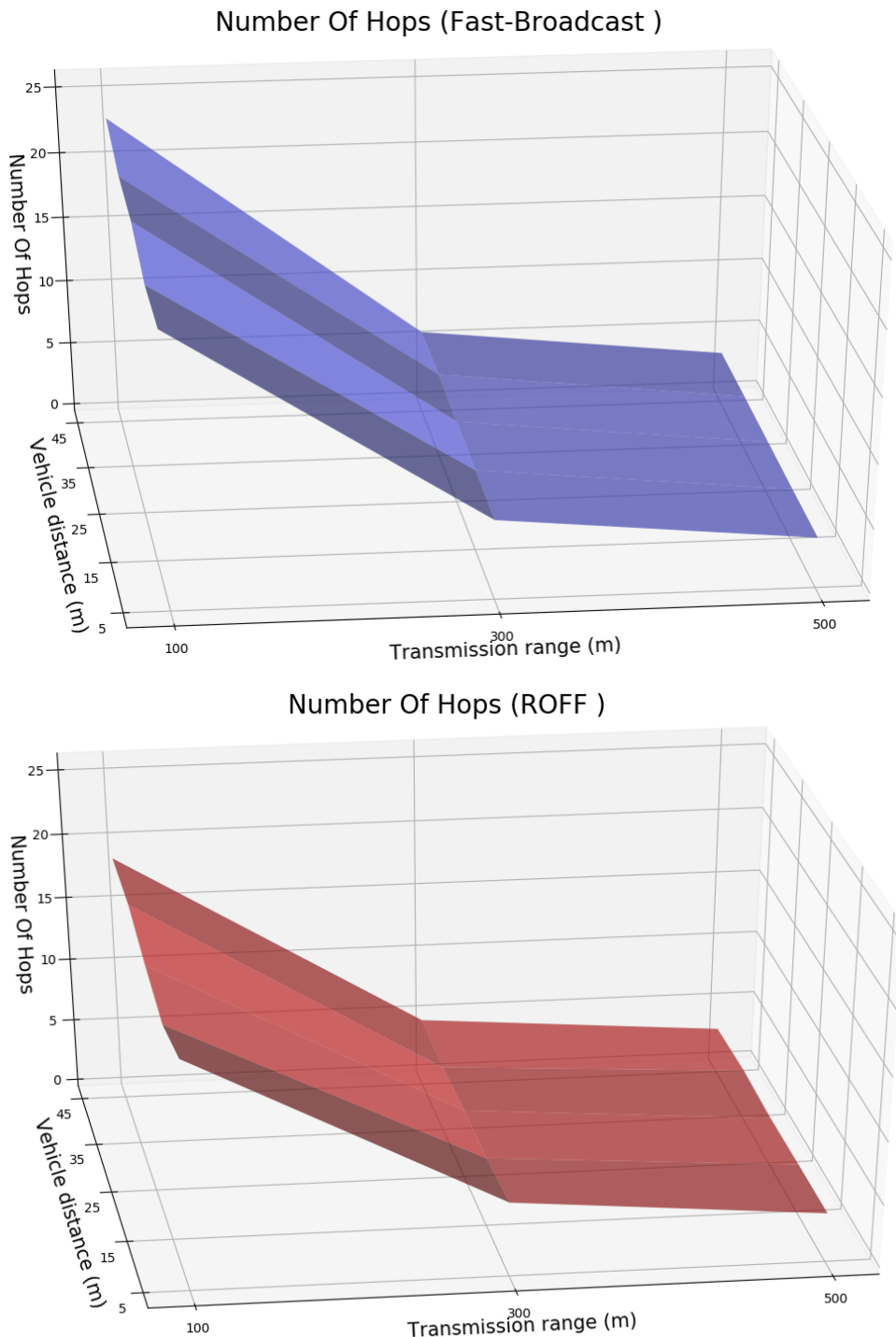


**Figure 6.38:** NOH for Fast-Broadcast (top) and ROFF (bottom) with different distance between vehicles and transmission ranges

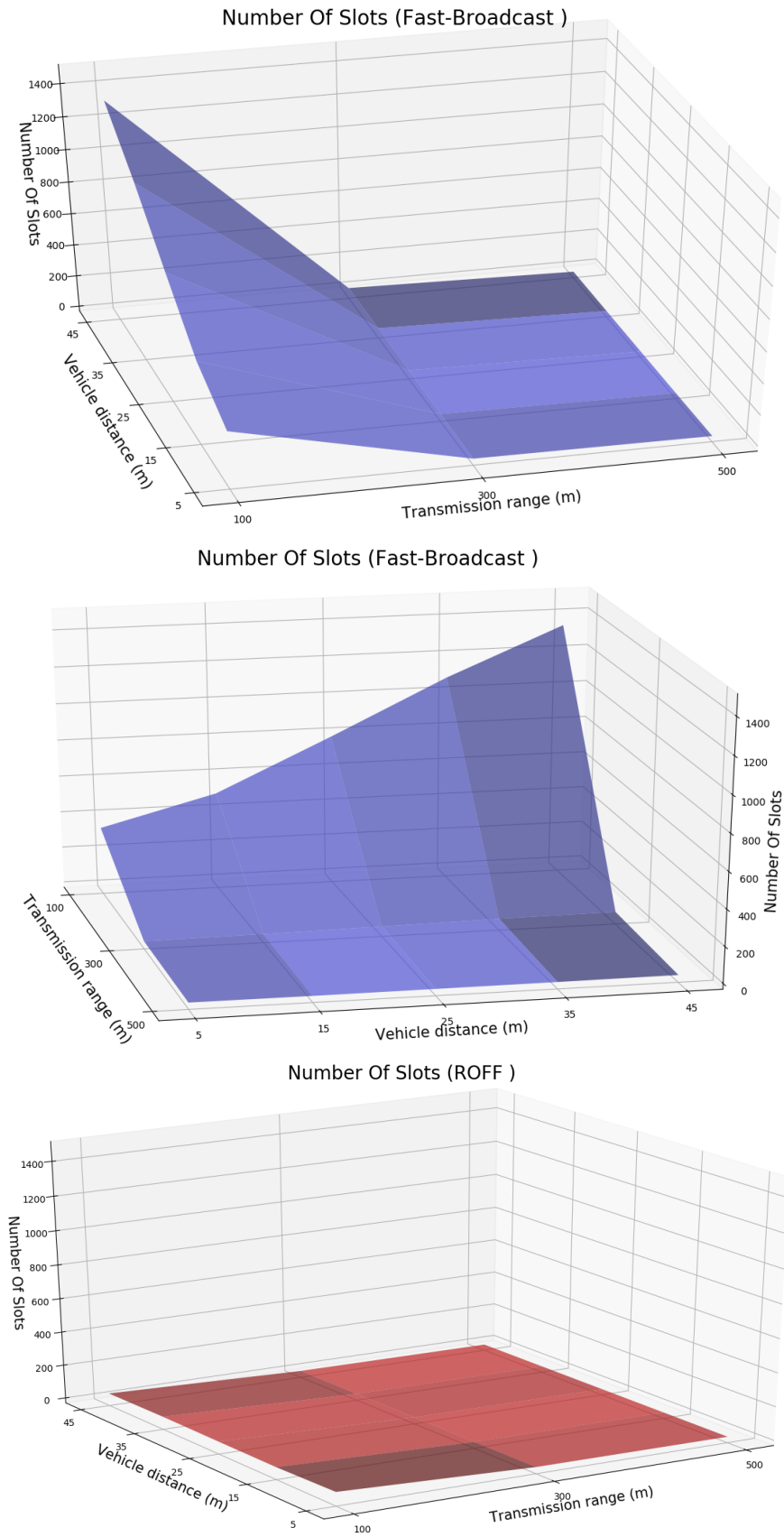


**Figure 6.39:** NOS for Fast-Broadcast (top) and ROFF (bottom) with different distance between vehicles and transmission ranges

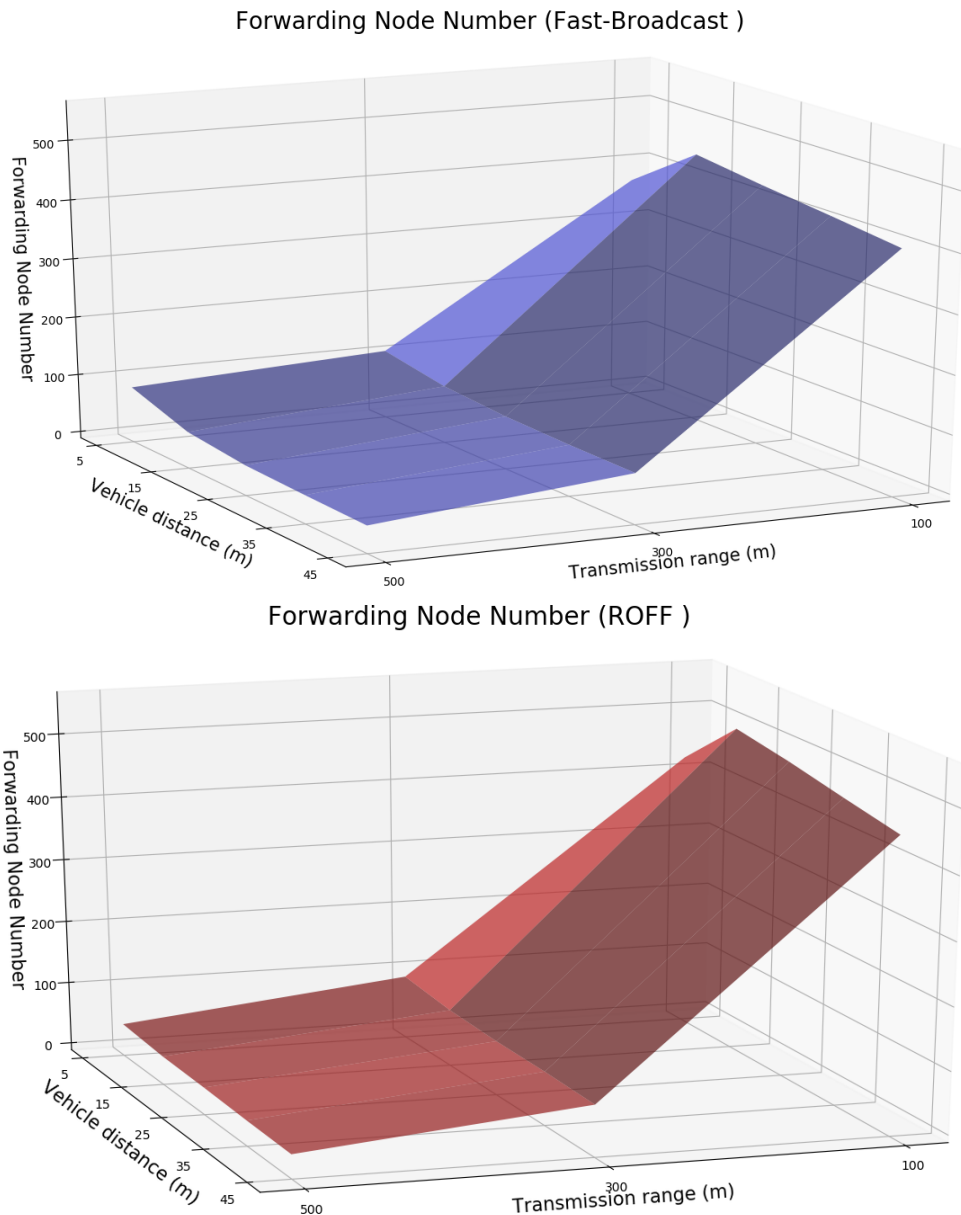


**Figure 6.40:** *FNN for Fast-Broadcast (top) with different distance between vehicles and transmission ranges*

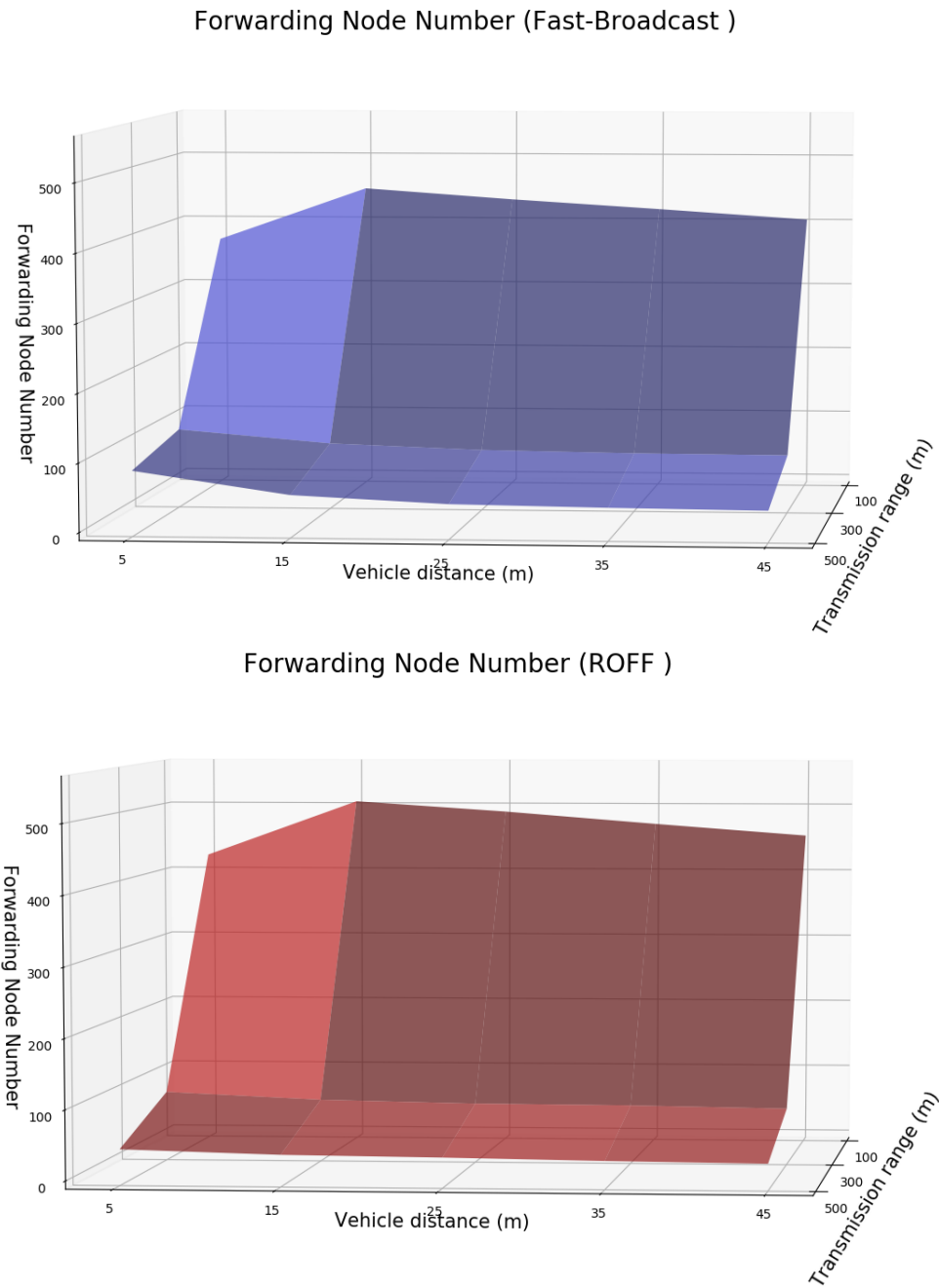


**Figure 6.41:** FNN for Fast-Broadcast (top) and ROFF (bottom) with different distance between vehicles and transmission ranges (alternative angle)

Figure 6.36 and 6.36 show optimal delivery ratios both total and on the circumference. We can see a small drop in the metrics' values for the 100 meters transmission range and 5 meters vehicle distance configurations. This might be due to higher collisions near the forwarders, which cause the signal to propagate unevenly to all areas of the

scenario. Despite this, the values are still acceptable for both algorithms.

Concerning NOS (Figure 6.38), we notice that ROFF achieves better results in every case. For both algorithms, different vehicle densities do not seem to affect the number of hops by much. This means that the algorithms manage to designate a distant PFC as next forwarder in both high and low density scenarios, with ROFF designation working better as noticed in previous tests.

Figure 6.39 show that *NOS* decreases as the transmission range decreases for Fast-Broadcast. This phenomenon is also due to the decrease in *NOH* noticed in the previous paragraph. We notice how *NOS* increases as the vehicle distance increases (hence the density decreases) under the 100 meters

## 6.9 Smaller contention window

All previous tests involving Fast-Broadcast have been carried out with a contention window ranging from 32 to 1024 slots. This interval is so wide in order to guarantee correct waiting time calculation even in high vehicle density scenarios. Fast-Broadcast's results on Number Of Slots could benefit from using a narrower contention window. In this scenario, based on the Los Angeles urban scenario, a contention window ranging from 16 to 128 slots will be utilized. Parameters for this scenario are reported in Table 6.18.

Parameter	Value
Network configuration	
Shadowing model	No
Junction modeling	No
Protocols configuration	
FB contention window	[16, 128], [32, 1024] slot
ROFF distance range ( $k$ parameter)	1
Number of simulations per configuration	600

**Table 6.18:** Contention window scenario configuration based on Los Angeles urban scenario

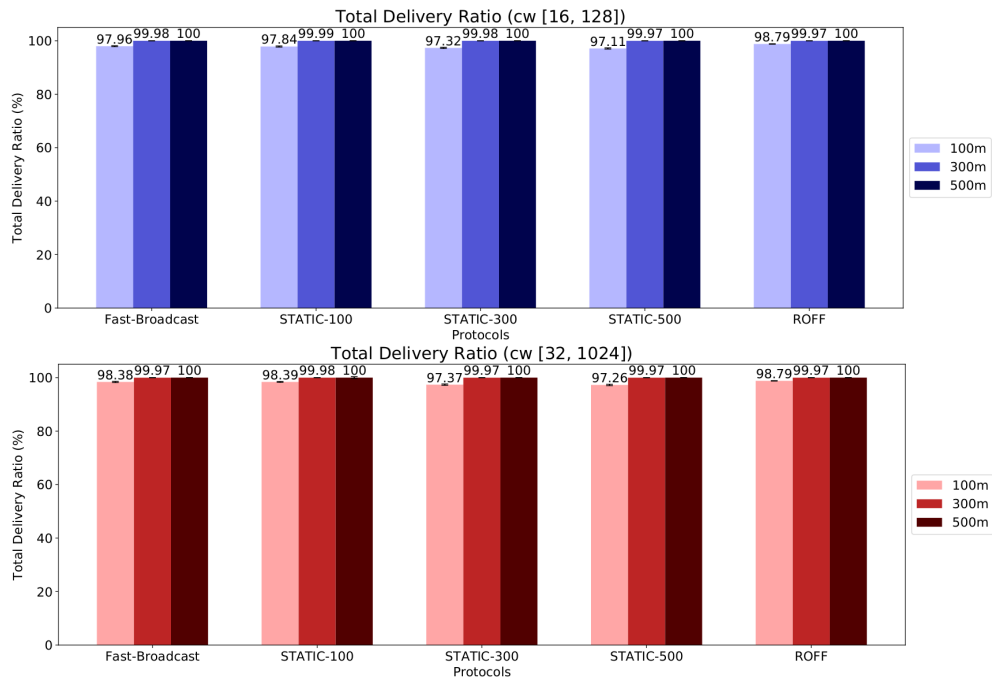


**Figure 6.42:** TDR for [16, 128] contention window (top) and [32, 1024] contention window (bottom)

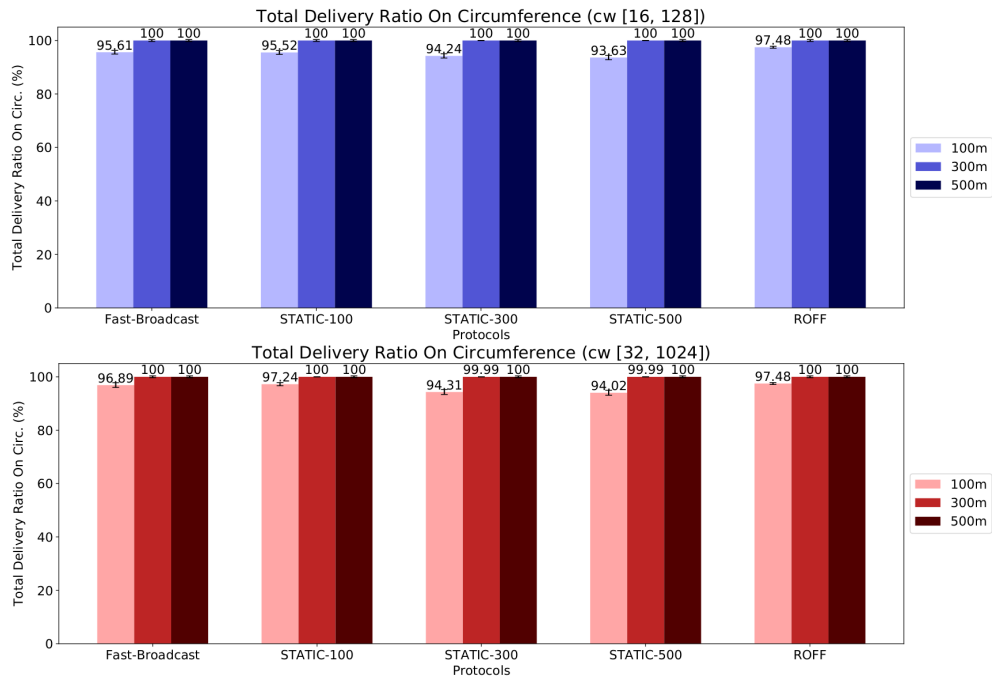


**Figure 6.43:** TDROC for [16, 128] contention window (top) and [32, 1024] contention window (bottom)

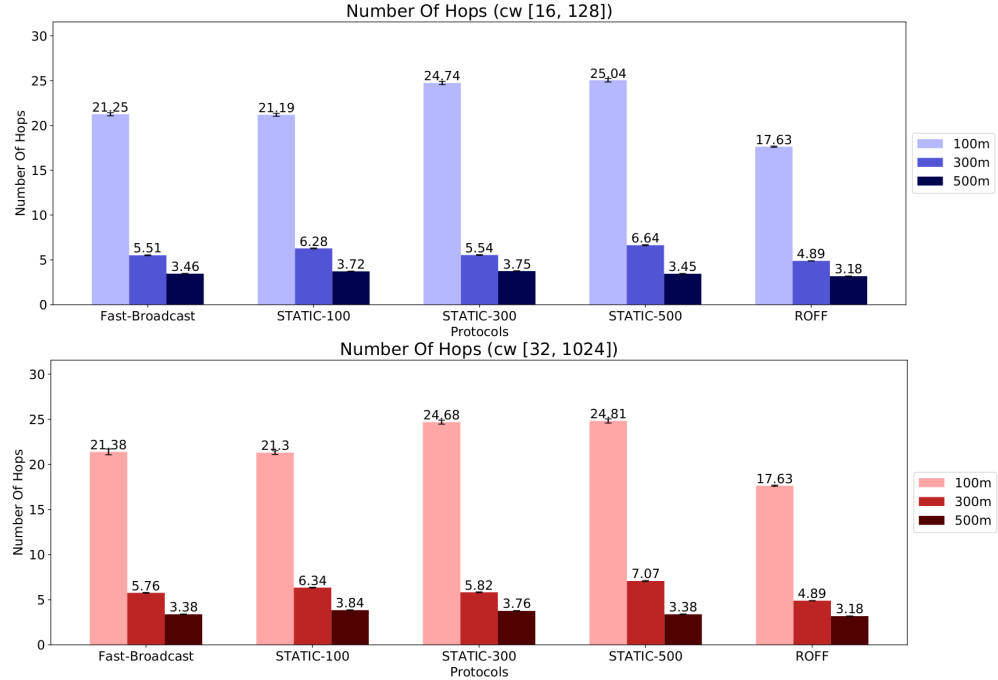


**Figure 6.44:** NOH for [16, 128] contention window (top) and [32, 1024] ] contention window (bottom)

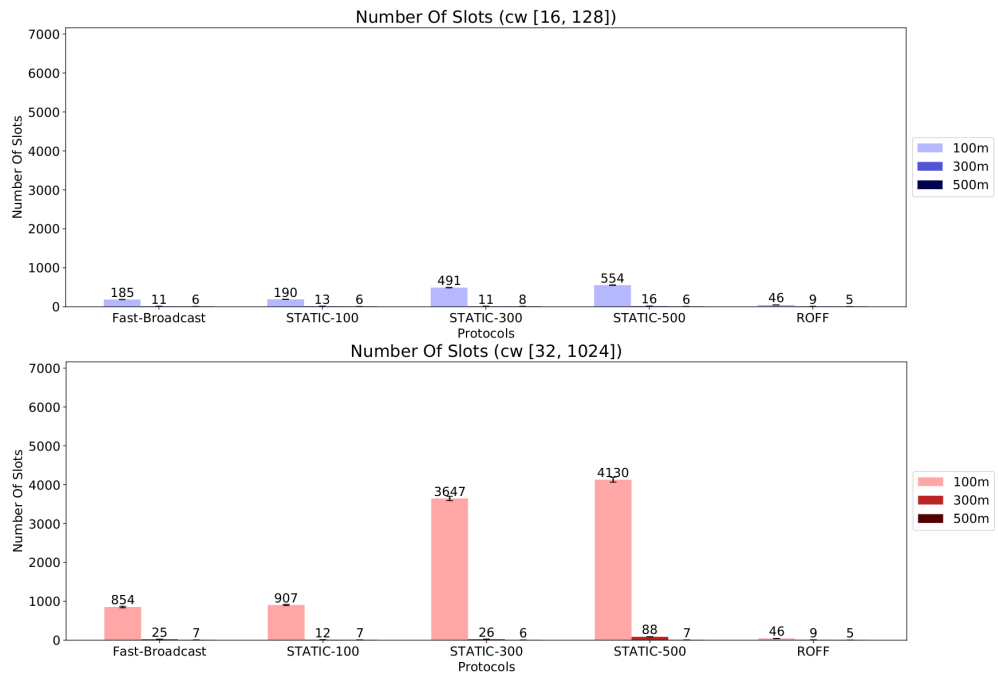


**Figure 6.45:** NOS for [16, 128] contention window (top) and [32, 1024] ] contention window (bottom)

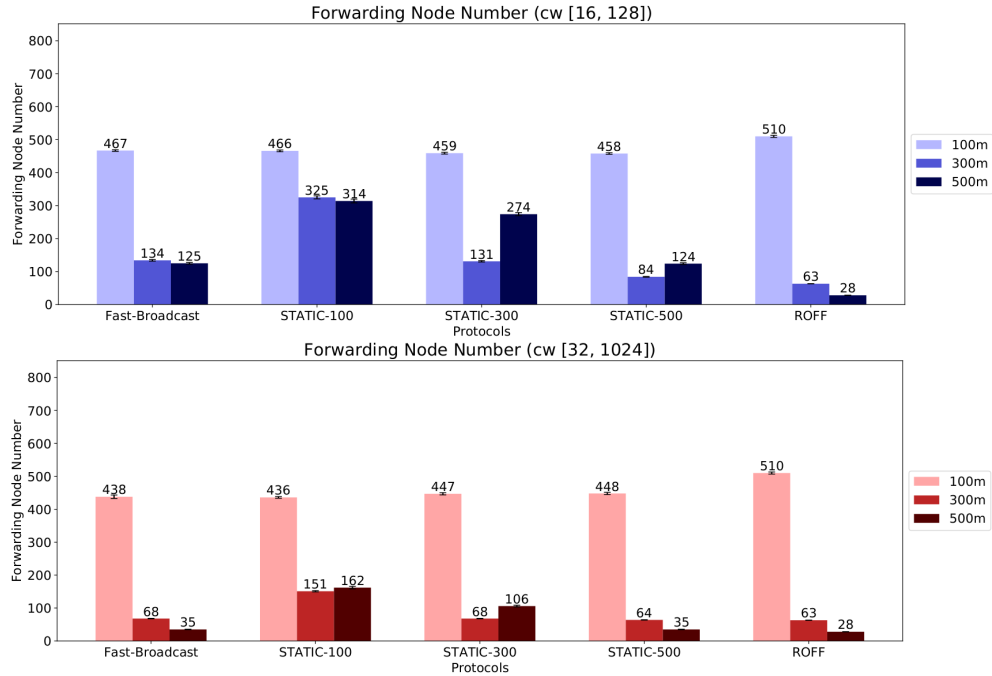


**Figure 6.46:** FNN for [16, 128] contention window (top) and [32, 1024] contention window (bottom)

Before starting to compare the metrics, we can notice that ROFF's results for both contention windows do not change: this is obvious, since the change in contention window affects only Fast-Broadcast (and its STATIC variants). Next, the same patterns between Fast-Broadcast and the STATIC protocols identified in previous tests regarding the underestimation, correct estimation and overestimation of transmission range continue to be true even for the lower contention window.

The two different contention windows do not cause any significant difference in delivery ratios and NOH. The smaller contention window brings about a big improvement in NOS, especially for the 100 meters transmission range configuration, where the metric improves by 361.62% for Fast-Broadcast. For the 300 meters transmission range, the metric improves by 56%, coming close to ROFF's value, equal to 9 slots. However, this improvement comes with a cost: looking at FNN (Figure 6.46), we can see that Fast-Broadcast's metric worsens by 97.05% and 254.29% for the two highest transmission range. This means that the waiting time difference between PFCs is not long enough to guarantee suppression of redundant transmission for the current vehicle density. Given a smaller contention window, more vehicles could end up waiting the exact same number of slots, hence resulting in multiple transmissions being fired simultaneously and needlessly. However, FNN does not increase by much for the 100 meters transmission range, and the decrease in NOS is the greatest: this means that for a lower number of PFCs (lower transmission range means lower number of neighbors for each node, hence a lower number of PFCs) the smaller contention window actually brings benefits all across the board.

These observations could suggest that a dynamic contention window, function of node density, number of neighbors or both could benefit Fast-Broadcast greatly.



# Acronyms

**LOS** Line of sight. [6](#)

**NIC** Network Interface Controller. [34](#)

**RPM** Radio Propagation Model. [5, 7](#)

**VANET** Vehicular Ad-Hoc Network. [1, 11](#)



# Bibliography

- [1] S. Panichpapiboon and W. Pattara-atikom, “A review of information dissemination protocols for vehicular ad hoc networks”, *IEEE Communications Surveys Tutorials*, vol. 14, no. 3, pp. 784–798, Third 2012, ISSN: 1553-877X. DOI: [10.1109/SURV.2011.070711.00131](https://doi.org/10.1109/SURV.2011.070711.00131).
- [2] Ting Zhong, Bo Xu, and Ouri Wolfson, “Disseminating real-time traffic information in vehicular ad-hoc networks”, in *2008 IEEE Intelligent Vehicles Symposium*, Jun. 2008, pp. 1056–1061. DOI: [10.1109/IVS.2008.4621303](https://doi.org/10.1109/IVS.2008.4621303).
- [3] T. Nadeem, S. Dashtinezhad, Chunyuan Liao, and L. Iftode, “Trafficview: A scalable traffic monitoring system”, in *IEEE International Conference on Mobile Data Management, 2004. Proceedings. 2004*, Jan. 2004, pp. 13–26. DOI: [10.1109/MDM.2004.1263039](https://doi.org/10.1109/MDM.2004.1263039).
- [4] T. Fujiki, M. Kirimura, T. Umedu, and T. Higashino, “Efficient acquisition of local traffic information using inter-vehicle communication with queries”, in *2007 IEEE Intelligent Transportation Systems Conference*, Sep. 2007, pp. 241–246. DOI: [10.1109/ITSC.2007.4357748](https://doi.org/10.1109/ITSC.2007.4357748).
- [5] Q. Yu and G. Heijenk, “Abiding geocast for warning message dissemination in vehicular ad hoc networks”, in *ICC Workshops - 2008 IEEE International Conference on Communications Workshops*, May 2008, pp. 400–404. DOI: [10.1109/ICCW.2008.81](https://doi.org/10.1109/ICCW.2008.81).
- [6] L. Wischhof, A. Ebner, and H. Rohling, “Information dissemination in self-organizing intervehicle networks”, *IEEE Transactions on Intelligent Transportation Systems*, vol. 6, no. 1, pp. 90–101, Mar. 2005, ISSN: 1524-9050. DOI: [10.1109/TITS.2004.842407](https://doi.org/10.1109/TITS.2004.842407).
- [7] G. Korkmaz, E. Ekici, F. Özgürner, and Ü. Özgürner, “Urban multi-hop broadcast protocol for inter-vehicle communication systems”, in *Proceedings of the 1st ACM International Workshop on Vehicular Ad Hoc Networks*, ser. VANET ’04, Philadelphia, PA, USA: ACM, 2004, pp. 76–85, ISBN: 1-58113-922-5. DOI: [10.1145/1023875.1023887](https://doi.org/10.1145/1023875.1023887). [Online]. Available: <http://doi.acm.org/10.1145/1023875.1023887>.
- [8] E. Fasolo, A. Zanella, and M. Zorzi, “An effective broadcast scheme for alert message propagation in vehicular ad hoc networks”, in *2006 IEEE International Conference on Communications*, vol. 9, Jun. 2006, pp. 3960–3965. DOI: [10.1109/ICC.2006.255700](https://doi.org/10.1109/ICC.2006.255700).
- [9] D. Li, H. Huang, X. Li, M. Li, and F. Tang, “A distance-based directional broadcast protocol for urban vehicular ad hoc network”, in *2007 International*

- Conference on Wireless Communications, Networking and Mobile Computing*, Sep. 2007, pp. 1520–1523. DOI: [10.1109/WICOM.2007.383](https://doi.org/10.1109/WICOM.2007.383).
- [10] Y. Tseng, R. Jan, C. Chen, C. Wang, and H. Li, “A vehicle-density-based forwarding scheme for emergency message broadcasts in vanets”, in *The 7th IEEE International Conference on Mobile Ad-hoc and Sensor Systems (IEEE MASS 2010)*, Nov. 2010, pp. 703–708. DOI: [10.1109/MASS.2010.5663803](https://doi.org/10.1109/MASS.2010.5663803).
  - [11] S. Khakbaz and M. Fathy, “A reliable method for disseminating safety information in vehicular ad hoc networks considering fragmentation problem”, in *2008 The Fourth International Conference on Wireless and Mobile Communications*, Jul. 2008, pp. 25–30. DOI: [10.1109/ICWMC.2008.74](https://doi.org/10.1109/ICWMC.2008.74).
  - [12] T. Osafune, L. Lin, and M. Lenardi, “Multi-hop vehicular broadcast (mhvb)”, in *2006 6th International Conference on ITS Telecommunications*, Jun. 2006, pp. 757–760. DOI: [10.1109/ITST.2006.289011](https://doi.org/10.1109/ITST.2006.289011).
  - [13] M. M. I. Taha and Y. M. Y. Hasan, “Vanet-dsrc protocol for reliable broadcasting of life safety messages”, in *2007 IEEE International Symposium on Signal Processing and Information Technology*, Dec. 2007, pp. 104–109. DOI: [10.1109/ISSPIT.2007.4458046](https://doi.org/10.1109/ISSPIT.2007.4458046).
  - [14] N. Wisitpongphan, O. K. Tonguz, J. S. Parikh, P. Mudalige, F. Bai, and V. Sadekar, “Broadcast storm mitigation techniques in vehicular ad hoc networks”, *IEEE Wireless Communications*, vol. 14, no. 6, pp. 84–94, Dec. 2007, ISSN: 1536-1284. DOI: [10.1109/MWC.2007.4407231](https://doi.org/10.1109/MWC.2007.4407231).
  - [15] H. Alshaer and E. Horlait, “An optimized adaptive broadcast scheme for inter-vehicle communication”, in *2005 IEEE 61st Vehicular Technology Conference*, vol. 5, May 2005, 2840–2844 Vol. 5. DOI: [10.1109/VETECS.2005.1543865](https://doi.org/10.1109/VETECS.2005.1543865).
  - [16] A. Wegener, H. Hellbruck, S. Fischer, C. Schmidt, and S. Fekete, “Autocast: An adaptive data dissemination protocol for traffic information systems”, in *2007 IEEE 66th Vehicular Technology Conference*, Sep. 2007, pp. 1947–1951. DOI: [10.1109/VETECF.2007.409](https://doi.org/10.1109/VETECF.2007.409).
  - [17] S. Panichpapiboon and G. Ferrari, “Irresponsible forwarding”, in *2008 8th International Conference on ITS Telecommunications*, Oct. 2008, pp. 311–316. DOI: [10.1109/ITST.2008.4740277](https://doi.org/10.1109/ITST.2008.4740277).
  - [18] S. Busanelli, G. Ferrari, and S. Panichpapiboon, “Efficient broadcasting in ieee 802.11 networks through irresponsible forwarding”, in *GLOBECOM 2009 - 2009 IEEE Global Telecommunications Conference*, Nov. 2009, pp. 1–6. DOI: [10.1109/GLOCOM.2009.5426212](https://doi.org/10.1109/GLOCOM.2009.5426212).
  - [19] M. Romanelli, C. Palazzi, and A. Bujari, “Propagazione di messaggi tra veicoli con modello urbano realistico”, Master’s thesis, University of Padua, 2017.
  - [20] C. E. Palazzi, S. Ferretti, M. Roccetti, G. Pau, and M. Gerla, “How do you quickly choreograph inter-vehicular communications? a fast vehicle-to-vehicle multi-hop broadcast algorithm, explained”, in *2007 4th IEEE Consumer Communications and Networking Conference*, Jan. 2007, pp. 960–964. DOI: [10.1109/CCNC.2007.194](https://doi.org/10.1109/CCNC.2007.194).

- [21] H. Yoo and D. Kim, “Roff: Robust and fast forwarding in vehicular ad-hoc networks”, *IEEE Transactions on Mobile Computing*, vol. 14, no. 7, pp. 1490–1502, Jul. 2015, ISSN: 1536-1233. DOI: [10.1109/TMC.2014.2359664](https://doi.org/10.1109/TMC.2014.2359664).
- [22] M. Stoffers and G. Riley, “Comparing the ns-3 propagation models”, in *2012 IEEE 20th International Symposium on Modeling, Analysis and Simulation of Computer and Telecommunication Systems*, Aug. 2012, pp. 61–67. DOI: [10.1109/MASCOTS.2012.17](https://doi.org/10.1109/MASCOTS.2012.17).
- [23] K. R. Schaubach, N. J. Davis, and T. S. Rappaport, “A ray tracing method for predicting path loss and delay spread in microcellular environments”, in */1992 Proceedings/ Vehicular Technology Society 42nd VTS Conference - Frontiers of Technology*, May 1992, 932–935 vol.2. DOI: [10.1109/VETEC.1992.245274](https://doi.org/10.1109/VETEC.1992.245274).
- [24] S.-C. Kim, B. J. Guarino, T. M. Willis, V. Erceg, S. J. Fortune, R. A. Valenzuela, L. W. Thomas, J. Ling, and J. D. Moore, “Radio propagation measurements and prediction using three-dimensional ray tracing in urban environments at 908 mhz and 1.9 ghz”, *IEEE Transactions on Vehicular Technology*, vol. 48, no. 3, pp. 931–946, May 1999, ISSN: 0018-9545. DOI: [10.1109/25.765022](https://doi.org/10.1109/25.765022).
- [25] I. Stepanov and K. Rothermel, “On the impact of a more realistic physical layer on manet simulations results”, *Ad Hoc Networks*, vol. 6, no. 1, pp. 61–78, 2008, ISSN: 1570-8705. DOI: <https://doi.org/10.1016/j.adhoc.2006.08.001>. [Online]. Available: <http://www.sciencedirect.com/science/article/pii/S1570870506000801>.
- [26] E. Giordano, R. Frank, G. Pau, and M. Gerla, “Corner: A step towards realistic simulations for vanet”, in *Proceedings of the Seventh ACM International Workshop on VehiculAr InterNETworking*, ser. VANET ’10, Chicago, Illinois, USA: ACM, 2010, pp. 41–50, ISBN: 978-1-4503-0145-9. DOI: [10.1145/1860058.1860065](https://doi.org/10.1145/1860058.1860065). [Online]. Available: <http://doi.acm.org/10.1145/1860058.1860065>.
- [27] K. N. Sridhar, S. Hao, M. C. Chan, and A. L. Ananda, “Egress: Environment for generating realistic scenarios for simulations”, in *2006 Tenth IEEE International Symposium on Distributed Simulation and Real-Time Applications*, Oct. 2006, pp. 15–24. DOI: [10.1109/DS-RT.2006.16](https://doi.org/10.1109/DS-RT.2006.16).
- [28] C. Sommer, D. Eckhoff, R. German, and F. Dressler, “A computationally inexpensive empirical model of ieee 802.11p radio shadowing in urban environments”, in *2011 Eighth International Conference on Wireless On-Demand Network Systems and Services*, Jan. 2011, pp. 84–90. DOI: [10.1109/WONS.2011.5720204](https://doi.org/10.1109/WONS.2011.5720204).
- [29] S. E. Carpenter and M. L. Sichitiu, “An obstacle model implementation for evaluating radio shadowing with ns-3”, in *Proceedings of the 2015 Workshop on Ns-3*, ser. WNS3 ’15, Barcelona, Spain: ACM, 2015, pp. 17–24, ISBN: 978-1-4503-3375-7. DOI: [10.1145/2756509.2756512](https://doi.org/10.1145/2756509.2756512). [Online]. Available: <http://doi.acm.org/10.1145/2756509.2756512>.
- [30] C. E. P. e. A. B. M. Barichello, “Propagazione rapida di messaggi in scenario veicolare urbano”, Master’s thesis, University of Padua, 2017.
- [31] E. P. for Intelligent Cities. (2019). European platform for intelligent cities, [Online]. Available: <http://web.archive.org/web/20080207010024/http://www.808multimedia.com/winnt/kernel.htm>.

- [32] D. Krajzewicz, J. Erdmann, M. Behrisch, and L. Bieker, “Recent development and applications of SUMO - Simulation of Urban MObility”, *International Journal On Advances in Systems and Measurements*, International Journal On Advances in Systems and Measurements, vol. 5, no. 3&4, pp. 128–138, Dec. 2012. [Online]. Available: <http://elib.dlr.de/80483/>.